Abstract and Applied Analysis

Modeling, Stability, Synchronization, and Chaos and their Applications to Complex Systems

Guest Editors: R. Yamapi, G. Filatrella, M. A. Aziz-Alaoui, and H. G. Enjieu Kadji

Modeling, Stability, Synchronization, and Chaos and their Applications to Complex Systems

Abstract and Applied Analysis

Modeling, Stability, Synchronization, and Chaos and their Applications to Complex Systems

Guest Editors: R. Yamapi, G. Filatrella, M. A. Aziz-Alaoui, and H. G. Enjieu Kadji

Editorial Board

Contents

Hindawi Publishing Corporation
Abstract and Applied Analysis
Volume 2014, Article ID 953813, 2 pages
http://dx.doi.org/10.1155/2014/953813

Editorial

Modeling, Stability, Synchronization, and Chaos and Their Applications to Complex Systems

R. Yamapi,[1] G. Filatrella,[2] M. A. Aziz-Alaoui,[3] and H. G. Enjieu Kadji[4]

[1] *Department of Physics, Faculty of Sciences, University of Douala, P.O. Box 24 157, Douala, Cameroon*
[2] *Dipartimento di Scienze Biologiche ed Ambientali, Università del Sannio, Via Port'Arsa 11, 82100 Benevento, Italy*
[3] *Laboratoire de Mathématiques Appliquées, Université du Le Havre, 25 rue Ph. Lebon, BP 540, 76600 Le Havre Cedex, France*
[4] *Monell Chemical Senses Center, 3500 Market Street, Philadelphia, PA 19104, USA*

Correspondence should be addressed to R. Yamapi; ryamapi@yahoo.fr

Received 15 January 2014; Accepted 15 January 2014; Published 27 February 2014

Issues related to chaotic dynamics, stability of oscillations, and their synchronization are widespread in nature, appearing ubiquitously in physics, chemistry, biology, engineering, and social science. Furthermore, potential applications in delicate areas, for instance, secure communication where transmitter and receiver are synchronized, explain the growing interest devoted to modeling and understanding.

In the current trend, collaborations and interdisciplinary researches are essential keys for mathematicians, chemists, physicists, biologists, and engineers to successfully investigate dynamical state in complex systems. This special issue addresses modeling, chaos, and synchronization processes in complex systems, based upon hypothesis or data from physics, chemistry, biophysics, and neuroscience. From 17 submissions, 5 papers are published in this special issue. Each paper was reviewed by at least two referees and revised accordingly by the authors. The themes include adaptive synchronization, stochastic chaotic systems, effective synchronization, exponential feedback coupling, distributed reduced-order observer-based protocol, nonlinear filtering, chaos synchronization, stability analysis, and control.

When it comes to synchronizing oscillations, different strategies have been investigated such as effective synchronization, adaptive synchronization, inverse synchronization, phase synchronization, and antiphase synchronization. This diversity of schemes is necessary because of the variety of systems under consideration. In Z. Wang et al.'s paper, an adaptive sliding mode controller is designed to realize the asymptotical synchronization in mean squares and the almost surely synchronization for two different stochastic chaotic systems, one with unknown parameters and another with uncertain terms. The robustness and efficiency of the technique are checked out using the Lorenz-Chen and Chen-Lu systems.

The exponential function-based nonlinear controller can also be utilized to achieve effective synchronization between two drive-response systems surrounded by the random perturbations. Such a technique was considered in P. Louodop et al.'s paper to obtain a new optimized controller which can lead to a much faster synchronization than the one based upon fixed feedback gain. Moreover, the new controller is easy to implement, for it does not need adaptation algorithm and it is based on a simple electrical system.

In the master-slave system configuration, chaotic synchronization can be effectively preserved via nonlinear filtering process. The synchronization phenomenon can occur in nonlinear interconnected structures that could have some useful applications for some chaotic systems in filtering waves. An example of application is the analysis of wave, originated from earthquakes and tsunamis inasmuch; they can generate resonance at particular frequencies. Such systems have been considered and investigated in J. S. González-Salas et al.'s paper.

The stability analysis and control of chaotic oscillations are also of great interest because of their impact in building up practical applications as those addressed in G. Zhou

et al.'s paper. Authors have considered in a new smooth Chua's system whose chaotic features are confirmed by the Lyapunov exponents. A linear controller and an adaptive controller are, respectively, proposed to globally synchronize two identical smooth Chua's systems estimated errors of uncertain parameters converge to zero as time increases.

When it comes to coordination control of multiagent systems, consensus problem is one of the most basic issues for the environment information changes and the communication links between agents may become unreliable. This particular matter concern is addressed in Y. Zhang et al.'s paper who have investigated a group of agents with high-dimensional linear coupling dynamics with an undirected switching interaction scheme.

Together, these papers represent an insightful investigation into the state of art in these majors' interdisciplinary topics. We hope this special issue captures the attention of the peers. We would like to acknowledge our gratitude to all the authors and reviewers who have made this special issue possible.

R. Yamapi
G. Filatrella
M. A. Aziz-Alaoui
H. G. Enjieu Kadji

Hindawi Publishing Corporation
Abstract and Applied Analysis
Volume 2013, Article ID 452549, 12 pages
http://dx.doi.org/10.1155/2013/452549

Research Article

Adaptive Synchronization for Two Different Stochastic Chaotic Systems with Unknown Parameters via a Sliding Mode Controller

Zengyun Wang,[1] Lihong Huang,[2,3] Xuxin Yang,[1] and Dingyang Lu[1]

[1] *Department of Mathematics, Hunan First Normal University, Changsha 410205, China*
[2] *College of Mathematics and Econometrics, Hunan University, Changsha 410082, China*
[3] *Hunan Women's University, Changsha 410003, China*

Correspondence should be addressed to Zengyun Wang; shunshuang1953@163.com

Received 31 January 2013; Accepted 19 March 2013

Academic Editor: René Yamapi

This paper investigates the problem of synchronization for two different stochastic chaotic systems with unknown parameters and uncertain terms. The main work of this paper consists of the following aspects. Firstly, based on the Lyapunov theory in stochastic differential equations and the theory of sliding mode control, we propose a simple sliding surface and discuss the occurrence of the sliding motion. Secondly, we design an adaptive sliding mode controller to realize the asymptotical synchronization in mean squares. Thirdly, we design an adaptive sliding mode controller to realize the almost surely synchronization. Finally, the designed adaptive sliding mode controllers are used to achieve synchronization between two pairs of different stochastic chaos systems (Lorenz-Chen and Chen-Lu) in the presence of the uncertainties and unknown parameters. Numerical simulations are given to demonstrate the robustness and efficiency of the proposed robust adaptive sliding mode controller.

1. Introduction

In the past few years, chaotic synchronization has received particular interests [1–3] mainly due to its wide applications in secure communications, ecological systems, system identification, and so forth. During the past decades, many methods and experimental techniques have been presented to realize the synchronization of two identical chaotic systems [4–10], such as adaptive control [4, 5], sliding mode control [6, 7], nonlinear feedback control [8, 9], and fuzzy system based control [10]. Among all these methods, sliding mode control method has been used widely to treat the unknown parameters and uncertainties [11, 12]. For example, synchronization and finite synchronization between two different chaotic systems with uncertainties and unknown parameters via sliding mode method are discussed in [13, 14], respectively. However, we have noted that in all of the above mentioned papers, the chaotic systems are deterministic differential equations without any random parameters or random excitation.

Recently, the stochastic modeling has played an important role in engineering application [15, 16] and there are some works in the field of control and synchronization on stochastic neural networks [17–25]. In accordance with the Lyapunov control theory, synchronization of stochastic delayed neural networks has been investigated in terms of linear matrix inequalities in [17]. Reference [18] discussed the adaptive lag synchronization between stochastic neural networks with time delay and [19] discussed the lag synchronization between stochastic neural networks with unknown parameters using adaptive control method. Reference [20] considered the robust decentralized adaptive control for stochastic delayed Hopfield neural networks using sling mode control method and [21, 22] discussed the almost surely exponential stability for stochastic neural networks. The almost surely synchronization between different stochastic chaotic systems is discussed in [23] using linear matrix equality technique. However, the parameters of the system need to be known, and the authors have not considered the chaotic system contained unknown parameters and uncertainties.

In [24], the authors designed an adaptive controller to make sure the synchronization error trajectories between two different stochastic Chua's systems enter a small zone around zero. The control of unstable periodic orbits of stochastic chaos is discussed in [25] using sliding mode method. As far as we know, there are no results on the asymptotical synchronization and almost surely synchronization for two different stochastic chaotic systems using adaptive sliding mode control method.

In this paper, we discussed the asymptotical synchronization and almost surely synchronization for two different stochastic chaotic systems with unknown parameters and uncertain terms using sliding mode method. The structure of this paper is outlined as follows. In Section 2, we introduce the model of chaotic systems with unknown parameters and uncertain terms and give several assumptions, definitions, and lemmas. Section 3 presents the main results of this paper; we design two adaptive sliding mode controllers to realize the synchronization. Numerical examples are given in Section 4 to show the effectiveness of our proposed results. Finally, some concluding remarks are made in Section 5.

2. Problem Statement and Mathematic Preliminaries

In this paper, we consider the following stochastic systems with uncertain parameters in the following form:

$$\begin{aligned} \mathrm{d}x_i = {} & \left(f_i\left(x_1,\ldots,x_n\right) + F_i\left(x_1,\ldots,x_n\right)\theta \right. \\ & \left. +\Delta f_i\left(x_1,\ldots,x_n\right)\right)\mathrm{d}t \\ & + \sigma_i\left(x_1,\ldots,x_n\right)\mathrm{d}w\left(t\right), \quad i = 1,2,\ldots,n \end{aligned} \tag{1}$$

or, in a compact form:

$$\mathrm{d}x = \left(f\left(x\right) + F\left(x\right)\theta + \Delta f\left(x\right)\right)\mathrm{d}t + \sigma\left(x\right)\mathrm{d}w\left(t\right). \tag{2}$$

We consider the model (1) as the drive system. The response chaotic system is

$$\begin{aligned} \mathrm{d}y_i = {} & \left(g_i\left(y_1,\ldots,y_n\right) + G_i\left(y_1,\ldots,y_n\right)\theta \right. \\ & \left. + \Delta g_i\left(y_1,\ldots,y_n\right) + u_i\left(t\right)\right)\mathrm{d}t \\ & + \sigma_i\left(y_1,\ldots,y_n\right)\mathrm{d}w\left(t\right), \quad i = 1,2,\ldots,n \end{aligned} \tag{3}$$

or, in a compact form:

$$\mathrm{d}y = \left(g\left(y\right) + G\left(y\right)\theta + \Delta g\left(y\right) + u\left(t\right)\right)\mathrm{d}t + \sigma\left(y\right)\mathrm{d}w\left(t\right), \tag{4}$$

where $x, y \in \mathfrak{R}^n$ are the state vectors, $u(t) \in \mathfrak{R}^n$ is the control input, $f(x), g(y) \in C^1(\mathfrak{R}^n, \mathfrak{R}^n)$, $F(x), G(y) \in C^1(\mathfrak{R}^n, \mathfrak{R}^{n\times m})$, and $\sigma(x), \sigma(y) \in C^1(\mathfrak{R}^n, \mathfrak{R}^{n\times p})$ are function matrices of x and y, respectively. $\theta \in \mathfrak{R}^m$ and $\psi \in \mathfrak{R}^m$ are the vectors of uncertain parameters, $\Delta f(x)$ and $\Delta g(y)$ represent the nonlinear vectors that may include unknown uncertainties and other external disturbances for the master system and slave system, and $w(t)$ is a p-dimensional Brown motion defined on a complete probability space $(\Omega, \mathscr{F}, \mathscr{P})$ with a natural filtration $\{\mathscr{F}_t\}$ generated by $\{w(s) : 0 \le s \le t\}$, where we associate Ω with the canonical space generated by $\{w(t)\}$ and denoted $\mathscr{F}$ the associated σ-algebra generated by $\{w(t)\}$ with the probability measure $\mathscr{P}$. Here the white noise $\mathrm{d}w_i(t)$ is independent of $\mathrm{d}w_j(t)$ for $i \ne j$.

(A1) The networks (2) and (4) are chaotic, and if x, y are bounded, then $|\Delta f_i(x)|$, $|\Delta g_i(x)|$ are bounded and satisfy $\Delta f_i(0) = \Delta g_i(0) = 0$ for $i = 1,\ldots,n$, that is,

$$\left|\Delta f_i\left(x\right)\right| \le \alpha_i, \qquad \left|\Delta g_i\left(x\right)\right| \le \beta_i, \tag{5}$$

where α_i and β_i are unknown parameters.

(A2) The noise intensity function matrices $\sigma_i : R^n \to R^p$ are locally Lipschitz continuous and satisfying the following condition. Moreover, σ_i satisfies

$$\left[\sigma_i\left(x\right) - \sigma_i\left(y\right)\right]^{\mathrm{T}}\left[\sigma_i\left(x\right) - \sigma_i\left(y\right)\right] \le \sum_{j=1}^{n} k_{ij}\left(x_j - y_j\right)^2, \tag{6}$$

where k_{ij} are unknown parameters.

Remark 1. Note that condition (A1) is very weak. We do not impose the usual conditions such as Lipschitz condition and differentiability on the unknown uncertainties functions. It can be discontinuous or even impulsive functions. Since the trajectories of chaotic systems are always bounded, hence, condition (A1) can be easily satisfied.

Remark 2. The condition (A2) is the linear growth condition in fact, it is easy to see this condition is equivalent to the condition in [23].

Throughout this paper, we always assume the nonlinear function matrix satisfies $f(0) = g(0) = F(0) = G(0) = 0$. It implies that (2) and (4) have a unique global solution on $t \ge 0$ for the initial conditions since (A1) and (A2) hold [26].

Let $e(t) = x(t) - y(t)$, then with subtracting (3) from (1) the error dynamics is obtained as follows:

$$\begin{aligned} \mathrm{d}e_i = {} & \left(f_i\left(x\right) - g_i\left(y\right) + F_i\left(x\right)\theta - G\left(y\right)\psi + \Delta f_i\left(x\right)\right. \\ & \left. -\Delta g_i\left(y\right) - u_i\left(t\right)\right)\mathrm{d}t + \left(\sigma_i\left(x\right) - \sigma_i\left(y\right)\right)\mathrm{d}w\left(t\right). \end{aligned} \tag{7}$$

It is clear that the synchronization problem can be transformed to be the equivalent problem of stabilizing the error system (7).

Remark 3. From the mathematical point of view, the model is more general. If the noise intensity function matrices $\sigma(x) = \sigma(y) = 0$, (7) becomes the model in [13]. Furthermore, if $\Delta f(x) = \Delta g(y) = 0$, the system will be the model in [14]. If $\Delta f(x) = \Delta g(y) = 0$ and θ, ψ are the known vectors, this will be the model discussed in [23].

Definition 4 (see [19]). The error system (7) is said to be globally stable in mean squares if for any given initial condition such that

$$\lim_{t\to\infty} E\left\|e\left(t\right)\right\|^2 = 0, \tag{8}$$

where $E[\cdot]$ is the mathematical expectation.

Definition 5 (see [26]). The trivial solution of the error system (7) is said to be almost surely exponentially stable, if for almost all sample paths of the solution $e(t)$, we have

$$\limsup_{t\to\infty}\frac{1}{t}\log\|e(t)\|<0, \tag{9}$$

that is, the the drive system and response system are almost surely synchronization.

Remark 6. If $e(t)=0$, this means that $x(t)=y(t)$, so $u(t)=f(x)+F(x)\theta+\Delta f(x)-g(y)-G(y)\psi-\Delta g(x)+(\sigma(x)-\sigma(y))\dot{w}(t)$, where $\dot{w}(t)=\mathrm{d}w(t)/\mathrm{d}t$. This implies that $u(t)$ directly depends on white Gaussian noises and it is an accessible causal signal; this means that the synchronization cannot be realized completely.

The purpose of this paper is to consider the adaptive feedback synchronization problem for stochastic chaotic systems with unknown parameters and uncertainties. The main work of this paper consists of the following aspects. (i) Design an adaptive controller such that the asymptotical stability of the error system (7) can be achieved in mean squares that $\lim_{t\to\infty}E\|e(t)\|^2=0$. (ii) Design an adaptive control such that the error system (7) can be almost surely stable, that means the almost surely synchronization could be achieved between drive system and response system.

Before proposing the main results, we introduce some lemmas which will be used in the following sections.

Lemma 7 (see [20, 27]). *The trivial solution of a stochastic differential equation as follows*

$$\mathrm{d}x(t)=a(t,x)\,\mathrm{d}t+b(t,x)\,\mathrm{d}\omega(t), \tag{10}$$

with $a(t,x)$ and $b(t,x)$ sufficiently differentiable maps, is globally asymptotically stable in probability if there exists a function $V(t,x)$ which is positive definite in the Lyapunov sense and satisfies

$$\mathscr{L}V(t,x)=V_t(t,x)+V_x(t,x)\cdot a(t,x)+\frac{1}{2}\operatorname{tr}\left\{b^{\mathrm{T}}(t,x)V_{xx}(t,x)b(t,x)\right\}<0, \tag{11}$$

for $x\neq 0$, where $V_t(t,x)=\partial V(t,x)/\partial t$, $V_x(t,x)=\partial V(t,x)/\partial x$, and $V_{xx}(t,x)=(\partial^2V(t,x)/\partial x_i\partial x_j)_{n\times n}$.

Lemma 8 (see [23, 26]). *Suppose there exist a nonnegative function $V(x,t)\in C^{2,1}(R^n\times[t_0,+\infty),R^+)$ and three positive numbers p, α, and λ such that, for all $x\neq 0$ and $t\geq t_0$,*

$$\alpha|x|^p\leq V(x,t),\qquad \mathscr{L}V(t,x)<-\lambda V(t,x) \tag{12}$$

holds, then for any $x_0\in R^n$, the trivial solution of (10) *is almost surely exponentially asymptotically stable; that is,*

$$\limsup_{t\to\infty}\frac{1}{t}\log\left|x(t,t_0,x_0)\right|<-\frac{\lambda}{p} \tag{13}$$

holds almost surely.

3. Main Results

To design the adaptive feedback controller to realize the synchronization for stochastic chaotic systems with unknown parameters and uncertainties, we use the sliding mode control method. In this section, the nonsingular terminal sliding mode is chosen as

$$s_i(t)=\lambda_i e_i(t),\quad i=1,\ldots,n, \tag{14}$$

where $s_i(t)\in R$, $s(t)=[s_1(t),s_2(t),\ldots,s_n(t)]^{\mathrm{T}}$ and $\lambda_i>0$ are constants.

3.1. Design of an Adaptive Controller to Realize Asymptotical Synchronization in Mean Squares. In this section, we are going to design an adaptive controller with updating laws such that the state trajectories will move to the sliding surface in mean squares. To ensure the occurrence of the sliding motion, an adaptive sliding mode controller is proposed as

$$\begin{aligned}u_i(t)&=f_i(x)+F_i(x)\widehat{\theta}-g_i(y)-G_i(y)\widehat{\psi}\\&\quad+\left(\widehat{\alpha}_i+\widehat{\beta}_i\right)\operatorname{sign}\left(s_i(t)\right)+k_is_i(t)\\&\quad+\sum_{j=1}^{n}\frac{\lambda_j^2}{\lambda_i^3}\widehat{k}_{ji}s_i(t),\quad i=1,2,\ldots,n,\end{aligned} \tag{15}$$

where $\widehat{\theta}$, $\widehat{\psi}$, $\widehat{\alpha}_i$, $\widehat{\beta}_i$, $\widehat{k}_{ij}$ are the estimations for θ, ψ, α_i, β_i, k_{ij}, respectively. $k_i>0$ is the switching gain and a constant, $i=1,2,\ldots,n$.

To tackle the uncertainties and unknown parameters, appropriate adaptive laws are defined as follows:

$$\begin{aligned}\dot{\widehat{\theta}}&=F^{\mathrm{T}}(x)\gamma(t),&\widehat{\theta}(0)&=\widehat{\theta}_0\\\dot{\widehat{\psi}}&=-G^{\mathrm{T}}(y)\gamma(t),&\widehat{\psi}(0)&=\widehat{\psi}_0\\\dot{\widehat{\alpha}}_i&=\lambda_i\left|s_i(t)\right|,&\widehat{\alpha}_i(0)&=\widehat{\alpha}_{i0}\\\dot{\widehat{\beta}}_i&=\lambda_i\left|s_i(t)\right|,&\widehat{\beta}_i(0)&=\widehat{\beta}_{i0}\\\dot{\widehat{k}}_{ij}&=\frac{\lambda_i^2}{\lambda_j^2}s_j^2(t),&\widehat{k}_{ij}(0)&=\widehat{k}_{ij0},\end{aligned} \tag{16}$$

where $\gamma(t)=[\lambda_1s_1(t),\lambda_2s_2(t),\ldots,\lambda_ns_n(t)]^{\mathrm{T}}$, and $\widehat{\theta}_0$, $\widehat{\psi}_0$, $\widehat{\alpha}_{i0}$, and $\widehat{\beta}_{i0}$ are the initial values of the update parameters, respectively.

The proposed control input in (15) with the updating laws in (16) will guarantee the reaching condition $\lim_{t\to\infty}E\|s(t)\|^2=0$ and ensure the occurrence of the sliding motion, which is proved in the following theorem.

Theorem 9. *Suppose that the assumption conditions (A1) and (A2) hold; consider the error dynamics* (7)*; this system is controlled by $u(t)$ in* (15) *with updating laws in* (16)*, then the error system trajectories will converge to the sliding surface $s(t)=0$ in mean squares.*

Proof. Select a positive definite function as a Lyapunov function candidate in the form of

$$V(t) = \frac{1}{2}\sum_{i=1}^{n}\left(s_i^2(t) + \left(\widehat{\alpha}_i - \alpha_i\right)^2 + \left(\widehat{\beta}_i - \beta_i\right)^2\right) + \frac{1}{2}\sum_{i=1}^{n}\sum_{j=1}^{n}\left(\widehat{k}_{ij} - k_{ij}\right)^2 + \frac{1}{2}\left\|\widehat{\theta} - \theta\right\|^2 + \frac{1}{2}\left\|\widehat{\psi} - \psi\right\|^2. \tag{17}$$

Since $\mathrm{d}s_i(t) = \lambda_i \mathrm{d}e_i(t)$, by Itô's differential rule, the stochastic derivative of $V(t)$ along trajectories of error system (7) can be obtained as follows:

$$\mathrm{d}V(t) = \mathscr{L}V(t)\,\mathrm{d}t + \sum_{i=1}^{n}\lambda_i s_i(t)\left(\sigma_i(x) - \sigma_i(y)\right)\mathrm{d}w(t), \tag{18}$$

where the weak infinitesimal operator $\mathscr{L}$ is given by

$$\begin{aligned}
&\mathscr{L}V(t)\\
&= \sum_{i=1}^{n}\left[\lambda_i s_i(t)\left(\left(f_i(x) - g_i(y) + F_i(x)\theta - G_i(y)\psi + \Delta f_i(x) - \Delta g_i(y) - u_i(t)\right)\right)\right]\\
&\quad + \sum_{j=1}^{n}\lambda_i^2\left(\sigma_i(x(t)) - \sigma_i(y(t))\right)^{\mathrm{T}}\\
&\quad \times\left(\sigma_i(x(t)) - \sigma_i(y(t))\right) + \left(\widehat{\alpha}_i - \alpha_i\right)\dot{\widehat{\alpha}}_i\\
&\quad + \left(\widehat{\beta}_i - \beta_i\right)\dot{\widehat{\beta}}_i\\
&\quad + \sum_{i=1}^{n}\sum_{j=1}^{n}\left(\widehat{k}_{ij} - k_{ij}\right)\dot{\widehat{k}}_{ij} + \left(\widehat{\theta} - \theta\right)^{\mathrm{T}}\dot{\widehat{\theta}} + \left(\widehat{\psi} - \psi\right)^{\mathrm{T}}\dot{\widehat{\psi}}\\
&\le \sum_{i=1}^{n}\Big[\lambda_i s_i(t) F_i(x)\left(\theta - \widehat{\theta}\right) - \lambda_i s_i(t) G_i(y)\left(\psi - \widehat{\psi}\right)\\
&\qquad + \alpha_i\lambda_i\left|s_i(t)\right| + \beta_i\lambda_i\left|s_i(t)\right| - \widehat{\alpha}_i\lambda_i\left|s_i(t)\right|\\
&\qquad - \widehat{\beta}_i\lambda_i\left|s_i(t)\right| - k_i\lambda_i s_i(t)^2\\
&\qquad - \lambda_i s_i(t)\sum_{j=1}^{n}\frac{\lambda_j^2}{\lambda_i^3}\widehat{k}_{ji}s_i(t) + \sum_{j=1}^{n}\lambda_i^2 k_{ij}e_j^2(t)\\
&\qquad + \left(\widehat{\alpha}_i - \alpha_i\right)\dot{\widehat{\alpha}}_i + \left(\widehat{\beta}_i - \beta_i\right)\dot{\widehat{\beta}}_i\Big]\\
&\quad + \sum_{i=1}^{n}\sum_{j=1}^{n}\left(\widehat{k}_{ij} - k_{ij}\right)\dot{\widehat{k}}_{ij} + \left(\widehat{\theta} - \theta\right)^{\mathrm{T}}\dot{\widehat{\theta}} + \left(\widehat{\psi} - \psi\right)^{\mathrm{T}}\dot{\widehat{\psi}}.
\end{aligned} \tag{19}$$

Using the facts $\sum_{i=1}^{n}\lambda_i s_i(t)F_i(x)\theta = \theta^{\mathrm{T}}F^{\mathrm{T}}(x)\gamma(t)$, $\sum_{i=1}^{n}\lambda_i s_i(t)G_i(x)\psi = \psi^{\mathrm{T}}G^{\mathrm{T}}(x)\gamma(t)$ and the updating laws in (16), one has

$$\mathscr{L}V(t) \le -\sum_{i=1}^{n}k_i\lambda_i s_i^2 = -\sum_{i=1}^{n}\eta_i s_i^2 = -\eta s^{\mathrm{T}}(t)\,s(t), \tag{20}$$

where $\eta_i = k_i\lambda_i$, $i = 1, 2, \ldots, n$ and $\eta = \min\{\eta_1, \eta_2, \ldots, \eta_n\} > 0$.

Taking mathematical expectation on both sides of (20), in view of (18) and the definition of $V(t)$, we obtain

$$\frac{1}{2}E\|s(t)\|^2 \le EV(t) \le EV(0) - \eta\int_0^t E\|s(\tau)\|^2\mathrm{d}\tau. \tag{21}$$

Based on the LaSalle invariance principle of stochastic differential equation, which was developed in [28, 29], we have $s(t) \to 0$ when $t \to \infty$, which in turn illustrates that $\lim_{t\to\infty}E\|s(t)\|^2 = 0$. This complete the proof. □

Remark 10. If $\sigma(x) = \sigma(y) = 0$, this theorem is an extension of Theorem 1 in [13]. If $\sigma(x) = \sigma(y) = 0$ and $\Delta f(x) = \Delta g(x)$, this is a similar result of Theorem 2 in [14].

Remark 11. Since the control law (15) contains the sign function as a hard switcher, the undesirable chattering phenomenon occurs. According to Lemma 2 and Remark 2 in [13], we can replace the $\mathrm{sign}(s_i)$ function by $\tanh(\epsilon s_i)$, $\epsilon > 0$.

Remark 12. From the proof of Theorem 9, we know that $\mathscr{L}V(t) \le 0$ as long as $s(t) \ne 0$. Therefore, the trajectories $s(t)$ will converge to $s(t) = 0$ in mean squares. On the other hand, from the adaptive law (18) we can see $\dot{\widehat{\theta}}$, $\dot{\widehat{\psi}}$, $\dot{\widehat{\alpha}}_i$, $\dot{\widehat{\beta}}_i$, and $\dot{\widehat{k}}_{ij}$ turn to zero when $s(t) = 0$, which implies that $\widehat{\theta}$, $\widehat{\psi}$, $\widehat{\alpha}_i$, $\widehat{\beta}_i$, and $\widehat{k}_{ij}$ approach some constants as $s(t) \to 0$. However, this does not elaborate that $\widehat{\theta} \to \theta$, $\widehat{\psi} \to \psi$. This point is consistent with the results of [30].

In fact, the unknown parameters θ, ψ in (7) cannot identify with $\widehat{\theta}$, $\widehat{\psi}$. We offer the following theorem.

Theorem 13. *In Theorem 9, if $\Delta f(x) \ne \Delta g(y)$ and the synchronization between* (1) *and* (3) *is realized, the unknown parameters θ, ψ in* (7) *cannot identify with $\widehat{\theta}$, $\widehat{\psi}$ in* (17)*, respectively.*

Proof. We prove it by its contrapositive proposition. On the synchronization manifold $x(t) = y(t)$, it follows $s_i(t) = 0$ and $\mathrm{d}s_i = 0$. From (7) and (15), we have

$$0 = \Bigg[\lambda_i\left(F_i(x)\left(\theta - \widehat{\theta}\right) - G_i(y)\left(\psi - \widehat{\psi}\right) + \Delta f_i(x) - \Delta g_i(y) - \left(\widehat{\alpha}_i + \widehat{\beta}_i\right)\mathrm{sign}\,s_i(t) - k_i s_i(t)\right) - \sum_{j=1}^{n}\frac{\lambda_j^2}{\lambda_i^2}\widehat{k}_{ji}s_i(t)\Bigg]\mathrm{d}t + \lambda_i\left(\sigma_i(x(t)) - \sigma_i(y(t))\right)\mathrm{d}w(t). \tag{22}$$

Suppose $\widehat{\theta} = \theta$ and $\widehat{\psi} = \psi$; we have $\Delta f_i(x) = \Delta g_i(y) = \Delta g_i(x)$; this means $\Delta f(x) = \Delta g(x)$, which is a contradiction. This completes the proof. □

If $\Delta f(x) = \Delta g(y) = 0$, we can get the following theorem.

Theorem 14. *Suppose that the assumption condition (A2) holds. Then under the controller* (15) *with updating laws* (16), *the response system and the drive system are asymptotical synchronized in mean squares. Moreover, if $F_{ij}(x)$, $G_{ij}(y)$ are linearly independent of the synchronization manifold, then* $\lim_{t\to\infty}(\widehat{\theta}-\theta)=\lim_{t\to\infty}(\widehat{\psi}-\psi)=0$.

Proof. It is easy to get the following error system:

$$\begin{aligned} \mathrm{d}e_i &= \left(f_i(x)-g_i(y)+F_i(x)\theta-G(y)\psi-u_i(t)\right)\mathrm{d}t \\ &\quad+\left(\sigma_i(x)-\sigma_i(y)\right)\mathrm{d}w(t). \end{aligned} \tag{23}$$

Define the following Lyapunov function candidate

$$\begin{aligned} V_1(t) &= \frac{1}{2}\sum_{i=1}^{n}s_i(t)^2+\frac{1}{2}\sum_{i=1}^{n}\sum_{j=1}^{n}\left(\widehat{k}_{ij}-k_{ij}\right)^2 \\ &\quad+\frac{1}{2}\left\|\widehat{\theta}-\theta\right\|^2+\frac{1}{2}\left\|\widehat{\psi}-\psi\right\|^2. \end{aligned} \tag{24}$$

Since $\mathrm{d}s_i(t)=\lambda_i\mathrm{d}e_i(t)$, by Itô's differential rule, the stochastic derivative of $V(t)$ along trajectories of error system (7) can be obtained as follows:

$$\mathrm{d}V_1(t)=\mathscr{L}V_1(t)\,\mathrm{d}t+\sum_{1}^{n}\lambda_i s_i\left(\sigma_i(x)-\sigma_i(y)\right)\mathrm{d}w(t), \tag{25}$$

where the weak infinitesimal operator $\mathscr{L}$ is given by

$$\begin{aligned} &\mathscr{L}V_1(t) \\ &=\sum_{i=1}^{n}\left[\lambda_i s_i(t)\left(\left(f_i(x)-g_i(y)\right.\right.\right. \\ &\qquad\left.\left.\left.+F_i(x)\theta-G_i(y)\psi-u_i(t)\right)\right)\right] \\ &\quad+\sum_{j=1}^{n}\lambda_i^2\left(\sigma_i(x(t))-\sigma_i(y(t))\right)^{\mathrm{T}} \\ &\qquad\times\left(\sigma_i(x(t))-\sigma_i(y(t))\right) \\ &\quad+\sum_{i=1}^{n}\sum_{j=1}^{n}\left(\widehat{k}_{ij}-k_{ij}\right)\dot{\widehat{k}}_{ij}+\left(\widehat{\theta}-\theta\right)^{\mathrm{T}}\dot{\widehat{\theta}}+\left(\widehat{\psi}-\psi\right)^{\mathrm{T}}\dot{\widehat{\psi}} \\ &\le\sum_{i=1}^{n}\left[\lambda_i s_i(t)F_i(x)\left(\theta-\widehat{\theta}\right)\right. \\ &\qquad-\lambda_i s_i(t)G_i(y)\left(\psi-\widehat{\psi}\right) \\ &\qquad+\alpha_i\lambda_i\left|s_i(t)\right|+\beta_i\lambda_i\left|s_i(t)\right| \\ &\qquad-\widehat{\alpha}_i\lambda_i\left|s_i(t)\right|-\widehat{\beta}_i\lambda_i\left|s_i(t)\right|-k_i\lambda_i s_i(t)^2 \\ &\qquad-\lambda_i s_i(t)\sum_{j=1}^{n}\frac{\lambda_j^2}{\lambda_i^3}\widehat{k}_{ji}s_i(t) \\ &\qquad\left.+\sum_{j=1}^{n}\lambda_i^2k_{ij}e_j(t)^2\right] \\ &\quad+\sum_{i=1}^{n}\sum_{j=1}^{n}\left(\widehat{k}_{ij}-k_{ij}\right)\dot{\widehat{k}}_{ij} \\ &\quad+\left(\widehat{\theta}-\theta\right)^{\mathrm{T}}\dot{\widehat{\theta}}+\left(\widehat{\psi}-\psi\right)^{\mathrm{T}}\dot{\widehat{\psi}}. \end{aligned} \tag{26}$$

From the update laws (16), we can always choose the appropriate initial values of $\widehat{\alpha}_{i0}$ and $\widehat{\beta}_{i0}$ to make $\widehat{\alpha}_i>0$ and $\widehat{\beta}_i>0$. Since $\widehat{\alpha}_i s_i(t)\,\mathrm{sign}(s_i(t))\ge 0$ and $\widehat{\beta}_i s_i(t)\,\mathrm{sign}(s_i(t))\ge 0$. Using the facts $\sum_{i=1}^{n}\lambda_i s_i(t)F_i(x)\theta=\theta^{\mathrm{T}}F^{\mathrm{T}}(x)\gamma(t)$, $\sum_{i=1}^{n}\lambda_i s_i(t)G_i(x)\psi=\psi^{\mathrm{T}}G^{\mathrm{T}}(x)\gamma(t)$ and the updating laws in (18), with the same procedure of the proof of Theorem 9, we also arrive at $E\|s(t)\|^2\to 0$.

On the synchronization manifold $x(t)=y(t)$, it follows $s(t)=0$ and $\mathrm{d}s_i=0$. From (7) and (15), we have

$$0=\lambda_i\left[F_i(x)\left(\theta-\widehat{\theta}\right)-G_i(y)\left(\psi-\widehat{\psi}\right)\right]. \tag{27}$$

Since $F_{ij}(x)$, $G_{ij}(y)$ are linearly independent on the synchronization manifold, therefore, the above equality holds if and only if $\widehat{\theta}=\theta$ and $\widehat{\psi}=\psi$. □

Remark 15. Certainly, under the controller without $(\widehat{\alpha}_i+\widehat{\beta}_i)\,\mathrm{sign}\,s_i(t)$ term, the response system can also synchronize the drive system in mean squares. However, under the controller (15) with this term, it is more effective to realize the synchronization with this term. If $x_i(t)>y_i(t)$, this term will help to increase $y_i(t)$, and if $x_i(t)<y_i(t)$, this term will help to decrease $y_i(t)$. Hence, this term $(\widehat{\alpha}_i+\widehat{\beta}_i)\,\mathrm{sign}\,s_i(t)$ can enhance the synchronization speed.

3.2. Design of an Adaptive Controller to Realize Almost Surely Synchronization. In this section, we are going to design an adaptive controller with update laws such that the state trajectories will move to the sliding surface almost surely. We first introduce the following assumptions for the unknown parameters.

(A3) The unknown parameters vectors θ and ψ are norm bounded with known bounds, that is,

$$\|\theta\|\le\overline{\theta},\qquad\|\psi\|\le\overline{\psi}, \tag{28}$$

where $\overline{\theta}$ and $\overline{\psi}$ are two known positive constants.

(A4) Assume (A1) and (A2) hold, and α_i, β_i, and k_{ij} are known positive constants.

To ensure the occurrence of the sliding motion, an adaptive sliding mode controller is proposed as

$$\begin{aligned} u_i(t) &= f_i(x)+F_i(x)\widehat{\theta}-g_i(y)-G_i(y)\widehat{\psi} \\ &\quad+\left(\alpha_i+\beta_i\right)\mathrm{sign}\left(s_i(t)\right)+\frac{1}{2}k_i s_i(t) \\ &\quad-\eta\left(\left\|\widehat{\theta}\right\|^2+\overline{\theta}^2+\left\|\widehat{\psi}\right\|^2+\overline{\psi}^2\right) \\ &\quad\times\left(\frac{s_i(t)}{\lambda_i\|s(t)\|^2}\right)+\sum_{j=1}^{n}\frac{\lambda_j^2}{\lambda_i^3}k_{ji}s_i(t), \end{aligned} \tag{29}$$

where $\widehat{\theta}$, $\widehat{\psi}$ are the estimations for θ, ψ, respectively. $\eta_i = k_i\lambda_i$, $i = 1, 2, \ldots, n$ and $\eta = \min\{\eta_1, \eta_2, \ldots, \eta_n\} > 0$, $k_i > 0$ are the switching gain and constants, $i = 1, 2, \ldots, n$.

To tackle the uncertainties and unknown parameters, appropriate adaptive laws are defined as follows:

$$\begin{aligned} \dot{\widehat{\theta}} &= F^{\mathrm{T}}(x)\,\gamma(t), \qquad \widehat{\theta}(0) = \widehat{\theta}_0 \\ \dot{\widehat{\psi}} &= -G^{\mathrm{T}}(y)\,\gamma(t), \qquad \widehat{\psi}(0) = \widehat{\psi}_0, \end{aligned} \tag{30}$$

where $\gamma(t) = [\lambda_1 s_1(t), \lambda_2 s_2(t), \ldots, \lambda_n s_n(t)]^{\mathrm{T}}$, and $\widehat{\theta}_0$, $\widehat{\psi}_0$ are the initial values of the update parameters, respectively.

Based on the control input in (29) with the updating laws in (30) to guarantee the reaching condition $\lim_{t\to\infty} s(t) = 0$ almost surely holds and to ensure the occurrence of the sliding motion, a theorem is proposed and proved.

Theorem 16. *Suppose that the assumption conditions (A3) and (A4) hold; consider the error dynamics* (7)*; this system is controlled by* $u(t)$ *in* (29) *with updating laws in* (30)*, then the error system trajectories will converge to the sliding surface* $s(t) = 0$ *almost surely.*

Proof. Select a positive definite function as a Lyapunov function candidate in the form of

$$V(t) = \frac{1}{2}\sum_{i=1}^{n} s_i(t)^2 + \frac{1}{2}\left\|\widehat{\theta} - \theta\right\|^2 + \frac{1}{2}\left\|\widehat{\psi} - \psi\right\|^2. \tag{31}$$

Since $\mathrm{d}s_i(t) = \lambda_i \mathrm{d}e_i(t)$, by Itô's differential rule, the stochastic derivative of $V(t)$ along trajectories of error system (7) can be obtained as follows:

$$\mathrm{d}V(t) = \mathscr{L}V(t)\,\mathrm{d}t + \sum_{1}^{n} \lambda_i s_i(t)\left(\sigma_i(x) - \sigma_i(y)\right)\mathrm{d}w(t), \tag{32}$$

where the weak infinitesimal operator $\mathscr{L}$ is given by

$$\begin{aligned} &\mathscr{L}V(t) \\ &= \sum_{i=1}^{n}[\lambda_i s_i(t)((f_i(x) - g_i(y) + F_i(x)\theta \\ &\qquad -G_i(y)\psi + \Delta f_i(x) - \Delta g_i(y) - u_i(t)))] \\ &\quad + \sum_{j=1}^{n} \lambda_i^2\left(\sigma_i(x(t)) - \sigma_i(y(t))\right)^{\mathrm{T}}\left(\sigma_i(x(t)) - \sigma_i(y(t))\right) \\ &\qquad + \left(\widehat{\theta} - \theta\right)^{\mathrm{T}}\dot{\widehat{\theta}} + \left(\widehat{\psi} - \psi\right)^{\mathrm{T}}\dot{\widehat{\psi}} \\ &\le \sum_{i=1}^{n}\Bigg[\lambda_i s_i(t) F_i(x)\left(\theta - \widehat{\theta}\right) - \lambda_i s_i(t) G_i(y)\left(\psi - \widehat{\psi}\right) \\ &\qquad - \frac{1}{2}k_i\lambda_i s_i(t)^2 - \lambda_i s_i(t)\sum_{j=1}^{n}\frac{\lambda_j^2}{\lambda_i^3}k_{ji}s_i(t) \\ &\qquad + \lambda_i s_i(t)\,\eta\left(\left\|\widehat{\theta}\right\|^2 + \overline{\theta}^2 + \left\|\widehat{\psi}\right\|^2 + \overline{\psi}^2\right) \\ &\qquad \times\left(\frac{s_i(t)}{\lambda_i\|s(t)\|^2}\right) + \sum_{j=1}^{n}\lambda_i^2 k_{ij}e_j^2(t)\Bigg] \\ &\quad + \left(\widehat{\theta} - \theta\right)^{\mathrm{T}}\dot{\widehat{\theta}} + \left(\widehat{\psi} - \psi\right)^{\mathrm{T}}\dot{\widehat{\psi}}. \end{aligned} \tag{33}$$

Using the facts $\sum_{i=1}^{n}\lambda_i s_i(t)F_i(x)\theta = \theta^{\mathrm{T}}F^{\mathrm{T}}(x)\gamma(t)$, $\sum_{i=1}^{n}\lambda_i s_i(t)G_i(x)\psi = \psi^{\mathrm{T}}G^{\mathrm{T}}(x)\gamma(t)$ and the updating laws in (30), one has

$$\begin{aligned} &\mathscr{L}V(t) \\ &\le -\sum_{i=1}^{n}\frac{1}{2}k_i\lambda_i s_i^2 + \eta\left(\left\|\widehat{\theta}\right\|^2 + \overline{\theta}^2 + \left\|\widehat{\psi}\right\|^2 + \overline{\psi}^2\right) \\ &\le -\eta\left[\frac{1}{2}s^{\mathrm{T}}(t)\,s(t) - \left(\left\|\widehat{\theta}\right\|^2 + \overline{\theta}^2\right) - \left(\left\|\widehat{\psi}\right\|^2 + \overline{\psi}^2\right)\right]. \end{aligned} \tag{34}$$

Since $\left\|\widehat{\theta} - \theta\right\|^2 \le 2(\left\|\widehat{\theta}\right\|^2 + \|\theta\|^2) \le 2(\left\|\widehat{\theta}\right\|^2 + \overline{\theta}^2)$ and similarly we have $\left\|\widehat{\psi} - \psi\right\|^2 \le 2(\left\|\widehat{\psi}\right\|^2 + \overline{\psi}^2)$, so we can conclude that $-(\left\|\widehat{\theta}\right\|^2 + \overline{\theta}^2) \le -1/2\left\|\widehat{\theta} - \theta\right\|^2$ and $-(\left\|\widehat{\theta}\right\|^2 + \overline{\theta}^2) \le -1/2\left\|\widehat{\theta} - \theta\right\|^2$. So it is easy to get

$$\begin{aligned} \mathscr{L}V(t) \le -\eta\Bigg[&\frac{1}{2}s^{\mathrm{T}}(t)\,s(t) + \frac{1}{2}\left\|\widehat{\theta} - \theta\right\|^2 \\ &+\frac{1}{2}\left\|\widehat{\theta} - \theta\right\|^2\Bigg] \le -\eta V(t). \end{aligned} \tag{35}$$

Then from Lemma 8, we can obtain: $\lim_{t\to\infty} s(t) = 0$ almost surely. This completes the proof. □

Remark 17. From the proof, it is easy to see that the positive numbers in (A4) also could be unknown; we just modify the estimate parameters in the controller. To simplify, we discussed the problem under condition (A4).

Remark 18. The controller in (30) contains a discontinuous term $\eta(\left\|\widehat{\theta}\right\|^2 + \overline{\theta}^2 + \left\|\widehat{\psi}\right\|^2 + \overline{\psi}^2)(s_i/\lambda_i\|s\|^2)$ and thus chattering is unavoidable. In order to eliminate this chattering, this control term can be modified as $\eta(\left\|\widehat{\theta}\right\|^2 + \overline{\theta}^2 + \left\|\widehat{\psi}\right\|^2 + \overline{\psi}^2)(s_i/(\lambda_i\|s\|^2 + \epsilon))$, where ϵ is a sufficiently small positive constant.

Remark 19. With the similar method in Theorem 13 and Theorem 14, we can also discuss the problem of the identification between the unknown parameters θ, ψ in (7) and $\widehat{\theta}$, $\widehat{\psi}$ in (30).

4. Numerical Simulations

In this section, we will show that the proposed adaptive controllers are efficient and that the theoretical results are correct. Numerical simulations are performed using MATLAB software. The well-known stochastic chaos between Lorenz system and Chen systems is synchronized using the adaptive controller (15) in the first example. The synchronization between Chen system and Lu system is shown in the second example using the adaptive controller (29). The Lorenz,

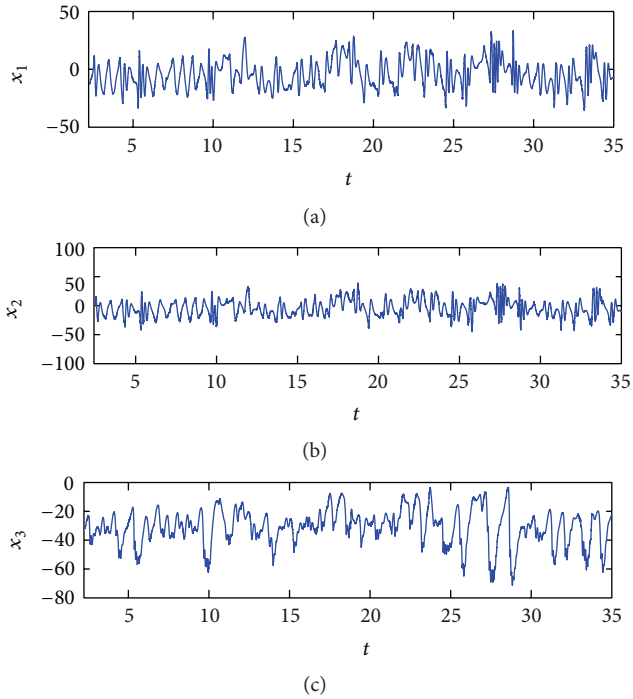

Figure 1: The trajectories of the error system without control input in Example 1.

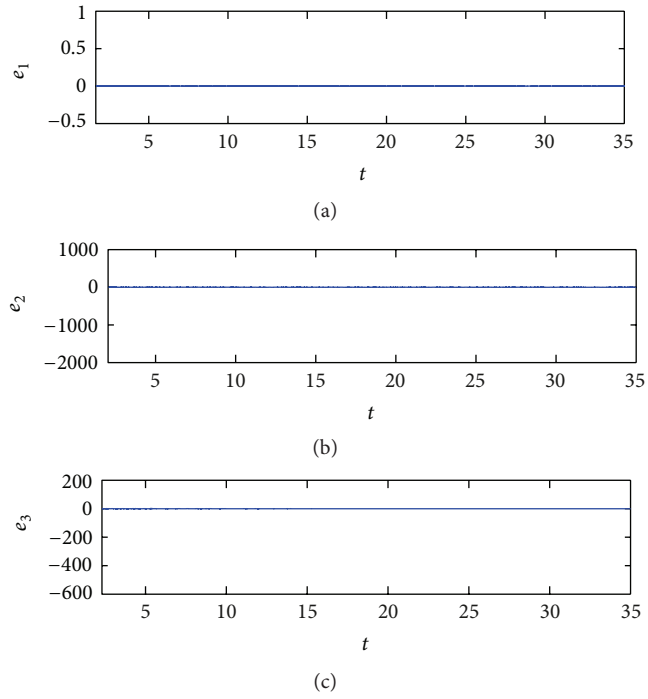

Figure 2: Time responses of error system under control input in Example 1.

Chen, and Lu systems are given by the following differential equations, respectively,

$$\begin{cases} \dot{x}_1 = 10\left(x_2 - x_1\right) \\ \dot{x}_2 = 28x_1 - x_2 - x_1x_3 \\ \dot{x}_3 = x_1x_2 - \dfrac{8x_3}{3} \end{cases}$$

$$\begin{cases} \dot{x}_1 = 35\left(x_2 - x_1\right) \\ \dot{x}_2 = 28x_2 - 7x_1 - x_1x_3 \\ \dot{x}_3 = x_1x_2 - 3x_3 \end{cases} \tag{36}$$

$$\begin{cases} \dot{x}_1 = 36\left(x_2 - x_1\right) \\ \dot{x}_2 = -20x_2 - x_1x_3 \\ \dot{x}_3 = x_1x_2 - 3x_3. \end{cases}$$

In all the cases, the uncertainties $\Delta f(x)$, $\Delta g(y)$, and $\sigma(x)$ and the noise intensity function are given as follows, respectively,

$$\begin{cases} \Delta f_1(x) = 0.5\sin\left(\pi x_1\right), \\ \Delta f_2(x) = 0.5\sin\left(2\pi x_2\right), \\ \Delta f_3(x) = 0.5\sin\left(3\pi x_3\right), \end{cases}$$

$$\begin{cases} \Delta g_1(y) = -5\sin\left(\pi y_1\right), \\ \Delta g_2(y) = -4\sin\left(2\pi y_2\right), \\ \Delta g_3(y) = -\sin\left(3\pi y_3\right), \end{cases}$$

$$\begin{cases} \sigma_1(x) = x_2^2 + 0.3x_3, \\ \sigma_2(x) = x_1^3 + 0.1x_3, \\ \sigma_3(x) = 0.2x_1 + x_1x_2. \end{cases} \tag{37}$$

In all simulations, we choose the initial value of the adaptive parameters vectors $\widehat{\theta}_0 = [5,5,5]^{\mathrm{T}}$, $\widehat{\psi}_0 = [3,3,3]^{\mathrm{T}}$, $\widehat{\alpha}_{i0} = \widehat{\beta}_{i0} = \widehat{k}_{ij0} = 2$, the constants $k_1 = 10$ and $\epsilon = 0.01$.

4.1. Example 1: Synchronization between Lorenz Systems and Chen Systems. The nonlinear part of master and slave systems can be rewritten in the form of (2) and (4) as follows:

$$f(x) = \begin{pmatrix} 0 \\ -x_1x_3 - x_2 \\ x_1x_2 \end{pmatrix}, \qquad F(x) = \begin{pmatrix} x_2 - x_1 & 0 & 0 \\ 0 & x_1 & 0 \\ 0 & 0 & -x_3 \end{pmatrix},$$

$$g(y) = \begin{pmatrix} 0 \\ -y_1y_3 \\ y_1y_2 \end{pmatrix}, \qquad G(y) = \begin{pmatrix} y_2 - y_1 & 0 & 0 \\ -y_1 & y_1 + y_2 & 0 \\ 0 & 0 & -y_3 \end{pmatrix}. \tag{38}$$

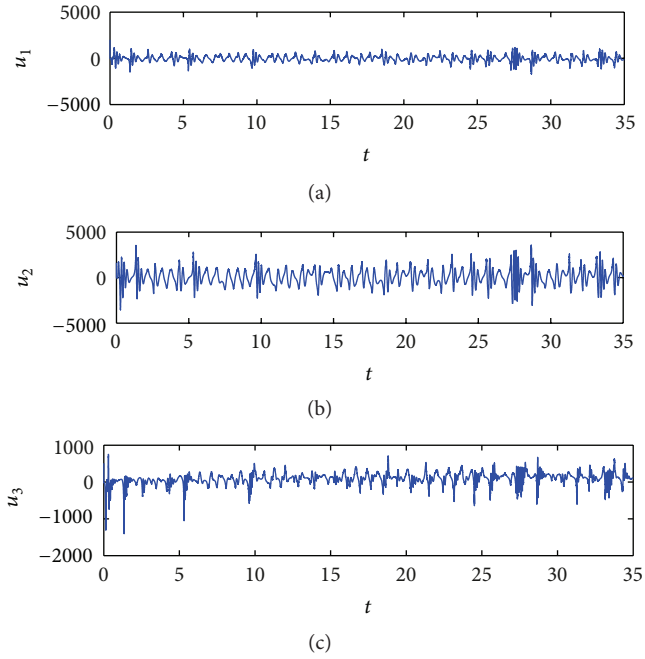

Figure 3: Time response of the control input in Example 1.

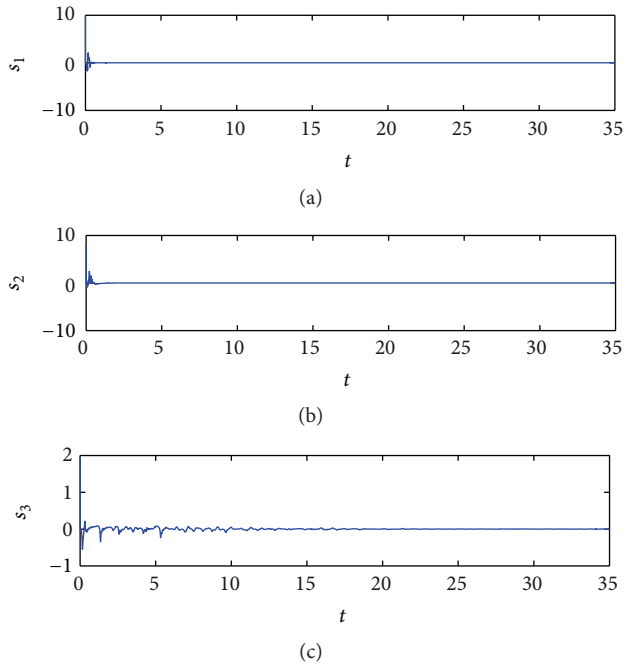

Figure 4: Time responses of the sliding mode surface $s(t)$ in Example 1.

Consequently, three sliding surfaces are chosen as

$$\begin{cases} s_1 = 10e_1(t), \\ s_2 = 8e_2(t), \\ s_3 = 2e_3(t). \end{cases} \tag{39}$$

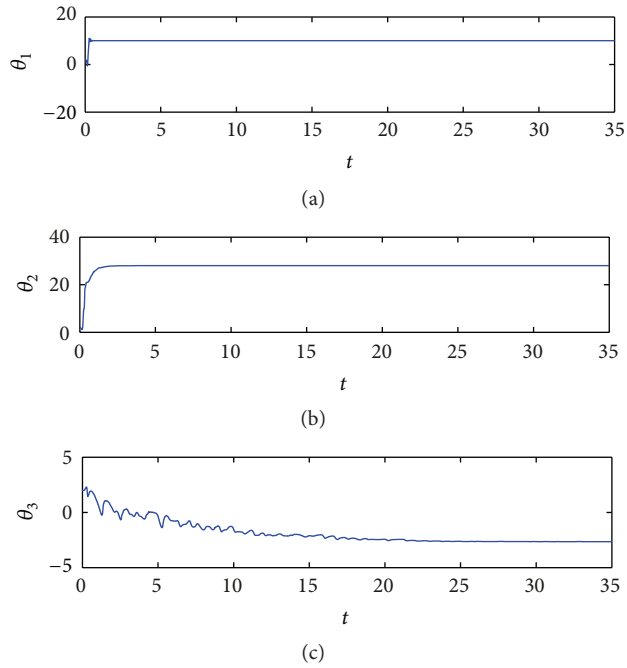

Figure 5: The trajectories of the adaptive laws of the parameter $\widehat{\theta}$ in Example 1.

The stochastic Lorenz and Chen systems are started with the initial conditions as follows: $x_0 = [1, 1.5, 2]^{\mathrm{T}}$ and $y_0 = [2, 2.5, 3]^{\mathrm{T}}$. The synchronization of the Lorenz and Chen systems without control input is shown in Figure 1 and the error simulation under the control input is shown in Figure 2. As one can see the synchronization errors converge to zero in mean squares. The control input is shown in Figure 3 and the sliding mode surface is shown in Figure 4. The updated vector parameters of $\widehat{\alpha}$, $\widehat{\beta}$, $\widehat{\theta}$, and $\widehat{\psi}$ are shown in Figures 5, 6, 7, and 8 and $\widehat{k}_{ij}$ are depicted in Figures 9, 10, and 11, respectively. Obviously, all of updated parameters approach some constants.

4.2. Example 2: Synchronization between Chen Systems and Lu Systems. The nonlinear part of master and slave systems can be rewritten in the form of (2) and (4) as follows:

$$f(x) = \begin{pmatrix} 0 \\ -x_1x_3 \\ x_1x_2 \end{pmatrix}, \qquad F(x) = \begin{pmatrix} x_2 - x_1 & 0 & 0 \\ -x_1 & x_1 + x_2 & 0 \\ 0 & 0 & -x_3 \end{pmatrix},$$
$$g(y) = \begin{pmatrix} 0 \\ -y_1y_3 \\ y_1y_2 \end{pmatrix}, \qquad G(y) = \begin{pmatrix} y_2 - y_1 & 0 & 0 \\ 0 & -y_2 & 0 \\ 0 & 0 & -y_3 \end{pmatrix}. \tag{40}$$

Consequently, the same sliding surfaces are chosen as in Example 1. To simplify, we choose the noise intensity function $\sigma(x) = [0.4x_2 + 0.3x_3, 0.2x_1 + 0.1x_3, 0.3x_1 + 0.2x_2]^{\mathrm{T}}$, so it is easy to see $\alpha_i = \beta_i = 0.5$ and $k_{11} = k_{22} = k_{33} = 0$, $k_{12} = 0.4$, $k_{13} = 0.3$, $k_{21} = 0.2$, $k_{23} = 0.1$, $k_{31} = 0.3$, and $k_{32} = 0.2$. The stochastic Chen and Lu systems are

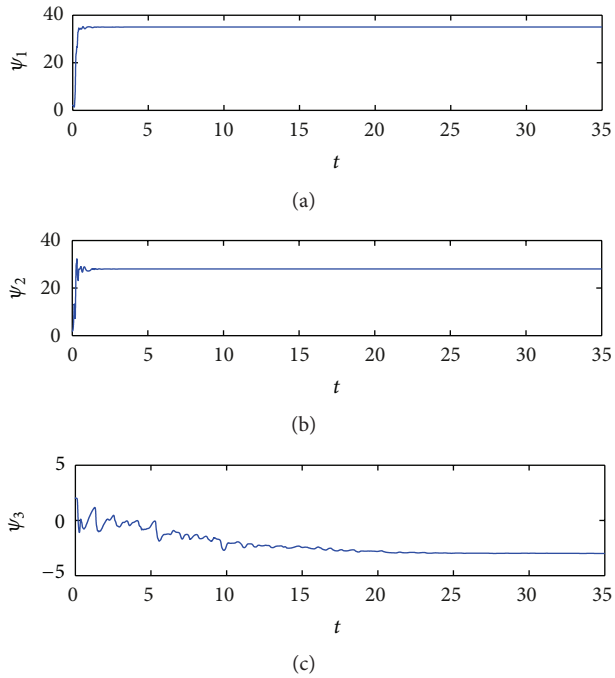

FIGURE 6: Time responses of the adaptive update laws $\widehat{\psi}$ in Example 1.

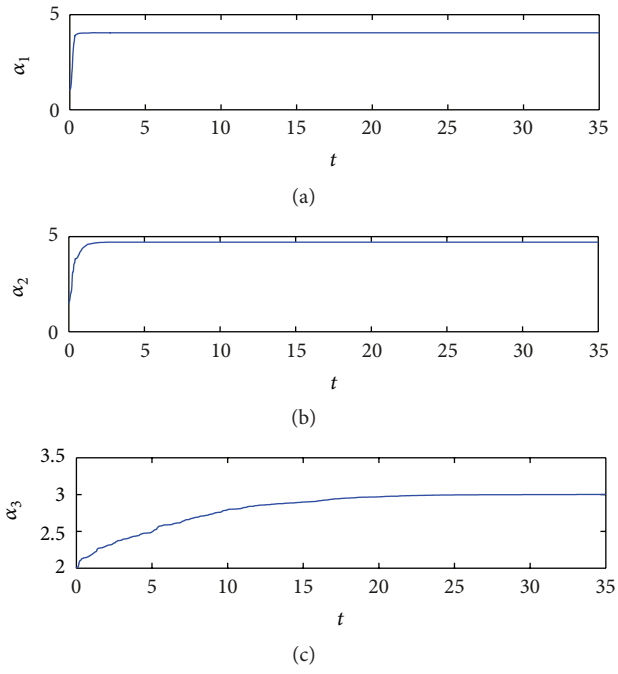

FIGURE 7: The trajectories of the adaptive laws α in Example 1.

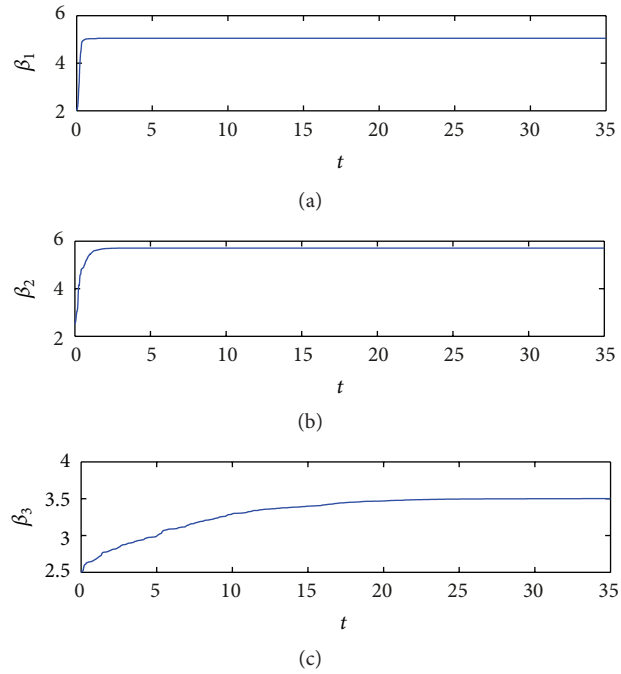

FIGURE 8: The trajectories of the adaptive laws β in Example 1.

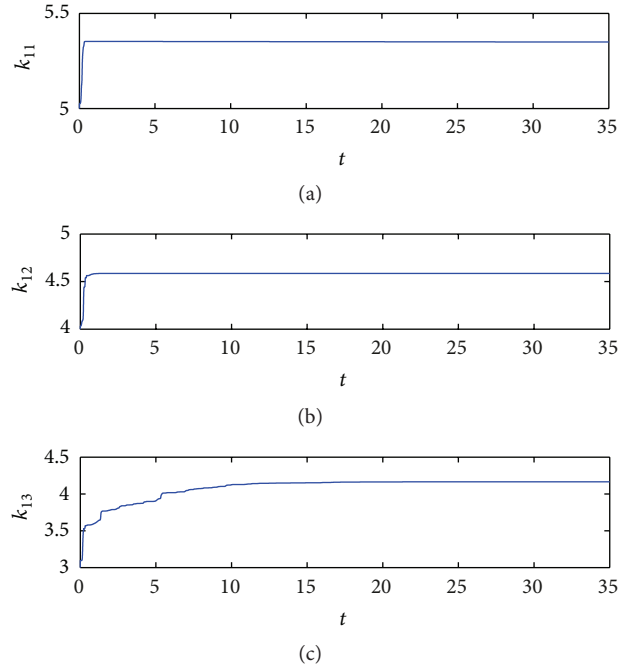

FIGURE 9: The trajectories of the adaptive laws k_{11}, k_{12}, and k_{13} in Example 1.

started with the initial conditions as follows: $x_0 = [8, 4, 7]^{\mathrm{T}}$ and $y_0 = [-10, -4, 2]^{\mathrm{T}}$. The synchronization of the Chen and Lu systems without control input is shown in Figure 12 and the error simulation under the control input is shown in Figure 13. As one can see the synchronization errors converge to zero almost surely. The control input is shown in Figure 14 and the sliding mode surface is shown in Figure 15. The updated vector parameters of $\widehat{\theta}$ and $\widehat{\psi}$ are depicted in Figures 16 and 17, respectively. Obviously, all of updated parameters approach some constants.

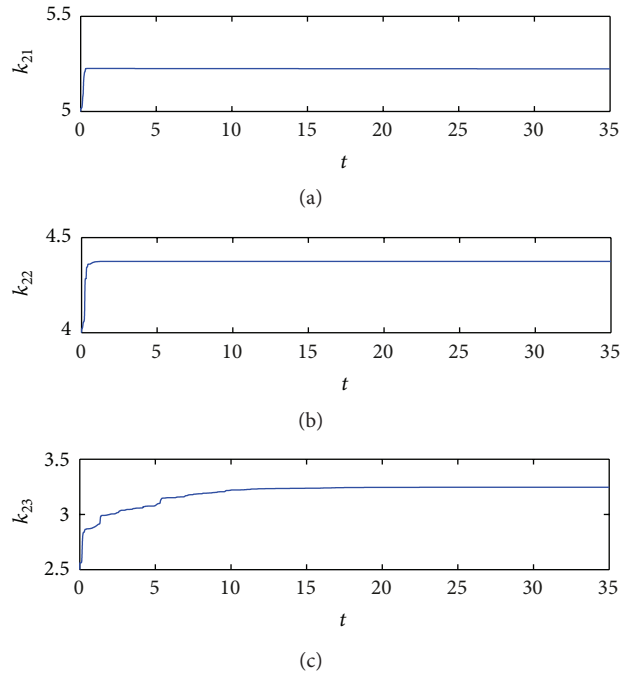

Figure 10: The trajectories of the adaptive laws k_{21}, k_{22}, and k_{23} in Example 1.

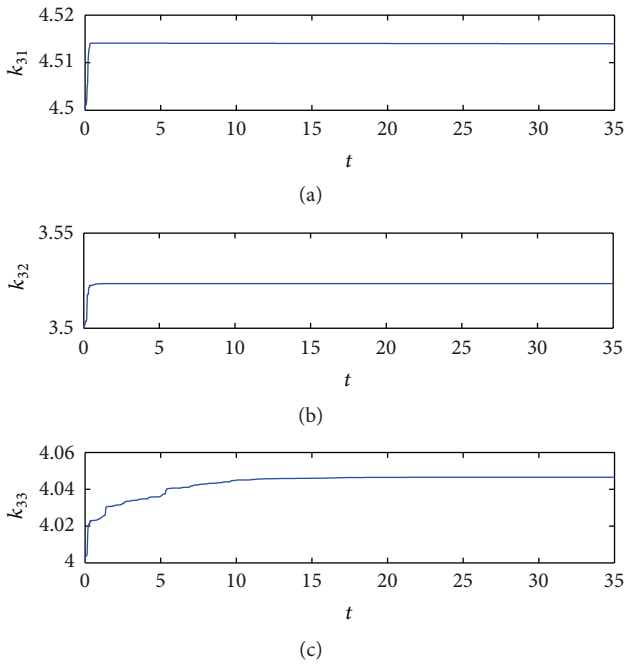

Figure 11: The trajectories of the adaptive laws k_{31}, k_{32}, and k_{33} in Example 1.

Remark 20. As it is observed in Figures 5, 6, 16, and 17, the limits of unknown parameter vectors $\widehat{\theta}$ and $\widehat{\psi}$ are not equal to the vectors θ and ψ in (36). This point is consistent with the results of Theorem 13, Theorem 14, and Remark 19.

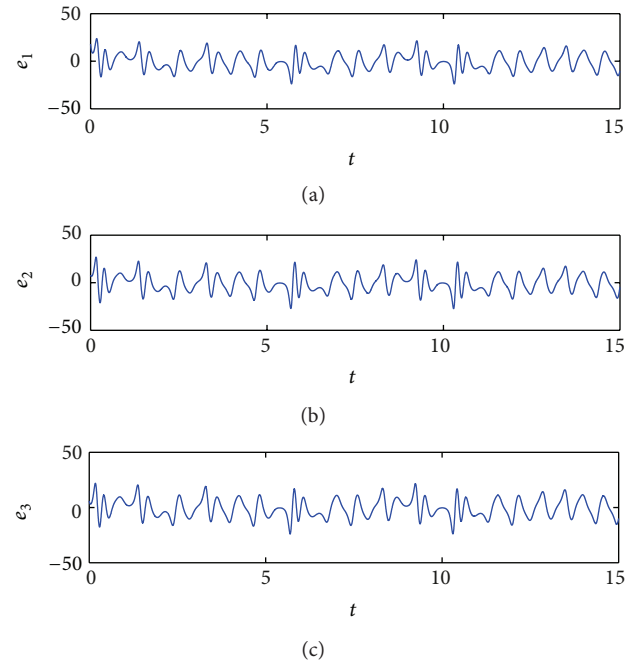

Figure 12: The trajectories of the error system without control input in Example 2.

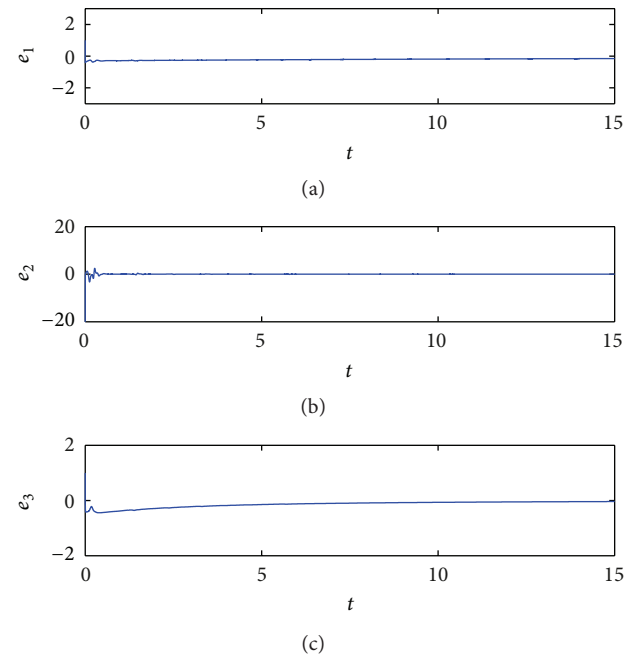

Figure 13: Time responses of error system under control input in Example 2.

5. Conclusion

In this paper, adaptive sliding mode controllers are designed to realize the asymptotical synchronization in mean squares and the almost surely synchronization for two different stochastic chaotic systems with unknown parameters and

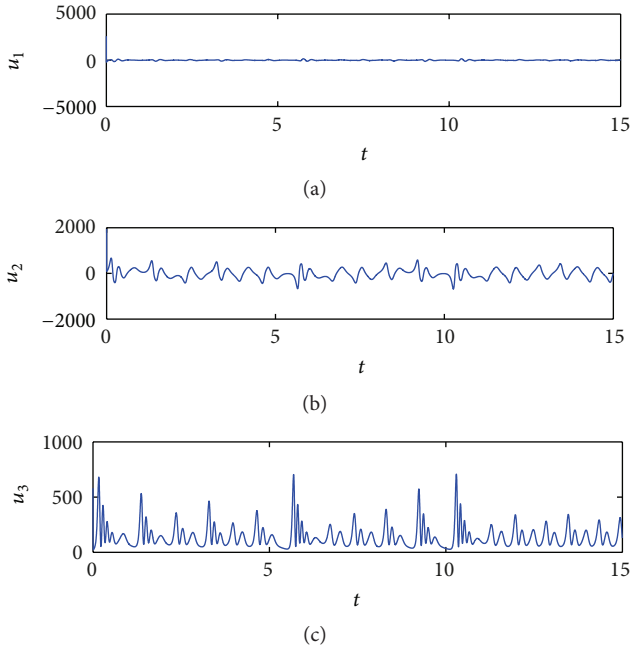

Figure 14: Time responses of the control input in Example 2.

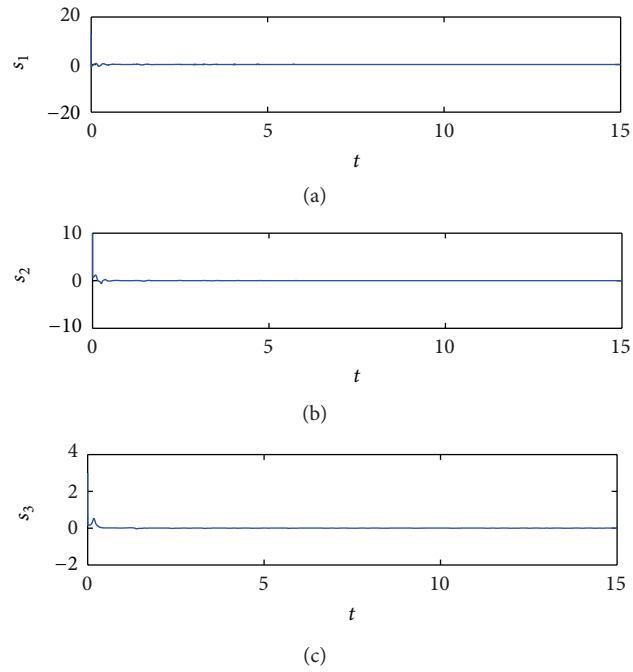

Figure 15: Time responses of the sliding mode surface $s(t)$ in Example 2.

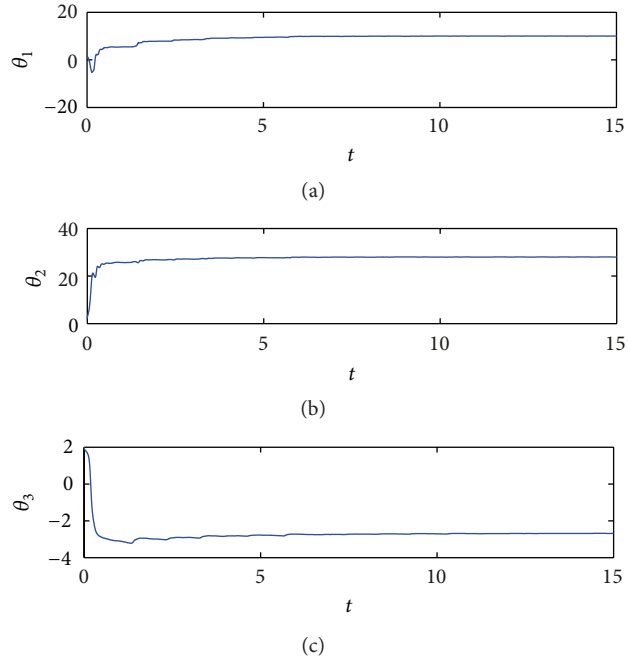

Figure 16: The trajectories of the adaptive laws of the parameter $\widehat{\theta}$ in Example 2.

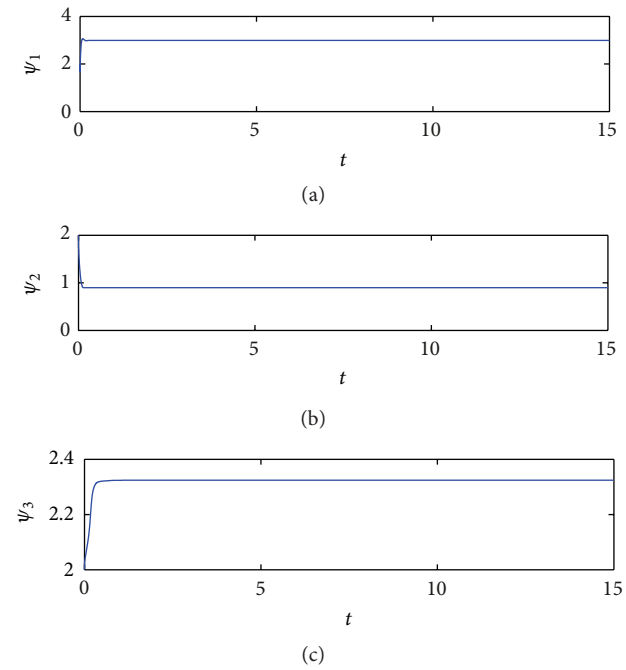

Figure 17: The trajectories of the adaptive laws of the parameter $\widehat{\psi}$ in Example 2.

uncertain terms, respectively. The designed controllers' robustness and efficiency are proved between two different pairs of stochastic chaos systems (Lorenz-Chen and Chen-Lu) with unknown parameters and uncertainties.

Acknowledgments

This work was supported by the National Natural Science Foundation of China (11071060), the Special Funds of the National Natural Science Foundation of China (11226143), the Natural Science Foundation of Hunan Province (13JJ4111),

the Scientific Research Fund of Hunan Provincial Education Department (11B029), and the Science Foundation of Hunan First Normal University (XYS10N11).

References

[1] L. M. Pecora and T. L. Carroll, "Synchronization in chaotic systems," *Physical Review Letters*, vol. 64, no. 8, pp. 821–824, 1990.

[2] T. L. Carroll and L. M. Pecora, "Synchronizing chaotic circuits," *IEEE Transactions on Circuits and Systems*, vol. 38, no. 4, pp. 453–456, 1991.

[3] L. Kocarev and U. Parlitz, "General approach for chaotic synchronization with applications to communication," *Physical Review Letters*, vol. 74, no. 25, pp. 5028–5031, 1995.

[4] Y. Yu and S. Zhang, "Adaptive backstepping synchronization of uncertain chaotic system," *Chaos, Solitons and Fractals*, vol. 21, no. 3, pp. 643–649, 2004.

[5] H. Salarieh and M. Shahrokhi, "Adaptive synchronization of two different chaotic systems with time varying unknown parameters," *Chaos, Solitons and Fractals*, vol. 37, no. 1, pp. 125–136, 2008.

[6] K. Konishi, M. Hirai, and H. Kokame, "Sliding mode control for a class of chaotic systems," *Physics Letters, Section A*, vol. 245, no. 6, pp. 511–517, 1998.

[7] J. M. Nazzal and A. N. Natsheh, "Chaos control using sliding-mode theory," *Chaos, Solitons and Fractals*, vol. 33, no. 2, pp. 695–702, 2007.

[8] J. Alvarez-Gallegos, "Nonlinear regulation of a Lorenz system by feedback linearization techniques," *Dynamics and Control*, vol. 4, no. 3, pp. 277–298, 1994.

[9] A. Alasty and H. Salarieh, "Nonlinear feedback control of chaotic pendulum in presence of saturation effect," *Chaos, Solitons and Fractals*, vol. 31, no. 2, pp. 292–304, 2007.

[10] A. Alasty and H. Salarieh, "Controlling the chaos using fuzzy estimation of OGY and Pyragas controllers," *Chaos, Solitons and Fractals*, vol. 26, no. 2, pp. 379–392, 2005.

[11] N. Luo and M. de la Sen, "State feedback sliding mode control of a class of uncertain time delay systems," *IEE Proceedings D*, vol. 140, no. 4, pp. 261–274, 1993.

[12] N. Luo, M. de la Sen, and J. Rodellar, "Robust stabilization of a class of uncertain time delay systems in sliding mode," *International Journal of Robust and Nonlinear Control*, vol. 7, no. 1, pp. 59–74, 1997.

[13] M. Pourmahmood, S. Khanmohammadi, and G. Alizadeh, "Synchronization of two different uncertain chaotic systems with unknown parameters using a robust adaptive sliding mode controller," *Communications in Nonlinear Science and Numerical Simulation*, vol. 16, no. 7, pp. 2853–2868, 2011.

[14] M. P. Aghababa, S. Khanmohammadi, and G. Alizadeh, "Finite-time synchronization of two different chaotic systems with unknown parameters via sliding mode technique," *Applied Mathematical Modelling*, vol. 35, no. 6, pp. 3080–3091, 2011.

[15] L. Billings, E. M. Bollt, and I. B. Schwartz, "Phase-space transport of stochastic chaos in population dynamics of virus spread," *Physical Review Letters*, vol. 88, no. 23, pp. 2341011–2341014, 2002.

[16] W. J. Freeman, "A proposed name for aperiodic brain activity: stochastic chaos," *Neural Networks*, vol. 13, no. 1, pp. 11–13, 2000.

[17] X. Z. Mou, W. N. Zhou, L. Pan, and Q. Zhu, "Synchronization control of stochastically coupled neural networks with mixed time-delays," in *Proceedings of the Chinese Control and Decision Conference (CCDC '09)*, pp. 3156–3161, June 2009.

[18] Y. Tang, R. Qiu, J.-A. Fang, Q. Miao, and M. Xia, "Adaptive lag synchronization in unknown stochastic chaotic neural networks with discrete and distributed time-varying delays," *Physics Letters A*, vol. 372, no. 24, pp. 4425–4433, 2008.

[19] X. S. Yang, Q. X. Zhu, and C. X. Huang, "Lag stochastic synchronization of chaotic mixed time-delayed neural networks with uncertain parameters or perturbations," *Neurocomputing*, vol. 74, no. 10, pp. 1617–1625, 2011.

[20] Z. Y. Wang and L. H. Huang, "Robust decentralized adaptive control for stochastic delayed Hopfield neural networks," *Neurocomputing*, vol. 74, pp. 3695–3699, 2011.

[21] C. X. Huang, P. Chen, Y. He, L. Huang, and W. Tan, "Almost sure exponential stability of delayed Hopfield neural networks," *Applied Mathematics Letters*, vol. 21, no. 7, pp. 701–705, 2008.

[22] C. X. Huang and J. D. Cao, "Almost sure exponential stability of stochastic cellular neural networks with unbounded distributed delays," *Neurocomputing*, vol. 72, no. 13–15, pp. 3352–3356, 2009.

[23] Y. Z. Sun and J. Ruan, "Synchronization between two different chaotic systems with noise perturbation," *Chinese Physics Letters*, vol. 19, no. 7, Article ID 070513, 2010.

[24] H. Salarieh and A. Alasty, "Adaptive chaos synchronization in Chua's systems with noisy parameters," *Mathematics and Computers in Simulation*, vol. 79, no. 3, pp. 233–241, 2008.

[25] H. Salarieh and A. Alasty, "Control of stochastic chaos using sliding mode method," *Journal of Computational and Applied Mathematics*, vol. 225, no. 1, pp. 135–145, 2009.

[26] X. Mao, *Stochastic Differential Equation and Application*, Horwood, Chichester, UK, 1997.

[27] R. Z. Khasminskii, *Stochastic Stability of Differential Equations*, vol. 7 of *Monographs and Textbooks on Mechanics of Solids and Fluids: Mechanics and Analysis*, Sijthoff & Noordhoff, Amsterdam, The Netherlands, 1980.

[28] X. Mao, "A note on the LaSalle-type theorems for stochastic differential delay equations," *Journal of Mathematical Analysis and Applications*, vol. 268, no. 1, pp. 125–142, 2002.

[29] Y. Shen, Q. Luo, and X. Mao, "The improved LaSalle-type theorems for stochastic functional differential equations," *Journal of Mathematical Analysis and Applications*, vol. 318, no. 1, pp. 134–154, 2006.

[30] M. Chen and W. H. Chen, "Robust adaptive neural network synchronization controller design for a class of time delay uncertain chaotic systems," *Chaos, Solitons and Fractals*, vol. 41, no. 5, pp. 2716–2724, 2009.

Hindawi Publishing Corporation
Abstract and Applied Analysis
Volume 2013, Article ID 620286, 10 pages
http://dx.doi.org/10.1155/2013/620286

Research Article

Stability Analysis and Control of a New Smooth Chua's System

Guopeng Zhou,[1,2] Jinhua Huang,[3] Xiaoxin Liao,[4] and Shijie Cheng[1]

[1] *College of Electrical and Electronic Engineering, Huazhong University of Science and Technology, Wuhan 430074, China*
[2] *College of Electronic and Information Engineering, Hubei University of Science and Technology, Xianning 437100, China*
[3] *Department of Electric and Electronic Engineering, Wuhan Institute of Shipbuilding Technology, Wuhan 430050, China*
[4] *Department of Control and Engineering, Huazhong University of Science and Technology, Wuhan 430074, China*

Correspondence should be addressed to Jinhua Huang; angela_icec@yahoo.com.cn

Received 3 December 2012; Accepted 7 April 2013

Academic Editor: René Yamapi

This paper is concerned with the stability analysis and control of a new smooth Chua's system. Firstly, the chaotic characteristic of the system is confirmed with the aid of the Lyapunov exponents. Secondly, it is proved that the system has globally exponential attractive set and positive invariant set. For the three unstable equilibrium points of the system, a linear controller is designed to globally exponentially stabilize the equilibrium points. Then, a linear controller and an adaptive controller are, respectively, proposed so that two similar types of smooth Chua's systems are globally synchronized, and the estimation errors of the uncertain parameters converge to zero as t tends to infinity. Finally, the numerical simulations are also presented.

1. Introduction

It is well known that Chua's system is the first analog circuit to realize chaos in experiments. The original Chua's system is described by the following ordinary differential equations [1]:

$$\begin{aligned} \dot{x} &= p\left(y - x - g\left(x\right)\right), \\ \dot{y} &= x - y + z, \\ \dot{z} &= -qy, \end{aligned} \tag{1}$$

where $x, y, z \in R$ are state variables and $g(x) = G_b x + (1/2)(G_a - G_b)(|x - E| - |x - E|)$, $p > 0$, $q > 0$, and G_a, G_b are constants. Due to the form of a simple circuit, there are a large literature on the dynamical behavior of Chua's system [2–8]. By changing the parameters or the corresponding functions of Chua's system, the chaotic phenomenon is very rich, and it is more convenient to study the chaotic mechanism and characteristics [6–8].

For the chaotic systems, Lagrange stability, stability of equilibrium points and, synchronization are three important problems which attracted more and more attention (refer to [9–16] and the reference therein). In [11–13], the authors studied the Lagrange stability by applying the attractive set and positive invariant set of the chaotic systems. Moreover, the researchers examined the stabilization of the unstable equilibrium points and the synchronization control for the chaotic systems with linear controllers [7, 14]. Recently, adaptive controllers are used in synchronous control of chaotic systems when the parameters of the systems are uncertain [15–17].

Motivated by the previous results, the main purpose of this paper is to construct a new smooth Chua's system and

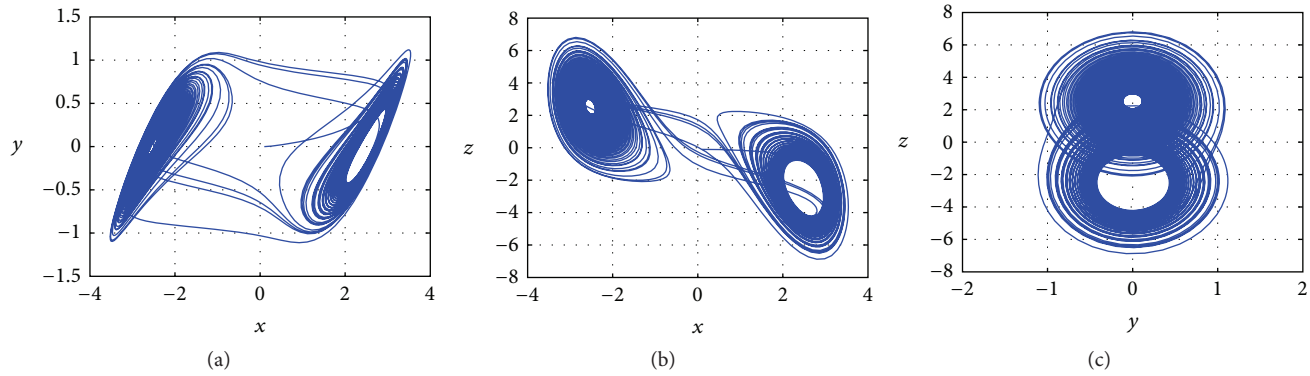

Figure 1: The phase portraits of Chua's system (2).

investigate the stability and control problems. More precisely, we will consider the following smooth Chua's system:

$$\begin{aligned} \dot{x} &= p\left(x + y - x\ln\sqrt{1+x^2}\right), \\ \dot{y} &= x - y + z, \\ \dot{z} &= -qy, \end{aligned} \tag{2}$$

where $x, y, z \in R$ are state variables and $p > 0$, $q > 0$ are constants.

We will show that the chaotic characteristics are depended on the parameters p and q and the initial state values of the system (2). All equilibrium points of system (2) are examined to be unstable when $p = 11$ and $q = 14.87$ (see in Section 3). By computing with MATLAB, the maximum Lyapunov exponent of the system (2) is 0.0021, where the embedding dimension m is 3 and the delay time τ is 5. Since the maximum Lyapunov exponent is greater than 0, the Chua's system is chaotic. It will be of great significance if the solution of (2) is ultimately bounded (Lagrange asymptotically stable). The chaotic phase diagrams of such system is obtained by simulation with MATLAB. Figure 1 shows the phase diagrams of the system (2) with $x(0) = -3$, $y(0) = 2$, and $z(0) = 1$, the phase diagrams of Chua's system exhibits chaotic.

The remains of this paper are organized as follows. The existence of globally exponential attractive set and positive invariant set for the system (2) will be discussed in Section 2. The asymptotic stability of the equilibrium points will be studied in Section 3, and the synchronization control for two similar types of the Chua's systems will be discussed in Section 4. In Section 5, we will give the numerical simulations to demonstrate the correctness of our results, and finally we will give the conclusions in Section 6.

2. Existence of Globally Exponential Attractive Set and Positive Invariant Set

The Lagrange stability analysis of the system (2) will be studied in this section. To do so, we first give two definitions [7].

Definition 1. If there exists a radially unbounded, positive definite Lyapunov function $V(X(t))$ and positive numbers $l > 0$, $\alpha > 0$ such that for all $X_0 \in R^3$, when $V(X_0) > l$, the solution of the system (2), $X(t) = (x(t), y(t), z(t))$ along $V(X(t))$ satisfies $|V(X(t)) - l| \le |V(x_0) - l|e^{-\alpha(t-t_0)}$, then system (2) has a globally exponential attractive set $\Omega \triangleq \{X \mid V(X(t)) < l\}$.

Definition 2. Let $\Omega \subseteq R^3$, if $\forall X_0 \in \Omega$ and for all $t \ge t_0$, $X(t, t_0, X_0) \subseteq \Omega$, then Ω is called positive invariant set of the system (2).

It is easy to prove that the globally exponential attractive set is positive invariant. A system with global attractive set is always called Lagrange globally asymptotically stable system or ultimately bounded dissipative system. For the system (2), we will prove the following the Lagrange stability results.

Theorem 3. *The system* (2) *has the following globally exponential attractive and positive invariant set:*

$$\Omega = \begin{cases} |x| \le |x_b| = \min\left\{|x_{b1}|, |x_{b2}|\right\} \\ y^2 + \dfrac{1}{q}z^2 - \epsilon yz \le \dfrac{(5/4\eta)\,x_b^2}{-\tau_1\mu_M\left(G_2^-\right)/\lambda_M\left(G_2^+\right)} \\ |x_{b1}| > \sqrt{e^{((2-(\epsilon/4))^2/(2-\epsilon q-(\epsilon/4)))+(\epsilon/4)+2} - 1} \\ |x_{b2}| = \sup\limits_{\overline{\Omega}} |x|, \\ \overline{\Omega} \triangleq \left\{ x \mid \dfrac{1}{p}x^2 + y^2 + \dfrac{1}{q}z^2 - \epsilon yz \right. \\ \qquad\qquad \left. = \dfrac{x_{b1}^2 \ln\left(1 + x_{b1}^2\right)}{-\mu_M\left(G_1^-\left(x_{b1}\right)\right)/\lambda_M\left(G_1^+\right)} \right\}, \end{cases} \tag{3}$$

where $0 < \epsilon \ll 1$,

$$G_1^+ \triangleq \begin{bmatrix} \frac{1}{p} & 0 & 0 \\ 0 & 1 & -\frac{\epsilon}{2} \\ 0 & -\frac{\epsilon}{2} & \frac{1}{q} \end{bmatrix}, \qquad G_2^+ \triangleq \begin{bmatrix} 1 & -\frac{\epsilon}{2} \\ -\frac{\epsilon}{2} & \frac{1}{q} \end{bmatrix}, \tag{4}$$

are symmetric positive definite matrices, and

$$G_1^- \triangleq \begin{bmatrix} 2\left(1 - \ln\sqrt{1+x_{b1}^2}\right) & 2 & -\frac{\epsilon}{2} \\ 2 & \epsilon q - 2 & \frac{\epsilon}{2} \\ -\frac{\epsilon}{2} & \frac{\epsilon}{2} & -\epsilon \end{bmatrix}, \qquad G_2^- \triangleq \begin{bmatrix} \epsilon q - 2 & \frac{\epsilon}{2} \\ \frac{\epsilon}{2} & -\epsilon \end{bmatrix}, \tag{5}$$

are symmetric negative definite matrices. $\lambda_M(G_1^+)$, $\mu_M(G_1^-)$, $\lambda_M(G_2^+)$, *and* $\mu_M(G_2^-)$ *are the maximum eigenvalues of* G_1^+, G_1^-, G_2^+, *and* G_2^-, *respectively.* ϵ, x_{b1}, *and* x_{b2} *in* (3) *are chosen to guarantee that* G_1^+, G_2^+ *are positive definite and* G_1^-, G_2^- *are negative definite.* τ_1, τ_2, *and* η *are chosen such that* $\tau_1 > 0$, $\tau_2 > 0$, $\eta > 0$, $\tau_1 + \tau_2 = 1$, *and* $\tau_2\mu_M(G_2^-) + \eta \le 0$.

Proof. The proof is divided into three steps.

Step I. The existence of ϵ, x_{b1} such that G_1^+ is positive definite and G_1^- is negative definite.

It is well known that G_1^+ is positive definite if and only if all the order principal minors of G_1^+ are positive [18]. That is,

$$\frac{1}{p} > 0, \qquad \begin{vmatrix} \frac{1}{p} & 0 \\ 0 & 1 \end{vmatrix} > 0,$$
$$\begin{vmatrix} \frac{1}{p} & 0 & 0 \\ 0 & 1 & -\frac{\epsilon}{2} \\ 0 & -\frac{\epsilon}{2} & \frac{1}{q} \end{vmatrix} = \frac{1}{p}\left(\frac{1}{q} - \frac{\epsilon^2}{4}\right) > 0. \tag{6}$$

Let $|\epsilon| < 2/\sqrt{q}$; it is easy to see that G_1^+ is positive definite since $p > 0$, $q > 0$.

Next, let

$$S_{11} = \begin{bmatrix} 2\left(1 - \ln\sqrt{1+x_{b1}^2}\right) & 2 \\ 2 & \epsilon q - 2 \end{bmatrix},$$
$$S_{12} = \begin{bmatrix} -\frac{\epsilon}{2} \\ \frac{\epsilon}{2} \end{bmatrix}, \qquad S_{21} = \left[-\frac{\epsilon}{2}, \frac{\epsilon}{2}\right], \qquad S_{22} = -\epsilon. \tag{7}$$

Then,

$$G_1^- = \begin{bmatrix} S_{11} & S_{12} \\ S_{21} & S_{22} \end{bmatrix}. \tag{8}$$

From Schur theorem [18], G_1^- is negative definite if and only if $S_{11} < 0$, $S_{22} - S_{21}S_{11}^{-1}S_{12} < 0$. Let $|\epsilon|$, x_{b1} satisfy

$$0 < \epsilon \ll 1,$$
$$|x_{b1}| > \sqrt{e^{((2-(\epsilon/4))^2/(2-\epsilon q-(\epsilon/4)))+(\epsilon/4)+2} - 1}. \tag{9}$$

It is easy to verify that G_1^- is negative definite.

Step II. Existence of globally exponential attractive set of x.

Let $\lambda_m(G_1^+)$ and $\lambda_m(G_1^-)$ be the minimum eigenvalues of G_1^+ and G_1^-, respectively. By constructing a radially unbounded Lyapunov function as follows:

$$V = \frac{1}{p}x^2 + y^2 + \frac{1}{q}z^2 - \epsilon yz = \begin{bmatrix} x \\ y \\ z \end{bmatrix}^T G_1^+ \begin{bmatrix} x \\ y \\ z \end{bmatrix}, \tag{10}$$

then, one can obtain that

$$\lambda_m(G_1^+)\left(x^2 + y^2 + z^2\right) \le V \le \lambda_M(G_1^+)\left(x^2 + y^2 + z^2\right). \tag{11}$$

The time derivative of V along the system (2) is given by

$$\begin{aligned} \left.\frac{dV}{dt}\right|_{(2)} &= \frac{2}{p}x\dot{x} + 2y\dot{y} + \frac{2}{q}z\dot{z} - \epsilon\dot{y}z - \epsilon y\dot{z} \\ &= \frac{2}{p}xp\left(x + y - x\ln\sqrt{1+x^2}\right) + 2y(x - y + z) \\ &\quad + \frac{2}{q}(-qy) - \epsilon(x - y + z)z - \epsilon y(-qy) \\ &= \begin{bmatrix} x \\ y \\ z \end{bmatrix}^T \begin{bmatrix} 2\left(1 - \ln\sqrt{1+x^2}\right) & 2 & -\frac{\epsilon}{2} \\ 2 & \epsilon q - 2 & \frac{\epsilon}{2} \\ -\frac{\epsilon}{2} & \frac{\epsilon}{2} & -\epsilon \end{bmatrix} \begin{bmatrix} x \\ y \\ z \end{bmatrix} \\ &= \begin{bmatrix} x \\ y \\ z \end{bmatrix}^T G_1^- \begin{bmatrix} x \\ y \\ z \end{bmatrix} - 2\left(\ln\sqrt{1+x^2} - \ln\sqrt{1+x_{b1}^2}\right)x^2. \end{aligned} \tag{12}$$

If $|x| > |x_{b1}|$, one has

$$\left.\frac{dV}{dt}\right|_{(2)} \le \begin{bmatrix} x \\ y \\ z \end{bmatrix}^T G_1^- \begin{bmatrix} x \\ y \\ z \end{bmatrix} \le \frac{\mu_M(G_1^-)}{\lambda_M(G_1^+)}V. \tag{13}$$

Then, the following inequality holds

$$V(X(t, t_0, X_0)) \le V(X_0)\, e^{(\mu_M(G_1^-)/\lambda_M(G_1^+))(t-t_0)}. \tag{14}$$

Thus, the trajectory of the system (2) will exponentially decay into the area $U = \{x \mid |x| \le |x_{b1}|\}$ if $|x| > |x_{b1}|$.

When the trajectory of the system (2) is in the area U, it holds that

$$\begin{aligned}\left.\frac{dV}{dt}\right|_{(2)} &= \begin{bmatrix} x \\ y \\ z \end{bmatrix}^T G_1^- \begin{bmatrix} x \\ y \\ z \end{bmatrix} + 2\left(\ln\sqrt{1+x_{b1}^2} - \ln\sqrt{1+x^2}\right)x^2 \\ &\le \frac{\mu_M(G_1^-)}{\lambda_M(G_1^+)}V + 2\left(\ln\sqrt{1+x_{b1}^2} - \ln\sqrt{1+x^2}\right)x^2 \\ &\le \frac{\mu_M(G_1^-)}{\lambda_M(G_1^+)}V + x_{b1}^2\ln\left(1+x_{b1}^2\right) \\ &= \frac{\mu_M(G_1^-)}{\lambda_M(G_1^+)}\left(\frac{V - x_{b1}^2\ln\left(1+x_{b1}^2\right)}{-\mu_M(G_1^-)/\lambda_M(G_1^+)}\right).\end{aligned} \tag{15}$$

Let $V_l \triangleq (x_{b1}^2\ln(1+x_{b1}^2))/(-\mu_M(G_1^-)/\lambda_M(G_1^+))$. If $V(X_0) > V_l$ and $V(X(t,t_0,X_0)) > V_l$, it holds that

$$V\left(X\left(t,t_0,X_0\right)\right) - V_l \le \left(V\left(X_0\right) - V_l\right)e^{(\mu_M(G_1^-)/\lambda_M(G_1^+))(t-t_0)}. \tag{16}$$

Let $\overline{\Omega} \triangleq \{X \mid V(X) = V_l\}$, $|x_{b2}| \triangleq \sup_{x\in\overline{\Omega}}|x|$. Then, $V(X(t,t_0,X_0)) - V_l$ exponentially decays when $|x| \ge |x_b| \triangleq \min\{|x_{b1}|, |x_{b2}|\}$. Thus, $\Omega_x \triangleq \{x \mid |x| \le |x_b|\}$ is the globally exponential attractive set of x.

Step III. Existence of globally exponential attractive set of y and z.

Let

$$G_2^+ \triangleq \begin{bmatrix} 1 & -\frac{\epsilon}{2} \\ -\frac{\epsilon}{2} & \frac{1}{q} \end{bmatrix}, \qquad G_2^- \triangleq \begin{bmatrix} \epsilon q - 2 & \frac{\epsilon}{2} \\ \frac{\epsilon}{2} & -\epsilon \end{bmatrix}, \tag{17}$$

then, G_2^+ is a positive matrix if $\epsilon \in (0, 2/\sqrt{q})$, and G_2^- is a negative matrix if $\epsilon \in (0, 8/(4q+1))$.

At the same time, it is easy to examine that G_2^+ is positive and G_2^- is negative if let $\epsilon \in (0, 8/(4q+1))$, since $q > 0$ and $8/(4q+1) = 2/(q+1/4) \le 2/\sqrt{q}$.

Let $\lambda_m(G_2^+)$, $\lambda_M(G_2^+)$ be, respectively, minimum and maximum eigenvalues of G_2^+, and let $\mu_m(G_2^-)$ and $\mu_M(G_2^-)$ be the minimum and maximum eigenvalues of G_2^-, respectively. Since $|x| \le |x_b|$, a radially unbounded and positive definite Lyapunov function about y and z is constructed as follows:

$$W = y^2 + \frac{1}{q}z^2 - \epsilon yz = \begin{bmatrix} y \\ z \end{bmatrix}^T G_2^+ \begin{bmatrix} y \\ z \end{bmatrix}. \tag{18}$$

Then, the time derivative of W along the system (2) yields

$$\begin{aligned}\left.\frac{dW}{dt}\right|_{(2)} &= 2y\dot{y} + \frac{2}{q}z\dot{z} - \epsilon\dot{y}z - \epsilon y\dot{z} \\ &= \begin{bmatrix} y \\ z \end{bmatrix}^T G_2^- \begin{bmatrix} y \\ z \end{bmatrix} + 2xy - \epsilon xz \\ &\le \mu_M(G_2^-)\left(y^2+z^2\right) + 2|x_b||y| + \epsilon|x_b||z| \\ &\le \tau_1\mu_M(G_2^-)\left(y^2+z^2\right) + \tau_2\mu_M(G_2^-)\left(y^2+z^2\right) \\ &\quad + \eta y^2 + \frac{x_b^2}{\eta} + \eta z^2 + \frac{x_b^2}{4\eta} \\ &\le \frac{\tau_1\mu_M(G_2^-)}{\lambda_M(G_2^+)}W + \left(\tau_2\mu_M(G_2^-) + \eta\right)\left(y^2+z^2\right) + \frac{5}{4\eta}x_b^2 \\ &\le \frac{\tau_1\mu_M(G_2^-)}{\lambda_M(G_2^+)}\left(W - \frac{(5/4\eta)x_b^2}{-\tau_1\mu_M(G_2^-)/\lambda_M(G_2^+)}\right),\end{aligned} \tag{19}$$

where τ_1, τ_2, and η are chosen such that $\tau_1 > 0$, $\tau_2 > 0$, $\eta > 0$, $\tau_1 + \tau_2 = 1$, and $\tau_2\mu_M(G_2^-) + \eta \le 0$.

Let $W_l \triangleq (5/4\eta)x_b^2/(-\tau_1\mu_M(G_2^-)/\lambda_M(G_2^+))$; if $W(X_0) > W_l$ and $W(X(t,t_0,X_0)) > W_l$, it holds that

$$\begin{aligned}&W\left(X\left(t,t_0,X_0\right)\right) - W_l \\ &\quad \le \left(W\left(X_0\right) - W_l\right)e^{(\tau_1\mu_M(G_2^-)/\lambda_M(G_2^+))(t-t_0)}.\end{aligned} \tag{20}$$

Similarly, if $W(X_0) \le W_l$, the state trajectory will stay in the area such that $W(X(t,t_0,X_0)) \le W_l$ holds. Hence, y and z are exponentially decreased and ultimately enter into the attractive region $W(X(t,t_0,X_0)) \le W_l$, that is,

$$y^2 + \frac{1}{q}z^2 - \epsilon yz \le \frac{(5/4\eta)x_b^2}{-\tau_1\mu_M(G_2^-)/\lambda_M(G_2^+)}. \tag{21}$$

Combining Steps I, II, and III, Theorem 3 is obtained and the proof is completed. □

Remark 4. In this section, a constructive method is proposed to prove the main results of existence of globally exponential attractive set and positive invariant set for the Chua's systems. By constructing the matrices G_1^+, G_1^-, G_2^+, G_2^-, and Lyapunov function candidate V and W, the problem is solved ingeniously.

3. Global Linear Stabilization of the Equilibrium Points

In this section, the stability of the equilibrium points for the system (2) will be discussed with the aid of a linear controller.

Firstly, it is easy to examine that the system (2) has three equilibrium points:

$$\begin{aligned}S_0 = (0,0,0), \qquad S_+ &= \left(\sqrt{e^2-1}, 0, -\sqrt{e^2-1}\right), \\ S_- &= \left(-\sqrt{e^2-1}, 0, \sqrt{e^2-1}\right).\end{aligned} \tag{22}$$

Moreover, the equilibrium points of the system is independent of parameters p and q. It should be mentioned that, however, the stability of the equilibrium points is depended on p and q. In the following, we will design a linear controller to stabilize the unstable equilibrium points.

Let $p = 11, q = 14.87$, and (x^*, y^*, z^*) be any equilibrium point of the system (2), the corresponding Jacobian matrix is given by

$$J_0 = \begin{bmatrix} p\left(-\ln\sqrt{1+x^{*2}} + \dfrac{1}{1+x^{*2}}\right) & p & 0 \\ 1 & -1 & 1 \\ 0 & -q & 0 \end{bmatrix}. \tag{23}$$

Then the characteristic equation of the corresponding local linearization system of system (2) is as follows:

$$a_0\lambda^3 + a_1\lambda^2 + a_2\lambda + a_3 = 0, \tag{24}$$

where $a_0 = 1, a_1 = 1 - pw, a_2 = -q - p - pw, a_3 = pqw$, and $w = -\ln\sqrt{1+x^{*2}} + (1/(1+x^{*2}))$.

(i) If $x^* = 0$, one has $a_0 = 1 > 0, a_1 = -10 < 0$. According to Hurwitz stability criterion [19], the necessary condition of stable equilibrium point is the same sign of the coefficients of the characteristic equation. Consequently, the equilibrium S_0 is unstable.

(ii) If $x^* = \pm\sqrt{e^2-1}$, one has $a_0 = 1, a_1 = 10.5113 > 0$, and $a_2 = -16.3587 < 0$. Similarly, one can obtain that S_+ and S_- are the unstable equilibrium points.

Now, we will discuss how to design a linear feedback controller such that the unstable equilibrium points are exponentially stable. For this purpose, we add the control terms to the system (2):

$$\begin{aligned} \dot{x} &= p\left(x + y - x\ln\sqrt{1+x^2}\right) + u_1, \\ \dot{y} &= x - y + z + u_2, \\ \dot{z} &= -qy + u_3. \end{aligned} \tag{25}$$

Let $X^* = (x^*, y^*, z^*)$ be any of the three unstable equilibrium points, let $X(t) = (x(t), y(t), z(t))$ be the solution of the system (25), and $\widetilde{X}(t) = (\tilde{x}, \tilde{y}, \tilde{z}) = X(t) - X^*$, then the error system is given by

$$\begin{aligned} \dot{\tilde{x}} &= p\left(\tilde{x} + \tilde{y} - x\ln\sqrt{1+x^2} + x^*\ln\sqrt{1+x^{*2}}\right) + u_1, \\ \dot{\tilde{y}} &= \tilde{x} - \tilde{y} + \tilde{z} + u_2, \\ \dot{\tilde{z}} &= -q\tilde{y} + u_3. \end{aligned} \tag{26}$$

Definition 5. $\forall X(0) = (x(0), y(0), z(0)) \in R^3$, if u_i $(i = 1, 2, 3)$ is appropriately selected such that

$$\left|\widetilde{X}\left(t, t_0, X_0\right)\right| \le \left|X\left(0\right) - X^*\right| e^{-\alpha(t-t_0)} \tag{27}$$

holds $(\alpha > 0)$. Then, the control input u_i $(i = 1, 2, 3)$ can globally exponentially stabilize the equilibrium point X^*.

Theorem 6. *If the following linear controller is added to the error system* (26)*,*

$$u_1 = -p\sigma_x\tilde{x}, \qquad u_2 = u_3 = 0, \tag{28}$$

where σ_x is any parameter given beforehand such that $\sigma_x > 2$; then the equilibrium point X^* is globally exponentially stable.

Proof. The proof is divided into two steps.

(1) We will find the existence of $\epsilon > 0$ such that G_3^+ is positive definite and G_3^- is negative definite, where

$$G_3^+ \triangleq \begin{bmatrix} \dfrac{1}{p} & 0 & 0 \\ 0 & 1 & -\dfrac{\epsilon}{2} \\ 0 & -\dfrac{\epsilon}{2} & \dfrac{1}{q} \end{bmatrix}, \qquad G_3^- \triangleq \begin{bmatrix} 2\left(1-\sigma_x\right) & 2 & -\dfrac{\epsilon}{2} \\ 2 & \epsilon q - 2 & \dfrac{\epsilon}{2} \\ -\dfrac{\epsilon}{2} & \dfrac{\epsilon}{2} & -\epsilon \end{bmatrix}. \tag{29}$$

It is easy to obtain that G_3^+ is positive definite if $|\epsilon| < 2/\sqrt{q}$. Now we focus on choosing $\epsilon > 0$ such that G_3^- is negative definite. By the Schur theorem [18], G_3^- is negative definite if and only if

$$\begin{aligned} &\epsilon > 0, \\ &\epsilon q + \frac{\epsilon}{4} - 2 < 0, \\ &\left(2\left(\sigma_x - 1\right) - \frac{\epsilon}{4}\right)\left(2 - \epsilon q - \frac{\epsilon}{4}\right) > \left(2 - \frac{\epsilon}{4}\right)^2, \end{aligned} \tag{30}$$

that is

$$\begin{aligned} &\epsilon > 0, \\ &\epsilon < \frac{8}{4q+1}, \\ &\sigma_x > \frac{64 - 16\epsilon + \epsilon^2}{64 - 32\epsilon q - 8\epsilon} + 1 + \frac{\epsilon}{8}. \end{aligned} \tag{31}$$

Obviously, G_3^- is negative definite if $0 < \epsilon \ll 1, \sigma_x > 2$.

(2) We construct a positive definite and radially unbounded Lyapunov function to prove the stability of closed-loop systems (26) with controller (28) which is written as

$$\begin{aligned} V_1\left(\widetilde{X}\left(t, t_0, \widetilde{X}_0\right)\right) &= \frac{1}{p}\tilde{x}^2 + \tilde{y}^2 + \frac{1}{q}\tilde{z}^2 - \epsilon\tilde{y}\tilde{z} \\ &= \begin{bmatrix} \tilde{x} \\ \tilde{y} \\ \tilde{z} \end{bmatrix}^T G_3^+ \begin{bmatrix} \tilde{x} \\ \tilde{y} \\ \tilde{z} \end{bmatrix}. \end{aligned} \tag{32}$$

Suppose $\lambda_m(G_3^+)$ and $\lambda_M(G_3^+)$ are minimum and maximum eigenvalues of the positive definite matrix G_3^+, respectively. Then, we have

$$\lambda_m\left(G_3^+\right)\left(\tilde{x}^2 + \tilde{y}^2 + \tilde{z}^2\right) \le V_1 \le \lambda_M\left(G_3^+\right)\left(\tilde{x}^2 + \tilde{y}^2 + \tilde{z}^2\right). \tag{33}$$

Let $f(\widetilde{x}) = x\ln\sqrt{1+x^2} - x^*\ln\sqrt{1+x^{*2}}$. Obviously, $x\ln\sqrt{1+x^2}$ is a monotonically increasing odd function. Then,

(i) if $\widetilde{x} \geq 0$, then $f(\widetilde{x}) \geq 0$ and

$$0 \leq \widetilde{x} f(\widetilde{x}) \leq +\infty, \tag{34}$$

(ii) if $\widetilde{x} \leq 0$, then $f(\widetilde{x}) \leq 0$ and

$$0 \leq \widetilde{x} f(\widetilde{x}) \leq +\infty. \tag{35}$$

Thus

$$0 \leq \widetilde{x} f(\widetilde{x}) \leq +\infty, \quad \forall \widetilde{x} \in R. \tag{36}$$

Differentiating V_1 with respect to time yields

$$\begin{aligned}\left.\frac{dV_1}{dt}\right|_{(26)} &= \frac{2}{p}\widetilde{x}\dot{\widetilde{x}} + 2\widetilde{y}\dot{\widetilde{y}} + \frac{2}{q}\widetilde{z}\dot{\widetilde{z}} - \epsilon\dot{\widetilde{y}}\widetilde{z} - \epsilon\widetilde{y}\dot{\widetilde{z}} \\ &= \begin{bmatrix}\widetilde{x}\\ \widetilde{y}\\ \widetilde{z}\end{bmatrix}^T G_3^- \begin{bmatrix}\widetilde{x}\\ \widetilde{y}\\ \widetilde{z}\end{bmatrix} - 2\widetilde{x} f(\widetilde{x}) \\ &\leq \mu_M(G_3^-)\left(\widetilde{x}^2 + \widetilde{y}^2 + \widetilde{z}^2\right) \\ &= \mu_M(G_3^-)\frac{\lambda_M(G_3^+)}{\lambda_M(G_3^+)}\left(\widetilde{x}^2 + \widetilde{y}^2 + \widetilde{z}^2\right) \leq \frac{\mu_M(G_3^-)}{\lambda_M(G_3^+)} V_1,\end{aligned} \tag{37}$$

where $\mu_M(G_3^-)$ is the maximum eigenvalues of the negative definite matrix G_3^-. Then,

$$\begin{aligned} &V_1\left(\widetilde{X}\left(t, t_0, \widetilde{X}_0\right)\right) \leq V_1\left(\widetilde{X}_0\right) e^{(\mu_M(G_3^-)/\lambda_M(G_3^+))(t-t_0)}, \\ &\widetilde{x}^2(t) + \widetilde{y}^2(t) + \widetilde{z}^2(t) \leq \frac{V_1\left(\widetilde{X}\left(t, t_0, \widetilde{X}_0\right)\right)}{\lambda_m(G_3^+)} \\ &\qquad \leq \frac{V_1\left(\widetilde{X}_0\right)}{\lambda_m(G_3^+)} e^{(\mu_M(G_3^-)/\lambda_M(G_3^+))(t-t_0)}. \end{aligned} \tag{38}$$

Hence, $\widetilde{x}^2(t)$, $\widetilde{y}^2(t)$, and $\widetilde{z}^2(t)$ converge to zero exponentially. According to Definition 5, the equilibrium point X^* is globally exponentially stable. The proof is complete. □

Remark 7. A constructive method to stabilize the unstable equilibrium points is proposed in this section, matrices G_3^+, G_3^-, and Lyapunov function candidate V_1 are given. Then, a linear controller is obtained to solve the problem. Comparing with nonlinear controller, linear controller is easy to implement in reality.

4. Globally Exponential Synchronization of Two Chua's Systems

In this section, the globally exponential synchronization of two Chua's systems will be discussed. The drive system is given by

$$\begin{aligned} \dot{x}_d &= p\left(x_d + y_d - x_d\ln\sqrt{1+x_d^2}\right), \\ \dot{y}_d &= x_d - y_d + z_d, \\ \dot{z}_d &= -q y_d, \end{aligned} \tag{39}$$

and the response system is described as follows:

$$\begin{aligned} \dot{x}_r &= p\left(x_r + y_r - x_r\ln\sqrt{1+x_r^2}\right) + u_1, \\ \dot{y}_r &= x_r - y_r + z_r + u_2, \\ \dot{z}_r &= -q y_r + u_3, \end{aligned} \tag{40}$$

where the subscripts d and r denote the drive and response systems and u_i $(i = 1, 2, 3)$ is feedback control input which satisfies $u_i(0, 0, 0) = 0$.

Let $e_x = x_r - x_d$, $e_y = y_r - y_d$, and $e_z = z_r - z_d$; one obtains that

$$\begin{aligned} \dot{e}_x &= p\left(e_x + e_y - x_r\ln\sqrt{1+x_r^2} + x_d\ln\sqrt{1+x_d^2}\right) + u_1, \\ \dot{e}_y &= e_x - e_y + e_z + u_2, \\ \dot{e}_z &= -q e_y + u_3. \end{aligned} \tag{41}$$

Theorem 8. *If the following controller is added to the error system* (41)*,*

$$u_1 = -p\delta_x\widetilde{x}, \qquad u_2 = u_3 = 0, \tag{42}$$

where δ_x is any parameter given beforehand with $\delta_x > 2$; then the zero solution of (41) *is globally exponentially stable and the systems* (39) *and* (40) *are globally exponentially synchronized.*

Proof. Since the proof of this theorem is parallel to that of Theorem 6, we omit it here. □

If the parameters p and q in the drive system are uncertain, one can construct the following controlled response system:

$$\begin{aligned} \dot{x}_r &= \widehat{p}\left(x_r + y_r - x_r\ln\sqrt{1+x_r^2}\right) + u_1, \\ \dot{y}_r &= x_r - y_r + z_r + u_2, \\ \dot{z}_r &= -\widehat{q} y_r + u_3, \end{aligned} \tag{43}$$

where $\widehat{p}$ and $\widehat{q}$ are the estimates of the uncertain parameters p and q, respectively. Let $e_x = x_r - x_d$, $e_y = y_r - y_d$, $e_z = z_r - z_d$,

$\widetilde{p} = \widehat{p} - p$, and $\widetilde{q} = \widehat{q} - q$, then, the error system of (39) and (43) is given by

$$\begin{aligned}\dot{e}_x &= \widehat{p}\left(e_x + e_y - x_r \ln\sqrt{1+x_r^2} + x_d \ln\sqrt{1+x_d^2}\right) \\ &\quad + \widetilde{p}\left(x_d + y_d - x_d \ln\sqrt{1+x_d^2}\right) + u_1, \\ \dot{e}_y &= e_x - e_y + e_z + u_2, \\ \dot{e}_z &= -\widehat{q}e_y - \widetilde{q}y_d + u_3.\end{aligned} \tag{44}$$

Theorem 9. *If the following adaptive controller is added to the error system* (44),

$$\begin{aligned}u_1 &= -\widehat{p}\left(e_x + e_y - x_r \ln\sqrt{1+x_r^2} + x_d \ln\sqrt{1+x_d^2}\right) - e_x, \\ u_2 &= -e_x - e_z, \\ u_3 &= \widehat{q}e_y - e_z, \\ \dot{\widehat{p}} &= \dot{\widetilde{p}} = -e_x\left(x_d + y_d - x_d \ln\sqrt{1+x_d^2}\right), \\ \dot{\widehat{q}} &= \dot{\widetilde{q}} = e_z y_d,\end{aligned} \tag{45}$$

then, we have the following.

(1) *The equilibrium points* ($\widetilde{p} = 0$, $\widetilde{q} = 0$, $e_x = 0$, $e_y = 0$, $e_z = 0$) *of the system* (44) *with adaptive control law* (45) *are globally stable; in addition,* $\lim_{t\to\infty} e_x = 0$, $\lim_{t\to\infty} e_y = 0$, *and* $\lim_{t\to\infty} e_z = 0$. *And thus, the two systems* (39) *and* (44) *are globally synchronized.*

(2) *The parameter estimates* $\widehat{p}$ *and* $\widehat{q}$ *will, respectively, converge to* p *and* q *as* t *tends to infinity.*

Proof. The proof contains two steps.

Firstly, a Lyapunov function candidate is constructed as follows:

$$V_2 = \frac{1}{2}\left(e_x^2 + e_y^2 + e_z^2 + \widetilde{p}^2 + \widetilde{q}^2\right). \tag{46}$$

Then, one has

$$\begin{aligned}\left.\frac{dV_2}{dt}\right|_{(44)} &= e_x\dot{e}_x + e_y\dot{e}_y + e_z\dot{e}_z + \widetilde{p}\dot{\widetilde{p}} + \widetilde{q}\dot{\widetilde{q}} \\ &= e_x\left(\widehat{p}\left(e_x + e_y - x_r \ln\sqrt{1+x_r^2} + x_d \ln\sqrt{1+x_d^2}\right) + u_1\right) \\ &\quad + e_y\left(e_x - e_y + e_z + u_2\right) \\ &\quad + e_z\left(-\widehat{q}e_y + u_3\right) - \widetilde{q}\left(e_z y_d - \dot{\widehat{q}}\right) \\ &\quad + \widetilde{p}\left(e_x\left(x_d + y_d - x_d \ln\sqrt{1+x_d^2}\right) + \dot{\widehat{p}}\right) \\ &= -e_x^2 - e_y^2 - e_z^2 \le 0.\end{aligned} \tag{47}$$

By LaSalle-Yoshizawa theorem [20], all the equilibrium points of the closed-loop systems are globally stable. Additionally, $\lim_{t\to\infty} e_x = 0$, $\lim_{t\to\infty} e_y = 0$, and $\lim_{t\to\infty} e_z = 0$. And thus, the two systems (39) and (43) are globally synchronized.

By referring to Lemma 4.1 in [21], $\lim_{t\to\infty}\widetilde{p} = 0$, $\lim_{t\to\infty}\widetilde{q} = 0$ if there exist two functions $f_1(t)$, $f_2(t)$ which satisfy persistency of excitation condition, such that

$$\begin{aligned}\lim_{t\to\infty}\dot{\widetilde{p}} &= 0, \qquad \lim_{t\to\infty}\dot{\widetilde{q}} = 0, \\ \lim_{t\to\infty}\widetilde{p}f_1(t) &= 0, \qquad \lim_{t\to\infty}\widetilde{q}f_2(t) = 0.\end{aligned} \tag{48}$$

Since $\lim_{t\to\infty} e_x = 0$, $\lim_{t\to\infty} e_z = 0$, it is easy to obtain from (45) that

$$\begin{aligned}\lim_{t\to\infty}\dot{\widetilde{p}} &= \lim_{t\to\infty} -e_x\left(x_d + y_d - x_d \ln\sqrt{1+x_d^2}\right) = 0, \\ \lim_{t\to\infty}\dot{\widetilde{q}} &= \lim_{t\to\infty} e_z y_d = 0.\end{aligned} \tag{49}$$

Add u_1 and u_3 from (45) to (44), we have

$$\begin{aligned}\lim_{t\to\infty}\dot{e}_x &= \lim_{t\to\infty} -e_x + \widetilde{p}\left(x_d + y_d - x_d \ln\sqrt{1+x_d^2}\right) \\ &= \lim_{t\to\infty}\widetilde{p}\left(x_d + y_d - x_d \ln\sqrt{1+x_d^2}\right) \\ &= 0, \\ \lim_{t\to\infty}\dot{e}_z &= \lim_{t\to\infty} -e_z - \widetilde{q}y_d \\ &= \lim_{t\to\infty} -\widetilde{q}y_d \\ &= 0.\end{aligned} \tag{50}$$

Let $f_1(t) \triangleq x_d + y_d - x_d \ln\sqrt{1+x_d^2}$ and $f_2(t) \triangleq y_d$; it is easy to see that $f_1(t)$ and $f_2(t)$ satisfy persistency of excitation condition [21]; thus, we have

$$\lim_{t\to\infty}\widetilde{p} = 0, \qquad \lim_{t\to\infty}\widetilde{q} = 0. \tag{51}$$

The proof is complete. □

Remark 10. Synchronization control methods for two Chua's systems are proposed in this section. A linear controller is given when parameters p and q are known. In the case of uncertain parameters p and q, an adaptive controller is proposed to solve the problem. Comparing with the results in reference [22, 23], the output tracking error only converges to a small neighborhood of the origin, yet the synchronization errors of Chua's systems can exponentially approach zero. On the other hand, compared with [23], a novel exponentially convergent method is used to solve the convergence of the estimation error of the uncertain parameters.

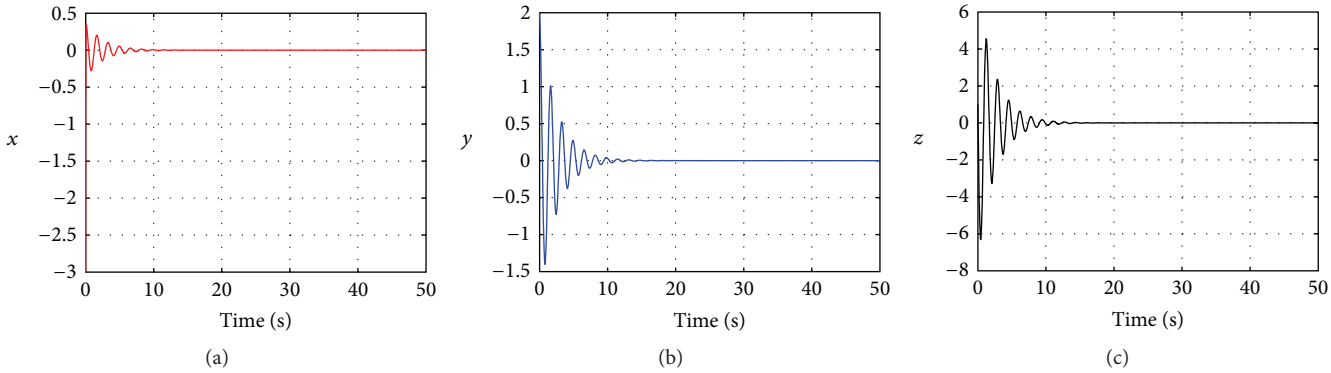

FIGURE 2: The asymptotic stability of S_0 with controller (28).

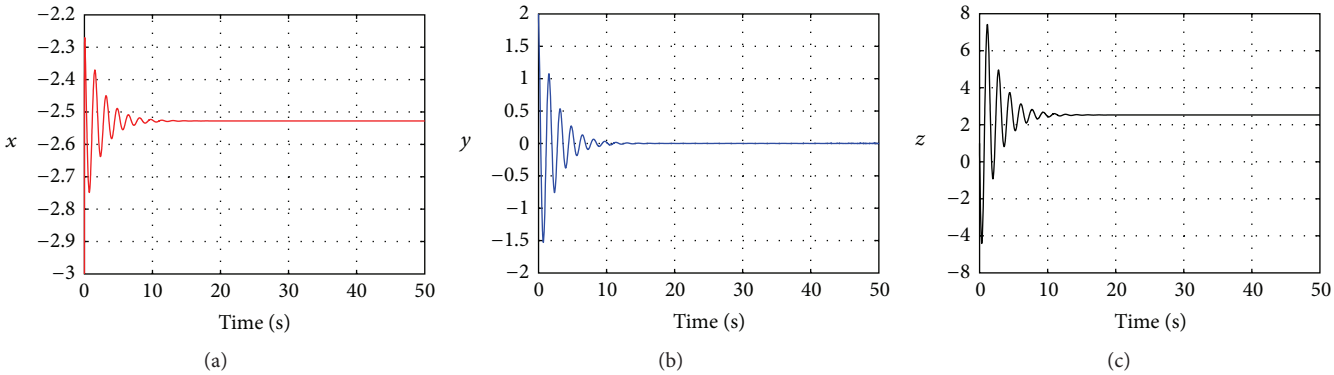

FIGURE 3: The asymptotic stability of S_- with controller (28).

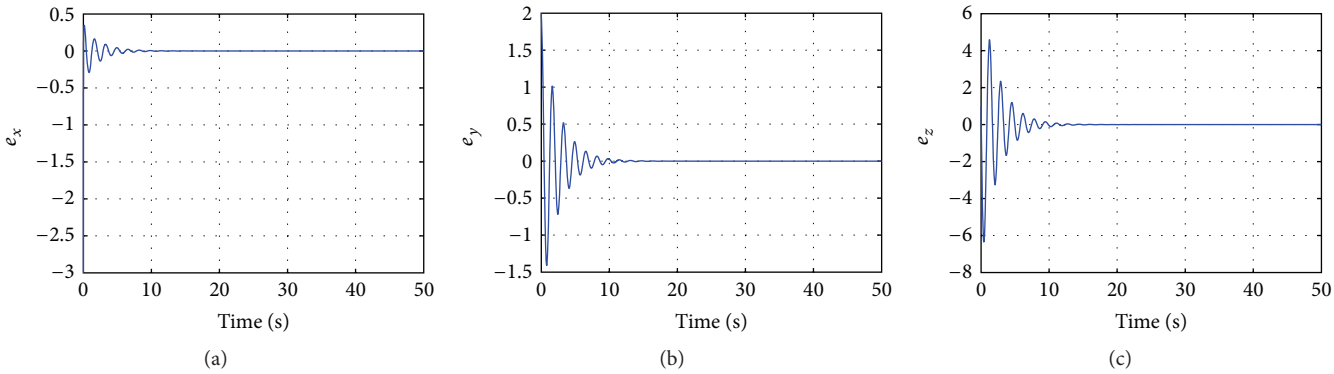

FIGURE 4: The synchronization errors of the system (39) and (40) with linear controller (42).

5. Numerical Simulations

In this section, several examples of numerical simulations are proposed to illustrate the theoretical results obtained in the previous sections. A fourth-order Runge-Kutta method is used to obtain the simulation results with MATLAB.

Chua's system (2) and the error systems (26), (41), and (44) are considered in this section for the numerical simulations. Let $p = 11$, $q = 14.87$, the initial state $x(0) = -3$, $y(0) = 2$, and $z(0) = 1$. Figure 2 shows the state trajectories of the closed-loop system (26) with linear control input (28); it is easy to see that the equilibrium point S_0 is asymptotically stable. Similarly, Figure 3 shows that, with the corresponding control input (28), the equilibrium point S_- is asymptotically stable. Figure 4 shows the synchronous errors of the system (39) and (40) with linear controller (42); it is easy to see that the two systems are globally asymptotically synchronized. When parameters p and q are uncertain, by using adaptive controller (45), the synchronous errors are asymptotically convergent to $e_x = 0$, $e_y = 0$, $e_z = 0$ (see Figure 5),

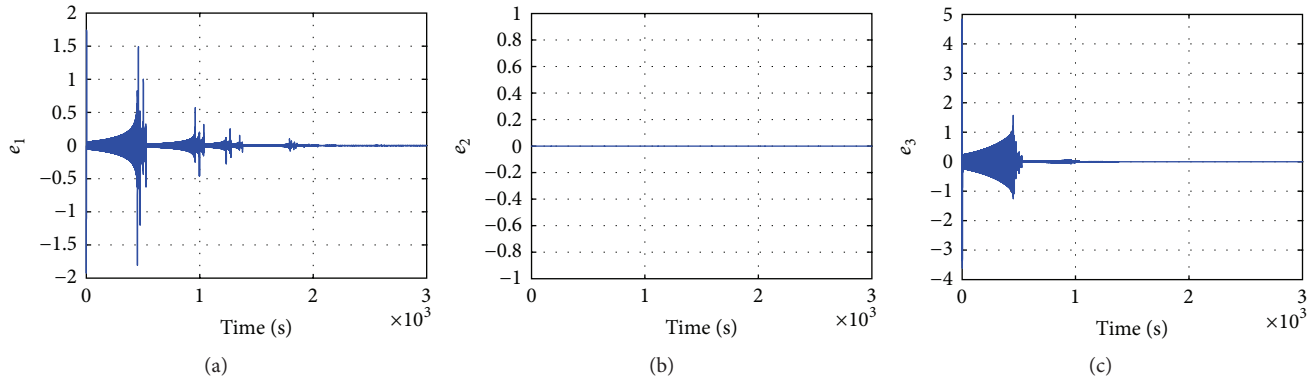

Figure 5: The synchronization errors of the system (39) and (43) with adaptive controller (45).

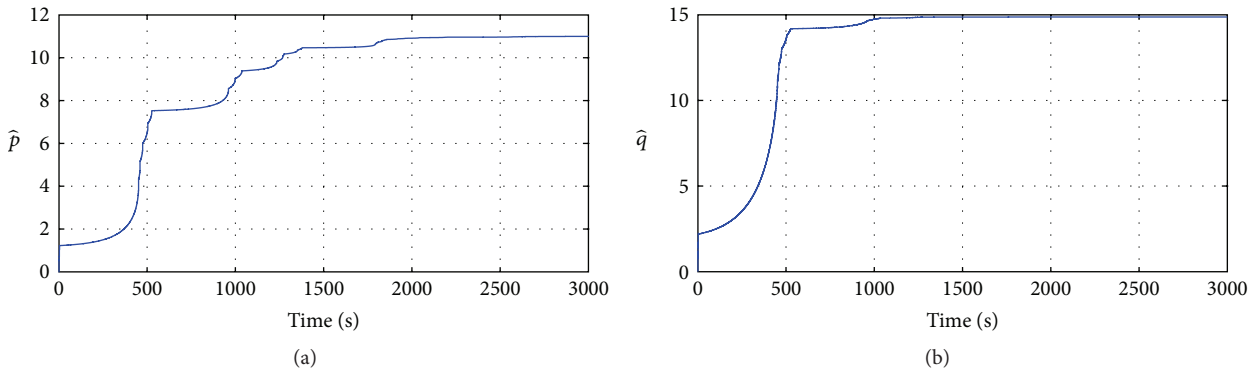

Figure 6: The convergence of parameters $\widehat{p}$ and $\widehat{q}$.

and the estimate values of the uncertain parameters p and q asymptotically converge to the real values $p = 11$, $q = 14.87$ (see Figure 6).

6. Conclusions

A new smooth Chua's system is constructed, and the chaotic characteristics is confirmed by computing the Lyapunov exponents of the system. A Constructive method is used to prove the existence of globally exponential attractive set and positive invariant set. For the three unstable equilibrium points of the system, a linear controller is designed to achieve globally exponential stability of the equilibrium points. Then, a linear controller and an adaptive controller are, respectively, proposed so that two similar types of smooth Chua's systems are globally synchronized, and the estimate errors of the uncertain parameters converge to zero as t tends to infinity.

Acknowledgments

The authors want to express their sincere thanks to the editor and the referee for their invaluable comments and suggestions which helped improve the paper greatly. This work was supported by the National Natural Science Foundation of China (50937002 and 51207063) and the Project of the Education Department of Hubei Province (T200910, T201009, and D20132801).

References

[1] L. O. Chua, "The genesis of Chua's circuit," *Archiv fur Elektronik und Ubertragungstechnik*, vol. 46, no. 4, pp. 250–257, 1992.

[2] L. P. Shil'nikov, "Chua's circuit: rigorous results and future problems," *International Journal of Bifurcation and Chaos*, vol. 4, no. 3, pp. 489–519, 1994.

[3] L. O. Chua, C. W. Wu, A. Huang, and G.-Q. Zhong, "A universal circuit for studying and generating chaos I: routes to chaos," *IEEE Transactions on Circuits and Systems I*, vol. 40, no. 10, pp. 732–744, 1993.

[4] L. O. Chua, "A zoo of strange attractor from the canonical Chua's circuits," in *Proceedings of the 35th Midwest Symposium on Circuits and Systems*, vol. 2, pp. 916–926, 1992.

[5] Y. F. Wang and J. G. Jiang, "The chaotic phenomena analysis of asymmetric nonlinear Chua's circuit," *Systems Engineering and Electronics*, vol. 29, no. 12, pp. 2029–2031, 2007.

[6] K. S. Tang, K. F. Man, G. Q. Zhong, and G. Chen, "Generating chaos via $x|x|$," *IEEE Transactions on Circuits and Systems I*, vol. 48, no. 5, pp. 636–641, 2001.

[7] X. Liao, P. Yu, S. Xie, and Y. Fu, "Study on the global property of the smooth Chua's system," *International Journal of Bifurcation and Chaos in Applied Sciences and Engineering*, vol. 16, no. 10, pp. 2815–2841, 2006.

[8] H. M. Deng, T. Li, Q. H. Wang et al., "Shaped Chua's chaotic system and its synchronization problem," *Systems Engineering and Electronics*, vol. 31, no. 3, pp. 638–641, 2009.

[9] G. A. Leonov, A. I. Bunin, and N. Koksch, "Attractor localization of the Lorenz system," *Zen and the Art of Motorcycle Maintenance*, vol. 67, no. 12, pp. 649–656, 1987.

[10] F. Zhou, Z. Y. Wang, G. P. Zhou, and F. X. Zhen, "Synchronization of two unsmooth Chua's circuits," *Mathematica Applicata*, vol. 25, no. 2, pp. 382–388, 2012.

[11] X. X. Liao, H. G. Luo, Y. L. Fu et al., "Positive invariant set and the globally exponentially attractive set of Lorenz system group," *Science in China-E*, vol. 37, no. 6, pp. 757–769, 2007.

[12] X. X. Liao, "New results for globally attractive set and positive invariant set of Lorenz system and application of chaos control and synchronization," *Science in China-E*, vol. 34, no. 12, pp. 1404–1419, 2004.

[13] J. G. Jian, X. L. Deng, and J. F. Wang, "New results of globally exponentially attractive set and synchronization controlling of the Qi chaotic system," *Advances in N Eural Networks-ISNN*, pp. 643–650, 2010.

[14] F. Q. Wang and C. X. Liu, "A new criterion for chaos and hyperchaos synchronization using linear feedback control," *Physics Letters A*, vol. 360, no. 2, pp. 274–278, 2006.

[15] H. R. Koofigar, F. Sheikholeslam, and S. Hosseinnia, "Robust adaptive synchronization for a general class of uncertain chaotic systems with application to Chuas circuit," *Chaos*, vol. 21, no. 4, Article ID 043134, 2011.

[16] H. G. Zhang, W. Huang, Z. L. Wang et al., "Adaptive synchronization between two different chaotic systems with unknown parameters," *Physics Letters A*, vol. 350, no. 5-6, pp. 363–366, 2006.

[17] F. Zhou, Z. Y. Wang, and G. P. Zhou, "Adaptive chronization of some modified smooth Chua's circuit," *Journal of Nanjing University of Information Science and Techology*, vol. 4, no. 2, pp. 186–189, 2012.

[18] X. X. Liao, *Theory Methods and Application of Stability*, Huazhong University of Science and Technology Press, 2nd edition, 2010.

[19] C. L. Phillips and J. Parr, *Feedback Control Systems*, Prentice Hall, 5th edition, 2010.

[20] M. Kristic, I. Kanellakopoulos, and P. Kokotovic, *Nonlinear and Adaptive Control Design*, John Wiley & Sons, New York, NY, USA, 1995.

[21] L. Liu, Z. Chen, and J. Huang, "Parameter convergence and minimal internal model with an adaptive output regulation problem," *Automatica*, vol. 45, no. 5, pp. 1306–1311, 2009.

[22] S. Tong and Y. Li, "Observer-based fuzzy adaptive control for strict-feedback nonlinear systems," *Fuzzy Sets and Systems*, vol. 160, no. 12, pp. 1749–1764, 2009.

[23] G. Zhou and C. Wang, "Deterministic learning from control of nonlinear systems with disturbances," *Progress in Natural Science*, vol. 19, no. 8, pp. 1011–1019, 2009.

Hindawi Publishing Corporation
Abstract and Applied Analysis
Volume 2013, Article ID 793276, 13 pages
http://dx.doi.org/10.1155/2013/793276

Research Article

On Distributed Reduced-Order Observer-Based Protocol for Linear Multiagent Consensus under Switching Topology

Yan Zhang, Lixin Gao, and Changfei Tong

Institute of Intelligent Systems and Decision, Wenzhou University, Zhejiang 325027, China

Correspondence should be addressed to Lixin Gao; gao-lixin@163.com

Received 21 January 2013; Accepted 18 March 2013

Academic Editor: H. G. Enjieu Kadji

We discuss linear multiagent systems consensus problem with distributed reduced-order observer-based protocol under switching topology. We use Jordan decomposition method to prove that the proposed protocols can solve consensus problem under directed fixed topology. By constructing a parameter-dependent common Lyapunov function, we prove that the distributed reduced-order observer-based protocol can also solve the continuous-time multi-agent consensus problem under the undirected switching interconnection topology. Then, we investigate the leader-following consensus problem and propose a reduced-order observer-based protocol for each following agent. By using similar analysis method, we can prove that all following agents can track the leader under a class of directed interaction topologies. Finally, the given simulation example also shows the effectiveness of our obtained result.

1. Introduction

Recently, a great number of researchers pay much attention to the coordination control of the multiagent systems, which have various subject background such as biology, physics, mathematics, information science, computer science, and control science in [1–4]. Consensus problem is one of the most basic problems of the coordination control of the multiagent systems, and the main idea is to design the distributed protocols which enable a group of agents to achieve an agreement on certain quantities of interest. The well-known early work [1] was done in the control systems community, which gave the theoretical explanation of the consensus behavior of the very famous Vicsek model [2]. Till now, many interesting results for solving similar or generalized consensus problems have been obtained.

The interaction topologies among agents include fixed and switching cases. Fixed topology may be easy to be handled by using eigenvalue decomposition method [5, 6]. Saber and Murray established a general model for consensus problems of the multiagent systems by introducing Lyapunov method to reveal the contract with the connectivity of the graph theory and the stability of the system in [7]. The Lyapunov-based approach is often chosen to solve high-order consensus problem [8, 9]. In most existing works, the dynamics of agents is assumed to be first-, second-, and, sometimes, high-order integrators, and the proposed consensus protocols are based on information of relative states among neighboring agents [10–13]. However, the interacting topology between agents may change dynamically due to the changes of environment, the unreliable communication links and time-delay. It is more difficult to deal with switching interaction topology in mathematics than fixed interaction topology. The common Lyapunov method is fit to probe the switching interaction topology [8]. Too many results have been established for multiagent consensus under switching topology [14–18]. Some other relevant research topics have also been addressed, such as oscillator network [19], cluster synchronization [20, 21], mean square consensus [22], fractional-order multiagent systems [23], descriptor multiagent system [24], random networks [25], and time-delay [26].

The leader-following configuration is very useful to design the multiagent systems. Leader-following consensus problems with first-order dynamics under jointly connected interacting topology were investigated by [1]. Hong et al. [8] considered a multiagent consensus problem with

a second-order active leader and variable interconnection topology. A distributed consensus protocol was proposed for first-order agent with distributed estimation of the general active leader's unmeasurable state variables in [15], while [16] extended the results of [15] to the case of communication delays among agents under switching topology. In [17], the authors considered leader-following problem in the multiagent system with general linear dynamics in both fixed topology case and switching topology case, respectively. The cooperative output regulation of linear multiagent systems can be viewed as a generalization of some results of the leader-following consensus problem of multiagent systems [27, 28].

In many practical systems, the state variables cannot be obtained directly. To achieve the state consensus, the agent has to estimate those unmeasurable state variables by output variables. In [8], the authors proposed a distributed observer-based tracking protocols for each first-order following agent. Under the assumption that the active leader's velocity cannot be measured directly, [29] proposed a distributed observer-based tracking protocol for each second-order following-agent. To track the accelerated motion leader, [30] proposed an observer-based tracking protocol for each second-order follower agent to estimate the acceleration of the leader. A robust adaptive observer based on the response system was constructed to practically synchronize a class of uncertain chaotic systems [31]. In [23], the author proposed an observer-type consensus protocol to the consensus problem for a class of fractional-order uncertain multiagent systems with general linear dynamics. For the multiagent system with general linear dynamics, [32] established a unified framework and proposed an observer-type consensus protocol, and [33] proposed a framework including full state feedback control, observer design, and dynamic output feedback control for leader-following consensus problem. The leader-following consensus problem was investigated under a class of directed switching topologies in [34]. In [35], distributed reduced-order observer-based consensus protocols were proposed for both continuous- and discrete-time linear multiagent systems. Other observer-based previous works include [36–38].

Motivated by the previous works, especially by [35], we do some further investigations on the reduced-order observer-based consensus protocol problem which had been studied by [35] under directed fixed interconnection topology. We first correct some errors and propose a new proof of the main result established in the aforementioned paper based on the Jordan decomposition method. Moreover, by constructing a parameter-dependent common Lyapunov function, we prove that the proposed protocol can guarantee the multiagent consensus system to achieve consensus under undirected switching topology. Although the Lyapunov function method is conservative and is not easy to be constructed, it is fit to solve the problem under the switching interconnection topology. We propose distributed protocol to solve leader-following consensus with a little simple modification to the reduced-order observer-based consensus protocol. Similarly, we can prove that all following agents can track the leader under a class of directed interaction topologies. As the special cases, the consensus conditions for balanced and undirected interconnection topology cases can be obtained directly. Although the leader-following consensus problem in this paper has been studied in many papers with the aid of internal model principle, we obtain a low-dimensional controller in our model.

The paper is organized as follows. In Section 2, some notations and preliminaries are introduced. Then, in Section 3 and Section 4, the main results on the consensus stability are obtained for both leaderless and leader-following cases, respectively. Following that, Section 5 provides a simulation example to illustrate the established results, and finally, the concluding remarks are given in Section 6.

2. Preliminaries

To make this paper more readable, we first introduce some notations and preliminaries, most of which can be found in [35]. Let $R^{m\times n}$ and $C^{m\times n}$ be the set of $m \times n$ real matrices and complex matrices, respectively. $\mathrm{Re}(\xi)$ denotes the real part of $\xi \in C$. I is the identity matrix with compatible dimension. A^T and A^H represent transpose and conjugate transpose of matrix $A \in C^{m\times n}$, respectively. $\mathbf{1}_n = [1, \ldots, 1]^T \in R^n$. For symmetric matrices A and B, $A > (\geq)\ B$ means that $A - B$ is positive (semi-) definite. $\otimes$ denotes the Kronecker product, which satisfies $(A \otimes B)(C \otimes D) = (AC) \otimes (BD)$ and $(A \otimes B)^T = A^T \otimes B^T$. A matrix is said to be Hurwitz stable if all of its eigenvalues have negative real parts.

A weighted digraph is denoted by $\mathcal{G} = \{\mathcal{V}, \varepsilon, A\}$, where $\mathcal{V} = \{v_1, v_2, \ldots, v_n\}$ is the set of vertices, $\varepsilon \subset \mathcal{V} \times \mathcal{V}$ is the set of edges, and a weighted adjacency matrix $A = [a_{ij}]$ has nonnegative elements a_{ij}. The set of all neighbor nodes of node v_i is defined by $\mathcal{N}_i = \{j \mid (v_i, v_j) \in \varepsilon\}$. The degree matrix $D = \{d_1, d_2, \ldots, d_n\} \in \mathcal{R}^{n\times n}$ of digraph $\mathcal{G}$ is a diagonal matrix with diagonal elements $d_i = \sum_{j\in\mathcal{N}_i} a_{ij}$. Then, the Laplacian matrix of $\mathcal{G}$ is defined as $L = D - A \in R^{n\times n}$, which satisfies $L\mathbf{1}_n = 0$. The Laplacian matrix has following interesting property.

Lemma 1 (see [14]). *The Laplacian matrix L associated with weighted digraph $\mathcal{G}$ has at least one zero eigenvalue and all of the non-zero eigenvalues are located on the open right half plane. Furthermore, L has exactly one zero eigenvalue if and only if the directed graph $\mathcal{G}$ has a directed spanning tree.*

A weighted graph is called undirected graph if for all $(v_i, v_j) \in \varepsilon$, we have $(v_j, v_i) \in \varepsilon$ and $a_{ij} = a_{ji}$. It is well known that Laplacian matrix of weighted undirected graph is symmetric positive semidefinite, which can be derived from Lemma 1 by noticing the fact that all eigenvalues of symmetric matrix are real and nonnegative. Furthermore, Laplacian matrix L has exactly one zero eigenvalue if and only if the undirected graph $\mathcal{G}$ is connected.

To establish our result, the well-known Schur Complement Lemma is introduced.

Lemma 2 (see [39]). *Let S be a symmetric matrix of the partitioned form $S = [S_{ij}]$ with $S_{11} \in R^{r\times r}$, $S_{12} \in R^{r\times(n-r)}$, and*

$S_{22} \in R^{(n-r)\times(n-r)}$. *Then,* $S < 0$ *if and only if*

$$S_{11} < 0, \quad S_{22} - S_{21}S_{11}^{-1}S_{12} < 0, \tag{1}$$

or equivalently,

$$S_{22} < 0, \quad S_{11} - S_{12}S_{22}^{-1}S_{21} < 0. \tag{2}$$

3. Multiagent Consensus Problem

Consider a multiagent system consisting of N identical agents, whose dynamics are modeled by

$$\dot{x}_i = Ax_i + Bu_i, \quad y_i = Cx_i\,, \quad i = 1, \ldots, N, \tag{3}$$

where $x_i \in R^n$ is the agent i's state, $u_i \in R^p$ agent i's control input, and $y_i \in R^q$ the agent i's measured output. A, B, and C are constant matrices with compatible dimensions. It is assumed that (A, B) is stabilizable, (A, C) is observable, and C has full row rank.

To solve consensus problem, a weighted counterpart of the distributed reduced-order observer-based consensus protocol proposed in [35] for agent i is given as follows:

$$\begin{aligned} \dot{v}_i &= Fv_i + Gy_i + \mathrm{T}Bu_i, \\ u_i &= \kappa KQ_1 \sum_{j\in\mathcal{N}_i(t)} a_{ij}(t)\left(y_i - y_j\right) \\ &\quad + \kappa KQ_2 \sum_{j\in\mathcal{N}_i(t)} a_{ij}(t)\left(v_i - v_j\right), \end{aligned} \tag{4}$$

where $v_i \in R^{n-q}$ is the protocol state, the weight $a_{ij}(t)$ is chosen as

$$a_{ij}(t) = \begin{cases} \alpha_{ij}, & \text{if agent } i \text{ is connected to agent } j, \\ 0, & \text{otherwise}, \end{cases} \tag{5}$$

κ is the coupling strength, and $F \in R^{(n-q)\times(n-q)}$, $G \in R^{(n-q)\times q}$, $T \in R^{(n-q)\times n}$, $Q_1 \in R^{n\times q}$ and, $Q_2 \in R^{n\times(n-q)}$ are constant matrices, which will be designed later.

For the multiagent system under consideration, the interconnection topology may be dynamically changing, which is assumed that there are only finite possible interconnection topologies to be switched. The set of all possible topology digraphs is denoted as $\mathcal{S} = \{\mathcal{G}_1, \mathcal{G}_2, \ldots, \mathcal{G}_M\}$ with index set $\mathcal{P} = \{1, 2, \ldots, M\}$. The switching signal $\sigma : [0, \infty) \to \mathcal{P}$ is used to represent the index of topology digraph; that is, at each time t, the underlying graph is $\mathcal{G}_{\sigma(t)}$. Let $0 = t_1, t_2, t_3, \ldots$ be an infinite time sequence at which the interconnection graph switches. Certainly, it is assumed that chattering does not occur when the switching interconnection topology is considered. The main objective of this section is to design protocol (4), which is used to solve the consensus problem under switching interconnection topology.

Let $x = [x_1^T, x_2^T, \ldots, x_N^T]^T$ and $v = [v_1^T, v_2^T, \ldots, v_N^T]^T$. Then, after manipulation with combining (3) and (4), the closed-loop system can be expressed as

$$\begin{aligned} &\frac{d}{dt}\begin{bmatrix} x \\ v \end{bmatrix} \\ &= \begin{bmatrix} I_N \otimes A + L_{\sigma(t)} \otimes (\kappa BKQ_1C) & L_{\sigma(t)} \otimes (\kappa BKQ_2) \\ I_N \otimes (GC) + L_{\sigma(t)} \otimes (\kappa TBKQ_1C) & I_N \otimes F + L_{\sigma(t)} \otimes (\kappa TBKQ_2) \end{bmatrix} \\ &\quad \times \begin{bmatrix} x \\ v \end{bmatrix}. \end{aligned} \tag{6}$$

We first discuss consensus problem under fixed interconnection topology, which has been investigated by [35]. In this case, the subscript $\sigma(t)$ in closed-loop system (6) should be dropped. Algorithm 3.1 in [35] is slightly modified to present as follows, which is used to choose control parameters in protocol (4).

Algorithm 3. Given (A, B, C) with properties that (A, B) is stabilizable, (A, C) is observable, and C has full row rank q, the control parameters in the distributed consensus protocol (4) are selected as follows.

(1) Select a Hurwitz matrix $F \in R^{(n-q)\times(n-q)}$ with a set of desired eigenvalues that contains no eigenvalues in common with those of A. Select $G \in \mathrm{R}^{(n-q)\times q}$ randomly such that (F, G) is controllable.

(2) Solve Sylvester equation

$$TA - FT = GC \tag{7}$$

to get the unique solution T, which satisfies that $\left[\begin{smallmatrix} C \\ T \end{smallmatrix}\right]$ is nonsingular. If $\left[\begin{smallmatrix} C \\ T \end{smallmatrix}\right]$ is singular, go back to Step 2 to select another G, until $\left[\begin{smallmatrix} C \\ T \end{smallmatrix}\right]$ is nonsingular. Compute matrices $Q_1 \in R^{n\times q}$ and $Q_2 \in R^{n\times(n-q)}$ by $[Q_1\ Q_2] = \left[\begin{smallmatrix} C \\ T \end{smallmatrix}\right]^{-1}$.

(3) For a given positive definite matrix Q, solve the following Riccati equation:

$$A^TP + PA - PBB^TP + Q = 0, \tag{8}$$

to obtain the unique positive definite matrix P. Then, the gain matrix K is chosen by $K = -B^TP$.

(4) Select the coupling strength $\kappa \geq 1/(2\min_{\lambda_i \neq 0}\{\mathrm{Re}(\lambda_i)\})$, where λ_i is the ith eigenvalue of Laplacian matrix L.

Remark 4. According to Theorem 8.M6 in [40], if A and F have no common eigenvalues, then the matrix $\left[\begin{smallmatrix} C \\ T \end{smallmatrix}\right]$ is nonsingular only if (A, C) is observable and (F, G) is controllable. Thus, the assumptions that (A, C) is detectable and (F, G) is stabilizable in Algorithm 3.1 of [35] may be questionable. Step 3 of Algorithm 3.1 in [35] is an LMI inequality. Here, we propose the Riccati equation to replace the LMI inequality in Step 3 of the algorithm. If we use the LMI design approach proposed by [35], all our following analysis process is also right as long as we do some sight modification. The Riccati equation has been widely studied in the subsequent centuries and has known an impressive range of applications in control

theory, which will make the condition expressed in Riccati equation easy to be generalized to other cases such as descriptor multiagent system. If (A, B) is stabilizable and Q is a positive definite matrix, the Riccati equation (8) has a unique positive definite matrix P, which can be found in many books such as [41]. On the other hand, it is convenient for us to solve Riccati equation by using Matlab toolbox.

The following theorem is a modified vision of Theorem 3.3 in [35], which is the main result of [35]. To prove Theorem 3.3 in [35], the authors mainly use the following assumption. Let $U \in R^{N\times N}$ be such a unitary matrix that $U^T L U = \Lambda = \left[\begin{smallmatrix} 0 & 0 \\ 0 & \Delta \end{smallmatrix}\right]$, where the diagonal entries of Δ are the nonzero eigenvalues of L. Unfortunately, this assumption is not right.

Since Laplacian matrix L of directed topology graph $\mathcal{G}$ is not symmetric, it can only be assumed that there exists a unitary matrix U satisfying $U^H L U = \left[\begin{smallmatrix} 0 & * \\ 0 & \Delta \end{smallmatrix}\right]$, where Δ is an upper triangular matrix and $*$ is a nonzero row vector (see [39]). Thus, I think the proof in [35] is not strict too. On the other hand, the limit function of $v_i(t)$ in Theorem 3.3 of [35] is not right, which should be $T\varpi(t)$. Now, we propose a strict proof, which is based on Jordan decomposition and may be easier to be understood. Before giving our proof, we present the theorem as follows.

Theorem 5. *For the multiagent system* (3) *whose interconnection topology graph $\mathcal{G}$ contains a directed spanning tree, the dynamic protocol* (4) *constructed by Algorithm 3 can solve the consensus problem. Moreover,*

$$x_i(t) \longrightarrow \varpi(t) \triangleq \left(r^T \otimes e^{At}\right) \begin{bmatrix} x_1(0) \\ \vdots \\ x_N(0) \end{bmatrix} = e^{At} \sum_{j=1}^{N} r_j x_j(0),$$
$$v_i \longrightarrow T\varpi(t), \quad i = 1, 2, \ldots, N, \ \text{as } t \longrightarrow \infty, \tag{9}$$

where $r = (r_1, r_2, \ldots, r_N)^T \in R^N$ is a nonnegative vector such that $r^T L = 0$ and $r^T \mathbf{1} = 1$.

Proof. By Lemma 1, the assumption that $\mathcal{G}$ contains a directed spanning tree means that zero is a simple eigenvalue of L and all other eigenvalues of L have positive real parts. From Jordan decomposition of L, let S be nonsingular matrix such $S^{-1} L S = J = \left[\begin{smallmatrix} 0 & 0 \\ 0 & J_1 \end{smallmatrix}\right]$, where the Jordan matrix $J_1 \in C^{(N-1)\times(N-1)}$ is an upper triangular matrix and the diagonal entries of J_1 are the nonzero eigenvalues of L.

Let $\overline{x} = (S^{-1} \otimes I_n)x$ and $\overline{v} = (S^{-1} \otimes I_{n-q})v$. Then, system (6) can be represented in terms of $\overline{x}$ and $\overline{v}$ as follows:

$$\frac{d}{dt}\begin{bmatrix} \overline{x} \\ \overline{v} \end{bmatrix} = \begin{bmatrix} I_N \otimes A + J \otimes (\kappa BKQ_1C) & J \otimes (\kappa BKQ_2) \\ I_N \otimes (GC) + J \otimes (\kappa TBKQ_1C) & I_N \otimes F + J \otimes (\kappa TBKQ_2) \end{bmatrix} \times \begin{bmatrix} \overline{x} \\ \overline{v} \end{bmatrix}. \tag{10}$$

Certainly, system (10) can be divided into the following two subsystems: one is

$$\frac{d}{dt}\begin{bmatrix} \overline{x}^0 \\ \overline{v}^0 \end{bmatrix} = \begin{bmatrix} A & 0 \\ GC & F \end{bmatrix} \begin{bmatrix} \overline{x}^0 \\ \overline{v}^0 \end{bmatrix} \tag{11}$$

and the other one is

$$\frac{d}{dt}\begin{bmatrix} \overline{x}^1 \\ \overline{v}^1 \end{bmatrix} = \begin{bmatrix} I_{N-1} \otimes A + J_1 \otimes (\kappa BKQ_1C) & J_1 \otimes (\kappa BKQ_2) \\ I_{N-1} \otimes (GC) + J_1 \otimes (\kappa TBKQ_1C) & I_{N-1} \otimes F + J_1 \otimes (\kappa TBKQ_2) \end{bmatrix} \times \begin{bmatrix} \overline{x}^1 \\ \overline{v}^1 \end{bmatrix}, \tag{12}$$

where $\overline{x} = [\overline{x}^{0T}, \overline{x}^{1T}]^T$ and $\overline{v} = [\overline{v}^{0T}, \overline{v}^{1T}]^T$ with $\overline{x}^0$ and $\overline{v}^0$ being their first n and $n - p$ column, respectively.

Denote $z_i(k)$ for agent i as

$$z_i = x_i - \sum_{j=1}^{N} r_j x_j, \quad i = 1, \ldots, N. \tag{13}$$

Obviously, for all $i, j = 1, 2, \ldots, N$, $z_i = 0$ if and only if $x_i = x_j$; that is, the consensus is achieved. Let $z = [{z_1}^T, {z_2}^T, \ldots, {z_N}^T]^T$. Then, we have $z = ((I_N - 1r^T) \otimes I_n)x$. Let $\overline{z} = (S^{-1} \otimes I_n)z$. We know that $\overline{z} = 0$ if and only if $z = 0$. Since $LS = SJ$, the first column of S is right zero eigenvector w_r of L. Similarly, $S^{-1}L = JS^{-1}$ implies that the first row of S^{-1} is is left zero eigenvector w_l^T. Set $S = [w_r, S_1]$ and $S^{-1} = \left[\begin{smallmatrix} w_l^T \\ Y_1 \end{smallmatrix}\right]$. Due to $S^{-1}S = I$, we have $w_l^T w_r = 1$, $w_l^T S_1 = 0$, and $Y_1 w_r = 0$. Since $\mathbf{1}$ and r^T are the right and left zero eigenvectors of L, respectively, and zero is simple eigenvalue of L, there exists constant $\alpha \neq 0$ such that $w_r = \alpha\mathbf{1}$ and $w_l = (1/\alpha)r$. Then, we can verify directly that

$$S^{-1}\left(I_N - \mathbf{1}r^T\right)S = S^{-1}S - S^{-1}\mathbf{1}r^T S = S^{-1}S - S^{-1}w_r w_l^T S = \begin{bmatrix} 0 & 0 \\ 0 & I_{N-1} \end{bmatrix}. \tag{14}$$

Thus, we have

$$\overline{z} = \left(S^{-1} \otimes I_n\right)z = \left(S^{-1} \otimes I_n\right)\left(\left(I_N - \mathbf{1}r^T\right) \otimes I_n\right)\left(S \otimes I_n\right)\overline{x} = \left(\begin{bmatrix} 0 & 0 \\ 0 & I_{N-1} \end{bmatrix} \otimes I_n\right)\overline{x} = \begin{bmatrix} 0 \\ \overline{x}^1 \end{bmatrix}, \tag{15}$$

From the previous analysis, we know that $\overline{x}_1 = 0 \Leftrightarrow \overline{z} = 0 \Leftrightarrow z = 0$. Thus, the stability of system (12) implies that multiagent system (6) can achieve consensus. Let $\overline{T} = \left[\begin{smallmatrix} I_{N-1}\otimes I_n & 0 \\ -I_{N-1}\otimes T & I_{N-1}\otimes I_{n-q} \end{smallmatrix}\right]$, which is nonsingular and $\overline{T}^{-1} = \left[\begin{smallmatrix} I_{N-1}\otimes I_n & 0 \\ I_{N-1}\otimes T & I_{N-1}\otimes I_{n-q} \end{smallmatrix}\right]$. Let $\zeta = \overline{T}\left[\begin{smallmatrix} \overline{x}^1 \\ \overline{v}^1 \end{smallmatrix}\right]$. By Step (2) of Algorithm 3, system (12) is equivalent to the following system:

$$\zeta = \begin{bmatrix} I_{N-1} \otimes A + J_1 \otimes (\kappa BK) & J_1 \otimes (\kappa BKQ_2) \\ 0 & I_{N-1} \otimes F \end{bmatrix} \zeta \triangleq \overline{F}\zeta. \tag{16}$$

The matrix $\overline{F}$ is block upper triangular matrix with diagonal block matrix entries $A+\kappa\lambda_i BK$ ($i = 2, 3, \ldots, N$) and F. By Step (3) and Step (4) of Algorithm 3, the unique positive definite solution P of Riccati equation (8) satisfies

$$\begin{aligned}&\left(A + \lambda_i \kappa BK\right)^H P + P\left(A + \lambda_i \kappa BK\right)\\ &\quad = -Q + PBB^T P - 2\,\mathrm{Re}\left(\lambda_i\right)\kappa PBB^T P \le -Q;\end{aligned} \tag{17}$$

that is, $A+\kappa\lambda_i BK$ ($i = 2, 3, \ldots, N$) are stable. Thus, $\overline{F}$ is stable. Moreover, system (12) is asymptotically stable; that is, the consensus problem can be solved by protocol (4).

From the first equation of system (11), we have $\overline{x}^0(t) = e^{At}\overline{x}^0(0) = e^{At}(w_l^T \otimes I_n) \times [x_1^T(0), x_2^T(0), \ldots, x_N^T(0)]^T$. In addition, the solution of system (6) under fixed topology satisfies $x(t) = (S \otimes I_n)\overline{x}(t) = [\alpha\mathbf{1} \otimes I_n, S_1 \otimes I_n]\begin{bmatrix}\overline{x}^0(t)\\ \overline{x}^1(t)\end{bmatrix} \to [\alpha\mathbf{1} \otimes I_n, S_1 \otimes I_n]\begin{bmatrix}\overline{x}^0(t)\\ 0\end{bmatrix} = \begin{bmatrix}\alpha\overline{x}^0(t)\\ \vdots\\ \alpha\overline{x}^0(t)\end{bmatrix}$, as $t \to \infty$. Thus, $x_i(t) \to \alpha e^{At}(w_l^T \otimes I_n)[x_1^T(0), x_2^T(0), \ldots, x_N^T(0)]^T = e^{At}(r^T \otimes I_n)[x_1^T(0), x_2^T(0), \ldots, x_N^T(0)]^T = (r^T \otimes e^{At})\begin{bmatrix}x_1(0)\\ \vdots\\ x_N(0)\end{bmatrix}$, as $t \to \infty$. From the second equation of system (11), we have

$$\begin{aligned}&\frac{d}{dt}\left(\overline{v}^0(t) - T\overline{x}^0(t)\right)\\ &\quad = F\overline{v}^0(t) + GC\overline{x}^0(t) - TA\overline{x}^0(t) = F\left(\overline{v}^0(t) - T\overline{x}^0(t)\right).\end{aligned} \tag{18}$$

Since F is Hurwitz stable, we know that $\lim_{t\to\infty}(\overline{v}^0(t) - T\overline{x}^0(t)) = 0$. Noticing that $v = (S \otimes I_{n-q})\overline{v}$, we can also obtain $v_i(t) \to \alpha\overline{v}^0(t)$, as $t \to \infty$. Thus, we have $v_i(t) \to \alpha T\overline{x}^0(t) = T\varpi(t)$, as $t \to \infty$. The proof is now completed. □

Next, we probe the consensus problem under switching interconnection topology. For the switching interconnection topology case, we always assume that all interconnection topology graphs $\mathcal{G}_i$, $i \in \mathcal{P}$ are undirected and connected. Choose an orthogonal matrix with form $U = [(1/\sqrt{N})\mathbf{1}, U_1]$ with $U_1 \in R^{N\times(N-1)}$. Noticing that the Laplacian matrix L_i of $\mathcal{G}_i$ ($i \in \mathcal{P}$) is symmetric and $L_i\mathbf{1} = 0$, we have

$$U^T L_i U = \begin{pmatrix}0 & 0\\ 0 & \widetilde{L}_{1i}\end{pmatrix} := \widetilde{L}_i, \tag{19}$$

where $\widetilde{L}_{1i}$ is an $(N-1)\times(N-1)$ symmetric matrix. Since all $\mathcal{G}_i$ are undirected and connected, L_i is positive semidefinite and $\widetilde{L}_{1i}$ is positive definite.

Then, we can define

$$\begin{aligned}&\overline{\lambda} = \min_{i\in\mathcal{P}}\left\{\lambda_2\left(L_i\right) \mid \mathcal{G}_i \text{ is undirected and connected}\right\} > 0,\\ &\widetilde{\lambda} = \max_{i\in\mathcal{P}}\left\{\lambda_{\max}\left(L_i\right) \mid \mathcal{G}_i \text{ is undirected and connected}\right\} > 0,\end{aligned} \tag{20}$$

where $\lambda_2(L_i)$ is the second small eigenvalue of L_i. Since $\mathcal{P}$ is finite set, $\overline{\lambda}$ and $\widetilde{\lambda}$ are fixed and positive.

To measure the disagreement of $x_i(t)$ to the average state of all agents, denote $z_i(t)$ for agent i as

$$z_i = x_i - \frac{1}{N}\sum_{j=1}^{N} x_j. \tag{21}$$

Obviously, $z_i = 0$ for any $i = 1, 2, \ldots, N$ if and only if $x_i = x_j$, for any $i, j = 1, 2, \ldots, N$; that is, the consensus is achieved. Let $z = [z_1^T, z_2^T, \ldots, z_N^T]^T$. Then, we have

$$z = \left(L_o \otimes I_n\right)x, \tag{22}$$

where

$$L_o = I_N - \frac{1}{N}\mathbf{1}_N\mathbf{1}_N^T, \tag{23}$$

which satisfies $L_o\mathbf{1}_N = 0$. It can be verified that $U^T\mathbf{1}_N = [\sqrt{N}, 0, \ldots, 0]^T$, from which we have

$$U^T L_o U = U^T U - \frac{1}{N}U^T\mathbf{1}\mathbf{1}^T U = \begin{bmatrix}0 & 0\\ 0 & I_{N-1}\end{bmatrix} \triangleq \widetilde{L}_o. \tag{24}$$

Let $\widetilde{x} = (U^T \otimes I_n)x$, $\widetilde{v} = (U^T \otimes I_{n-q})v$, and $\widetilde{z} = (U^T \otimes I_n)z$. Then, system (6) can be expressed in terms of $\widetilde{x}$ and $\widetilde{v}$ as follows:

$$\begin{aligned}&\frac{d}{dt}\begin{bmatrix}\widetilde{x}\\ \widetilde{v}\end{bmatrix}\\ &= \begin{bmatrix}I_N \otimes A + \widetilde{L}_{\sigma(t)} \otimes (\kappa BKQ_1C) & \widetilde{L}_{\sigma(t)} \otimes (\kappa BKQ_2)\\ I_N \otimes (GC) + \widetilde{L}_{\sigma(t)} \otimes (\kappa TBKQ_1C) & I_N \otimes F + \widetilde{L}_{\sigma(t)} \otimes (\kappa TBKQ_2)\end{bmatrix}\\ &\quad \times \begin{bmatrix}\widetilde{x}\\ \widetilde{v}\end{bmatrix}.\end{aligned} \tag{25}$$

Similarly, system (25) can be divided into the following two subsystems:

$$\frac{d}{dt}\begin{bmatrix}\widetilde{x}^0\\ \widetilde{v}^0\end{bmatrix} = \begin{bmatrix}A & 0\\ GC & F\end{bmatrix}\begin{bmatrix}\widetilde{x}^0\\ \widetilde{v}^0\end{bmatrix}, \tag{26}$$

$$\begin{aligned}&\frac{d}{dt}\begin{bmatrix}\widetilde{x}^1\\ \widetilde{v}^1\end{bmatrix}\\ &= \begin{bmatrix}I_{N-1} \otimes A + \widetilde{L}_{1\sigma(t)} \otimes (\kappa BKQ_1C) & \widetilde{L}_{1\sigma(t)} \otimes (\kappa BKQ_2)\\ I_{N-1} \otimes (GC) + \widetilde{L}_{1\sigma(t)} \otimes (\kappa TBKQ_1C) & I_{N-1} \otimes F + \widetilde{L}_{1\sigma(t)} \otimes (\kappa TBKQ_2)\end{bmatrix}\\ &\quad \times \begin{bmatrix}\widetilde{x}^1\\ \widetilde{v}^1\end{bmatrix},\end{aligned} \tag{27}$$

where $\widetilde{x} = [\widetilde{x}^{0T}, \widetilde{x}^{1T}]^T$ and $\widetilde{v} = [\widetilde{v}^{0T}, \widetilde{v}^{1T}]^T$ with $\widetilde{x}^0$ and $\widetilde{v}^0$ being their first n and $n-p$ columns, respectively.

We know that $\widetilde{z} = 0$ if and only if $z = 0$. On the other hand, we have

$$\begin{aligned}\widetilde{z} &= \left(U^T \otimes I_n\right)z = \left(U^T \otimes I_n\right)\left(L_o \otimes I_n\right)x\\ &= \left(\widetilde{L}_o \otimes I_n\right)\widetilde{x} = \begin{bmatrix}0\\ \widetilde{x}^1\end{bmatrix},\end{aligned} \tag{28}$$

from which we know that $\widetilde{x}^1 = 0$ is equivalent to $z = 0$.

Thus, the stability of the switching system (27) implies that multiagent system (6) can achieve consensus.

Denote that $\xi = \begin{bmatrix} I_{N-1}\otimes I_n & 0 \\ -I_{N-1}\otimes T & I_{N-1}\otimes I_{n-q} \end{bmatrix} \begin{bmatrix} \tilde{x}^1 \\ \tilde{v}^1 \end{bmatrix}$. By Step (2) of Algorithm 3, system (27) is equivalent to the following switching system:

$$\dot{\xi} = \widetilde{F}_{\sigma(t)}\xi, \tag{29}$$

where

$$\widetilde{F}_{\sigma(t)} = \begin{bmatrix} I_{N-1}\otimes A + \widetilde{L}_{1\sigma(t)}\otimes(\kappa BK) & \widetilde{L}_{1\sigma(t)}\otimes(\kappa BKQ_2) \\ 0 & I_{N-1}\otimes F \end{bmatrix}. \tag{30}$$

Next, we investigate consensus problem of multiagent system under switching interconnection topology based on convergence analysis of the switching system (29) and present our main result as follows.

Theorem 6. *For the multiagent system* (3) *whose interconnection topology graph* $\mathcal{G}_{\sigma(t)}$ *associated with any interval* $[t_j, t_{j+1})$ *is assumed to be undirected and connected, suppose that the parameter matrices* F, G, T, K, Q_1, *and* Q_2 *used in control protocol* (4) *are constructed by Steps* (1)–(3) *of Algorithm 3 and the coupling strength* κ *is satisfied as*

$$\kappa \geq \frac{1}{2\overline{\lambda}}. \tag{31}$$

Then, the distributed control protocol (4) *can guarantee that the multiagent system achieves consensus from any initial condition. Moreover,*

$$x_i(t) \longrightarrow \varpi(t) \triangleq e^{At}\left[\frac{1}{N}\sum_{j=1}^{N} x_j(0)\right], \tag{32}$$

$$v_i(t) \longrightarrow T\varpi(t), \quad i = 1, 2, \ldots, N, \ \text{as } t \longrightarrow \infty.$$

Proof. Till now, we know that the multiagent system achieves consensus if the state ξ of systems (29) satisfies $\lim_{t\to\infty}\xi = 0$. Although system (29) is switching in $[0, \infty)$, it is time-invariant in any interval $[t_i, t_{i+1})$. Assume that $\sigma(t) = p$, which belongs to $\mathcal{P}$. Since $\mathcal{G}_p$ is undirected and connected, $\widetilde{L}_{1p}$ is positive definite. Let U_p be an orthogonal matrix such that

$$U_p\widetilde{L}_{1p}U_p^T = \Lambda_p \triangleq \operatorname{diag}\left\{\lambda_{1p}, \lambda_{2p}, \ldots, \lambda_{(N-1)_p}\right\}, \tag{33}$$

where λ_{ip} is ith eigenvalue of matrix $\widetilde{L}_{1p}$. The unique positive definite solution $P > 0$ of Riccati equation (8) satisfies

$$\begin{aligned}&\left(A + \lambda_{ip}\kappa BK\right)^T P + P\left(A + \lambda_{ip}\kappa BK\right) \\ &\quad = -Q + PBB^TP - 2\lambda_{ip}\kappa PBB^TP \leq -Q,\end{aligned} \tag{34}$$

from which we can obtain

$$\begin{aligned}&\left[I\otimes A + \Lambda_p\otimes(\kappa BK)\right]^T(I\otimes P) + (I\otimes P) \\ &\quad\times\left[I\otimes A + \Lambda_p\otimes(\kappa BK)\right] \leq -I\otimes Q < 0.\end{aligned} \tag{35}$$

Pre- and postmultiplying inequality (63) by $U_p\otimes I$ and its transpose, respectively, we get

$$\begin{aligned}&\left[I\otimes A + \widetilde{L}_{1p}\otimes(\kappa BK)\right]^T(I\otimes P) + (I\otimes P) \\ &\quad\times\left[I\otimes A + \widetilde{L}_{1p}\otimes(\kappa BK)\right] \leq -I\otimes Q < 0.\end{aligned} \tag{36}$$

In addition, for stable matrix F, there exist positive definite matrices $\overline{Q}$ and $\overline{P}$ satisfying the Lyapunov equation

$$F^T\overline{P} + \overline{P}F = -\overline{Q}, \tag{37}$$

or equivalently,

$$\begin{aligned}&\left(I_{N-1}\otimes F\right)^T\left(I_{N-1}\otimes\overline{P}\right) + \left(I_{N-1}\otimes\overline{P}\right)\left(I_{N-1}\otimes F\right) \\ &\quad = -\left(I_{N-1}\otimes\overline{Q}\right).\end{aligned} \tag{38}$$

Consider the parameter-dependent Lyapunov function for dynamic system (29)

$$V(\xi(t)) = \xi(t)^T\widetilde{P}\xi(t), \tag{39}$$

where matrix $\widetilde{P}$ has the form

$$\widetilde{P} = \begin{pmatrix} \frac{1}{\omega}I\otimes P & 0 \\ 0 & I\otimes\overline{P} \end{pmatrix} \tag{40}$$

with positive parameter ω. In interval $[t_i, t_{i+1})$, the time derivative of this Lyapunov function along the trajectory of system (29) is

$$\frac{d}{dt}V(\xi) = \xi^T\left(\widetilde{F}_\sigma^T\widetilde{P} + \widetilde{P}\widetilde{F}_\sigma\right)\xi \triangleq \xi^T\widetilde{Q}_\sigma\xi, \tag{41}$$

where

$$\widetilde{Q}_\sigma = \begin{pmatrix} \frac{1}{\omega}\widetilde{Q}_{1\sigma} & \frac{1}{\omega}\widetilde{L}_{1\sigma(t)}\otimes(\kappa PBKQ_2) \\ \frac{1}{\omega}\widetilde{L}_{1\sigma(t)}^T\otimes(\kappa PBKQ_2)^T & I\otimes\left(F^T\overline{P} + \overline{P}F^T\right) \end{pmatrix},$$

$$\begin{aligned}\widetilde{Q}_{1\sigma} = \frac{1}{\omega}\Big[&\left(I\otimes A + \widetilde{L}_{1\sigma(t)}\otimes(\kappa BK)\right)^T(I\otimes P) \\ &+ (I\otimes P)\left(I\otimes A + \widetilde{L}_{1\sigma(t)}\otimes(\kappa BK)\right)\Big].\end{aligned} \tag{42}$$

From (64) and (65), we have

$$\widetilde{Q}_\sigma \leq \begin{pmatrix} -\frac{1}{\omega}I\otimes Q & \frac{1}{\omega}\widetilde{L}_{1\sigma(t)}\otimes(\kappa PBKQ_2) \\ \frac{1}{\omega}\widetilde{L}_{1\sigma(t)}^T\otimes(\kappa PBKQ_2)^T & -I\otimes\overline{Q} \end{pmatrix}. \tag{43}$$

Since the constant ω can be chosen large enough to satisfy

$$\omega > \widetilde{\lambda}^2\kappa^2\lambda_{\max}\left(Q^{-1}(PBKQ_2)^T\overline{Q}^{-1}(PBKQ_2)\right), \tag{44}$$

this implies that

$$-\frac{1}{\omega}(I\otimes Q)+\frac{1}{\omega^2}\left[\widetilde{L}_{1\sigma(t)}\otimes\left(\kappa PBKQ_2\right)\right]\times\left(I\otimes\overline{Q}^{-1}\right)\left[\widetilde{L}_{1\sigma(t)}^{T}\otimes\left(\kappa PBKQ_2\right)^{T}\right]<0. \tag{45}$$

According to Lemma 2, we know that $\widetilde{Q}_\sigma$ is positive definite. Because there are only finite interconnection topology graphs to be switched, we know that system (29) is asymptotically stable; that is, system (6) achieves consensus. Similarly, we can prove that

$$x_i(t)\longrightarrow\varpi(t)\triangleq e^{At}\left[\frac{1}{N}\sum_{j=1}^{N}x_j(0)\right],\qquad v_i\longrightarrow T\varpi(t),\quad i=1,2,\ldots,N,\ \text{as } t\longrightarrow\infty. \tag{46}$$

The proof is now completed. □

Remark 7. Here, the topological graph is assumed to be undirected for convenience. If all graphs $\mathcal{G}_{\sigma(t)}$ are directed and balanced with a directed spanning tree, we also have

$$U^{T}L_\sigma(t)U=\begin{pmatrix}0 & 0\\ 0 & \widetilde{L}_{1\sigma(t)}\end{pmatrix}, \tag{47}$$

where $\widetilde{L}_{1\sigma(t)}$ is positive definite (see [18]). Define

$$\overline{\lambda}=\min_{l\in\mathcal{P}}\left\{\frac{1}{2}\lambda_2\left(L_l^{T}+L_l\right)\mid\mathcal{G}_l\text{ is balanced and has a directed spanning tree}\right\}>0, \tag{48}$$

where $\lambda_2(L_l^T+L_l)$ is the second small eigenvalue of $L_l^T+L_l$. Following the similar line to analyze the directed topology as Theorem 11 in the next section, it is not difficult to establish similar condition to guarantee that the multiagent system achieves consensus.

4. Multiagent Consensus Problem with a Leader

In this section, we consider the multiagent system consisting of N identical agent and a leader. The dynamics of the following agents are described by system (3), and the dynamics of the leader are given as

$$\dot{x}_0=Ax_0,\quad y_0=Cx_0,\quad x_0\in R^n,\ y_0\in R^q, \tag{49}$$

where x_0 is the state of the leader, and y_0 is the measured output of the leader.

Our aim is to construct the distributed control protocol for each agent to track the leader; that is, $x_i\to x_0, t\to\infty$ for any $i=1,2,\ldots N$. To this end, we propose a reduced-order observer-based consensus protocol for each agent as follows:

$$\begin{aligned}\dot{v}_i&=Fv_i+Gy_i+TBu_i,\\ u_i&=\kappa KQ_1\left[\sum_{j\in\mathcal{N}_i(t)}a_{ij}(t)\left(y_i-y_j\right)+d_i(t)\left(y_i-y_0\right)\right]\\ &\quad+\kappa KQ_2\left[\sum_{j\in\mathcal{N}_i(t)}a_{ij}(t)\left(v_i-v_j\right)+d_i(t)\left(v_i-Tx_0\right)\right],\end{aligned} \tag{50}$$

where $v_i\in R^{n-q}$ is the protocol state, $\kappa>0$ is the coupling strength, $a_{ij}(t)$ is chosen by (5), and $d_i(t)$ is chosen by

$$d_i(t)=\begin{cases}\beta_i, & \text{if agent } i \text{ is connected to the leader at time } t,\\ 0, & \text{otherwise,}\end{cases} \tag{51}$$

where β_i is positive connected weight of edge $(i,0)$.

Remark 8. The leader's dynamics is only based on itself, but its system matrices are the same as all following agents. In [17], the authors investigated this leader-following consensus problem by using the distributed state feedback control protocol. In this paper, we will solve the problem via the distributed reduced-order observer-based protocol (50), which needs to be assumed that only the neighbors of leader can obtain the state information of the leader.

In what follows, the digraph $\widehat{\mathcal{G}}$ of order $N+1$ is introduced to model interaction topology of the leader-following multiagent system, whose nodes v_i, $i=1,2,\ldots,N$, are used to label N following agents and v_0 is labeled leader. In fact, $\widehat{\mathcal{G}}$ contains graph $\mathcal{G}$, which models the topology relation of these N followers, and v_0 with the directed edges from some agents to the leader describes the topology relation among all agents. Node v_0 is said to be globally reachable, if there is a directed path from every other node to node v_0 in digraph $\widehat{\mathcal{G}}$.

Let $L_{\sigma(t)}$ be the Laplacian matrix of the interaction graph $\mathcal{G}_{\sigma(t)}$, and let $B_{\sigma(t)}$ be an $N\times N$ diagonal matrix whose ith diagonal element is $d_i(t)$ at time t. For convenience, denote that $H_{\sigma(t)}=L_{\sigma(t)}+B_{\sigma(t)}$. The matrix H has the following property.

Lemma 9 (see [9]). *Matrix $H=L+B$ is positive stable if and only if node 0 is globally reachable in $\widehat{\mathcal{G}}$.*

Let $\varepsilon_i=x_i-x_0$, and $\overline{\varepsilon}_i=v_i-Tx_0$. Then, the dynamics of ε_i and $\overline{\varepsilon}_i$ are described as follows:

$$\begin{aligned}\dot{\varepsilon}_i&=A\varepsilon_i+\kappa BKQ_1C\sum_{j\in N_i(t)}a_{ij}(t)\left[\left(\varepsilon_i-\varepsilon_j\right)+d_i(t)\varepsilon_i\right]\\ &\quad+\kappa KQ_2\left[\sum_{j\in N_i(t)}a_{ij}(t)\left(\overline{\varepsilon}_i-\overline{\varepsilon}_j\right)+d_i(t)\left(\overline{\varepsilon}_i\right)\right],\end{aligned} \tag{52}$$

$$\begin{aligned}\dot{\bar{\varepsilon}}_i &= \dot{v}_i - T\dot{x}_0 = Fv_i + GCx_i + \kappa BKQ_1C \\ &\times \left[\sum_{j\in N_i(t)} a_{ij}\left(x_i - x_j\right) + d_i(t)\left(x_i - x_0\right)\right] + \kappa KQ_2 \\ &\times \left[\sum_{j\in N_i(t)} a_{ij}\left(v_i - v_j\right) + d_i(t)\left(v_i - Tx_0\right)\right] - TAx_0.\end{aligned} \tag{53}$$

According to (7) and (53), we can obtain

$$\begin{aligned}\dot{\bar{\varepsilon}}_i &= F\bar{\varepsilon}_i + GC\varepsilon_i + \kappa BKQ_1C \\ &\times \left[\sum_{j\in N_i(t)} a_{ij}(t)\left(\varepsilon_i - \varepsilon_j\right) + d_i(t)\,\varepsilon_i\right] \\ &+ \kappa KQ_2\left[\sum_{j\in N_i(t)} a_{ij}(t)\left(\bar{\varepsilon}_i - \bar{\varepsilon}_j\right) + d_i(t)\left(\bar{\varepsilon}_i\right)\right].\end{aligned} \tag{54}$$

Let $\varepsilon = (\varepsilon_1^T, \varepsilon_2^T, \ldots, \varepsilon_N^T)^T$, $\bar{\varepsilon} = (\bar{\varepsilon}_1^T, \bar{\varepsilon}_2^T, \ldots, \bar{\varepsilon}_N^T)^T$, and $\xi^T = (\varepsilon^T, \bar{\varepsilon})^T$. From (52) and (54), the error dynamics can be represented as

$$\dot{\xi} = \begin{bmatrix} I_N \otimes A + H_\sigma \otimes (\kappa BKQ_1C) & H_\sigma \otimes (\kappa BKQ_2) \\ I_N \otimes (GC) + H_\sigma \otimes (\kappa TBKQ_1C) & I_N \otimes F + H_\sigma \otimes (\kappa TBKQ_2) \end{bmatrix}\xi. \tag{55}$$

Let $\eta = \begin{bmatrix} I_N \otimes I_n & 0 \\ -I_N \otimes T & I_N \otimes I_{n-q} \end{bmatrix}\xi$. Similarly, system (55) is equivalent to the following switching system:

$$\dot{\eta} = \widehat{F}_{\sigma(t)}\eta, \tag{56}$$

where

$$\widehat{F}_{\sigma(t)} = \begin{bmatrix} I_N \otimes A + H_\sigma \otimes (\kappa BK) & H_\sigma \otimes \left(\kappa BKQ_2\right) \\ 0 & I_N \otimes F \end{bmatrix} \tag{57}$$

From the previous transformation, we know that the stability of error system (29) means that all following agents can track the leader. First, we consider fixed topology case and give the result as follows.

Theorem 10. *For the leader-following multiagent systems* (3) *and* (49)*, whose interconnection topology graph $\widehat{\mathcal{G}}$ is fixed and has a globally reachable node v_0, suppose that the parameter matrices F, G, T, K, Q_1, and Q_2 in the dynamic protocol* (50) *are constructed by Steps* (1)–(3) *of Algorithm 3 and the coupling strength κ is satisfied as*

$$\kappa \geq \frac{1}{2\min_i\left\{\mathrm{Re}\left(\lambda_i(H)\right)\right\}}. \tag{58}$$

Then, the distributed control protocol (50) *guarantees that all following agents can track the leader from any initial condition.*

Proof. Of course, $\sigma(t)$ in dynamical equation can also be removed. According to Lemma 9, we know that H is positive stable; that is, all eigenvalues $\lambda_i(H)$ of H satisfy $\mathrm{Re}(\lambda_i(H)) > 0$. Similarly, we can do similarity transformation to matrix $\widehat{F}$, which can be similar to block upper triangle matrix with diagonal block matrix entries $A + \kappa\lambda_i(H)BK$ and F. Based on Step (3) of Algorithm 3 and (58), we know that $A + \kappa\lambda_i(H)BK$ is stable. Thus, the error system $\dot{\eta} = \widehat{F}\eta$ is stable.

Next, we probe the leader-following consensus problem under switching interconnection topology. Unlike undirected switching topology assumption in the previous section, we assume that the interconnection topology switches in a class of directed topologies. For convenience, the interconnection topology switches in finite set, which is defined by

$$\begin{aligned}\Gamma = \Big\{&\widehat{\mathcal{G}}_i \mid v_0 \text{ is globally reachable node} \\ &\text{in graph } \widehat{\mathcal{G}}_i \text{ and } H^T\left(\widehat{\mathcal{G}}_i\right) + H\left(\widehat{\mathcal{G}}_i\right) \\ &\text{is positive definite, } i \in \mathcal{P}_0\Big\}\end{aligned} \tag{59}$$

with index set $\mathcal{P}_0 = \{1, 2, \ldots, M_0\}$.

Therefore, define

$$\widehat{\lambda} := \min_{\widehat{\mathcal{G}}\in\Gamma}\left\{\lambda\left(H^T\left(\widehat{\mathcal{G}}\right) + H\left(\widehat{\mathcal{G}}\right)\right)\right\}. \tag{60}$$

Noticing that the set Γ is finite set and $H^T(\widehat{\mathcal{G}}) + H(\widehat{\mathcal{G}})$ is positive definite, we know that $\widehat{\lambda}$ is well defined, which is positive and depends directly on the constants, all constants a_{ij} and β_i $(i, j = 1, 2, \ldots, n)$ given in (5) and (51). □

Theorem 11. *For the leader-following multiagent system* (3) *and* (49)*, whose interconnection topology graph $\widehat{\mathcal{G}}_{\sigma(t)}$ associated with any interval $[t_j, t_{j+1})$ is assumed to have a globally reachable node v_0, suppose that the parameter matrices F, G, T, K, Q_1, and Q_2 used in control protocol* (50) *are constructed by Steps* (1)–(3) *of Algorithm 3 and the coupling strength κ is satisfied as*

$$\kappa \geq \frac{1}{2\widehat{\lambda}}. \tag{61}$$

Then, the distributed control protocol (50) *guarantees that all following agents can track the leader from any initial condition.*

Proof. In time interval $[t_i, t_{i+1})$, assume that $\sigma(t) = p \in \mathcal{P}_0$. There exists an orthogonal transformation U_p such that $U_p(H_p^T + H_p)U_p^T$ is a diagonal matrix $\Lambda_p = \mathrm{diag}\{\lambda_{1p}, \lambda_{2p}, \ldots, \lambda_{np}\}$, where λ_{ip} is ith eigenvalue of matrix $H_p^T + H_p$.

According to Algorithm 3 and condition (61), we can know that the unique solution $P > 0$ of Riccati equation satisfies

$$\begin{aligned}&P\left(A + \frac{1}{2}\lambda_{ip}\kappa BK\right)^T + \left(A + \frac{1}{2}\lambda_{ip}\kappa BK\right)P \\ &\quad = -Q + PBB^TP - \lambda_{ip}\kappa PC^TCP \leq -Q,\end{aligned} \tag{62}$$

form which we can obtain the following inequality:

$$\begin{aligned}&(I \otimes P)\left(I \otimes A + \frac{1}{2}\Lambda_p \otimes (\kappa BK)\right)^T \\ &\quad + \left(I \otimes A + \frac{1}{2}\Lambda_p \otimes (\kappa BK)\right)(I \otimes P) \leq -I \otimes Q < 0.\end{aligned} \tag{63}$$

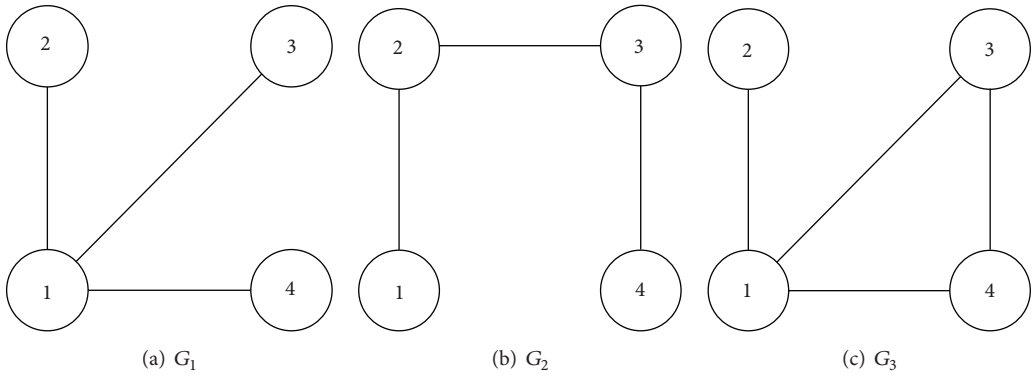

FIGURE 1: Three interconnection topology graphs.

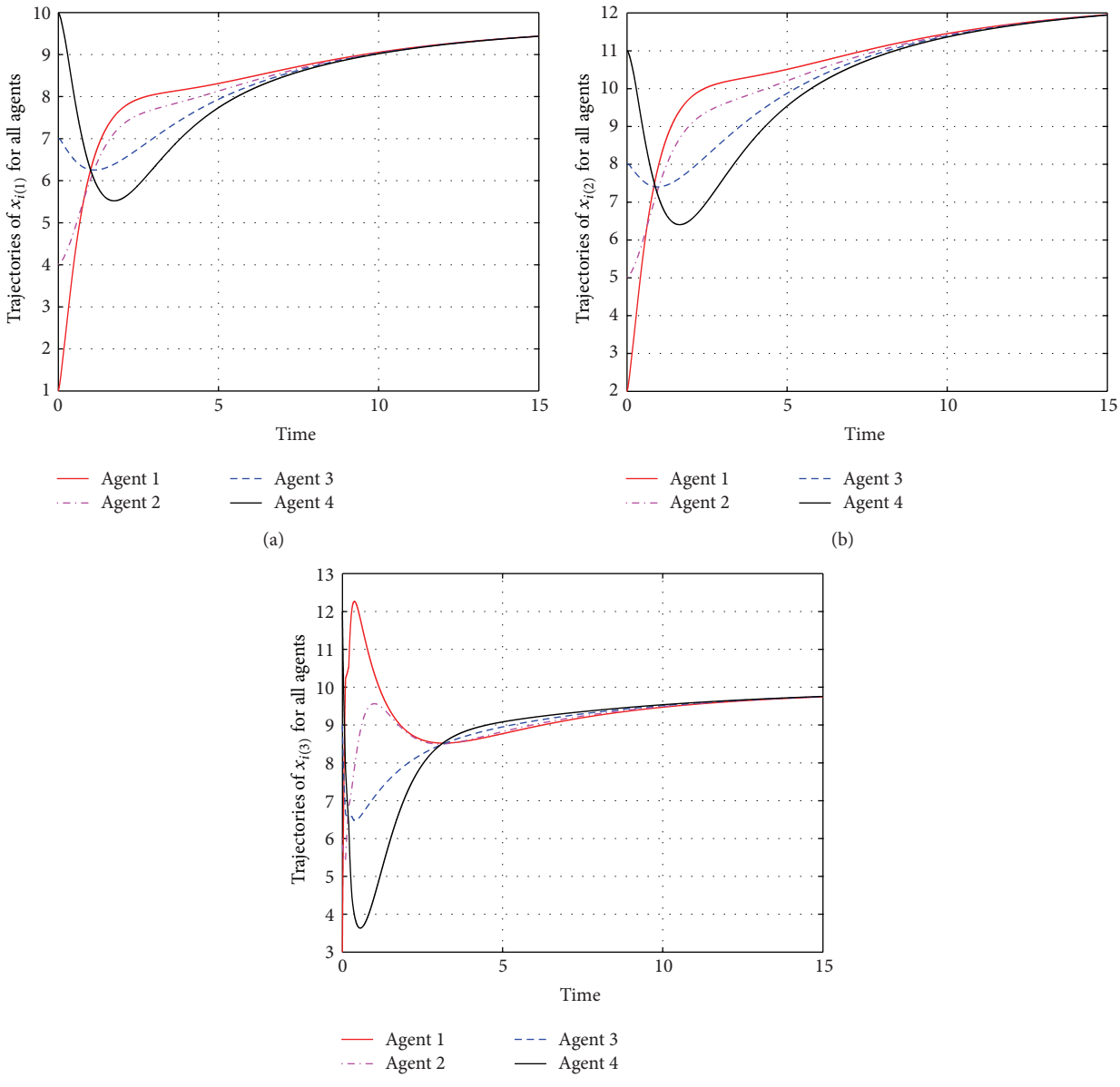

FIGURE 2: Trajectories $x_{i(j)}(t)$ $(j = 1, 2, 3)$ of four agents.

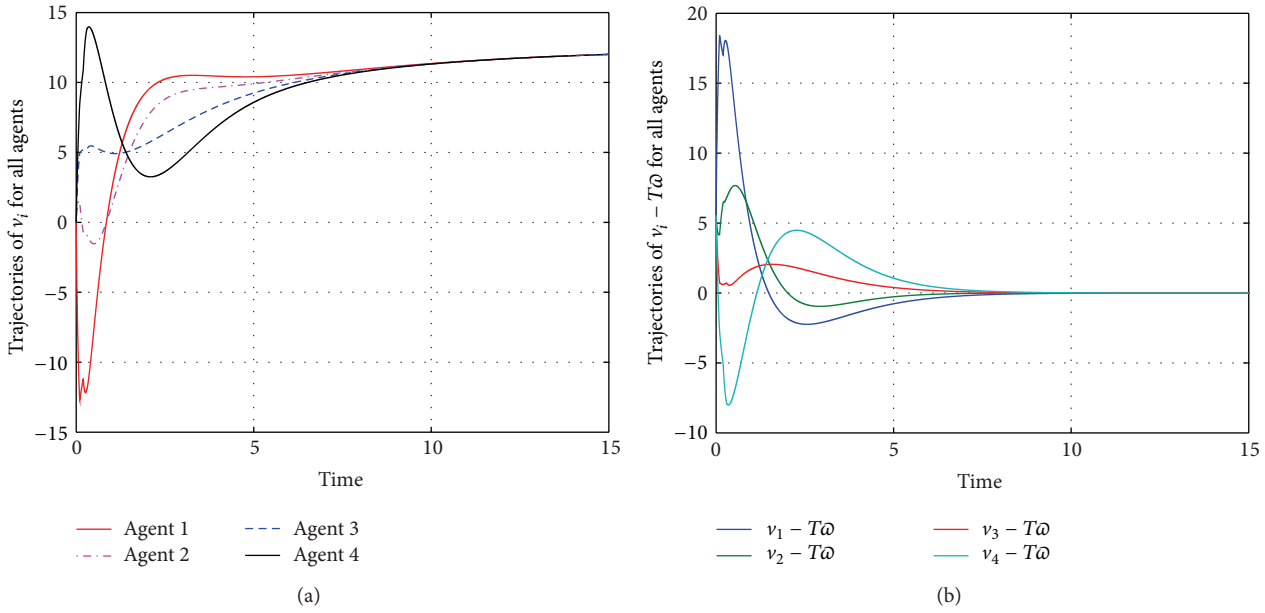

FIGURE 3: Trajectories $v_i^{(j)}(t)$ and $v_i(t) - T\omega(t)$ of four agents.

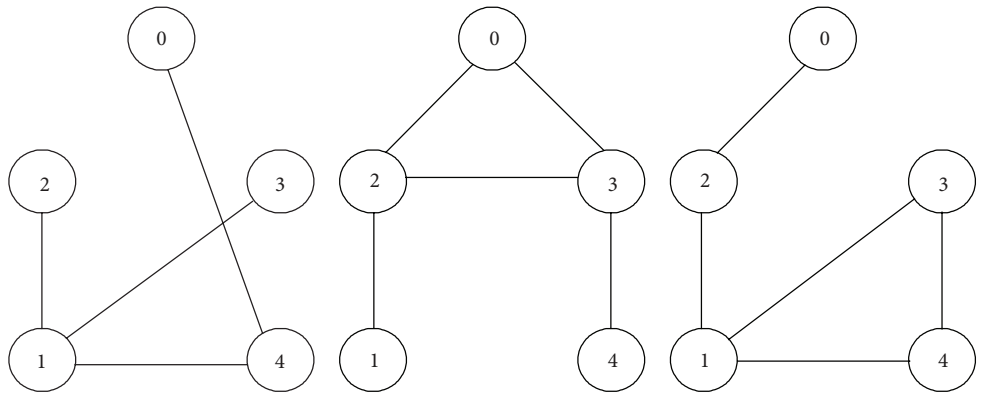

FIGURE 4: Three interconnection topology graphs.

By pre- and postmultiplying (63) with $U_p \otimes I$ and its transpose, respectively, we have

$$(I \otimes P)\left(I \otimes A + \frac{1}{2}\left(H_p^T + H_p\right) \otimes (\kappa BK)\right)^T + \left(I \otimes A + \frac{1}{2}\left(H_p^T + H_p\right) \otimes (\kappa BK)\right)(I \otimes P) \leq -I \otimes Q < 0. \tag{64}$$

Since PBK is a symmetric matrix, we know that the following inequality holds:

$$\begin{aligned}&(I \otimes P)\left(I \otimes A + H_p \otimes (\kappa BK)\right)^T + \left(I \otimes A + H_p \otimes (\kappa BK)\right)(I \otimes P)\\ &= (I \otimes P)\left[I \otimes A + \frac{1}{2}\left(H_p^T + H_p\right) \otimes (\kappa BK)\right]^T + \left[I \otimes A + \frac{1}{2}\left(H_p^T + H_p\right) \otimes (\kappa BK)\right](I \otimes P)\\ &\leq -I \otimes Q < 0.\end{aligned} \tag{65}$$

Similarly, as the proof of the stability of system (29) in the proof of Theorem 6, we can prove that the error system $\dot{\eta} = \widehat{F}_{\sigma(t)}\eta$ is stable. □

5. Simulation Example

The multiagent system contains four agents with each one modeled by the following linear dynamics:

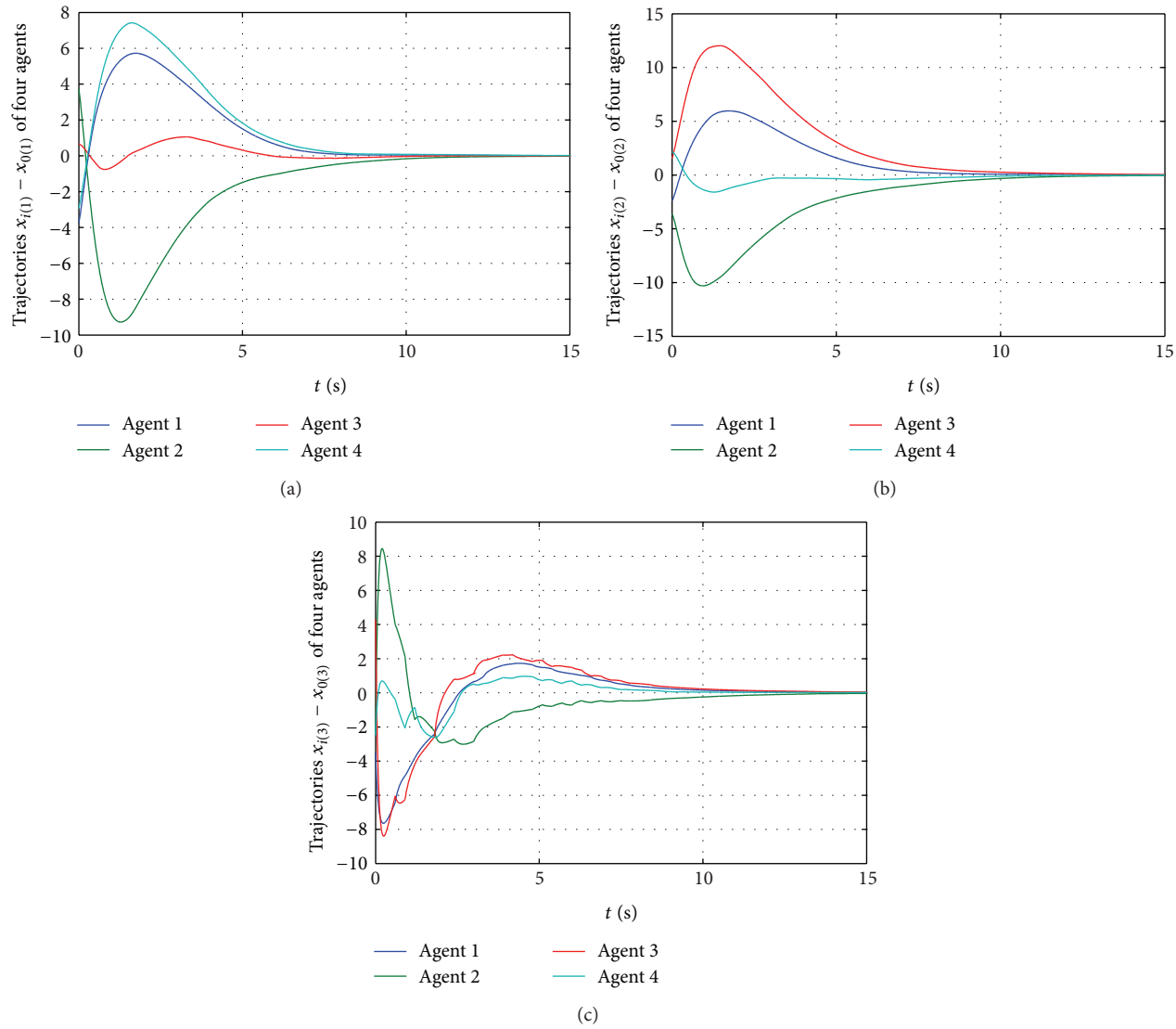

FIGURE 5: Trajectories $x_{i(j)}(t) - x_{0(j)}$ $(j = 1, 2, 3)$ of four agents.

$$\dot{x}_i(t) = \begin{bmatrix} -2.1622 & 1.1469 & 0.6921 \\ -2.0497 & 0.9585 & 0.8159 \\ -1.9817 & 1.1558 & 0.5047 \end{bmatrix} x_i(t) + \begin{bmatrix} 0 \\ 0 \\ 1 \end{bmatrix} u_i(t),$$
$$y_i(t) = \begin{bmatrix} 1 & 0 & 0 \\ 0 & 1 & 0 \end{bmatrix} x_i(t). \tag{66}$$

The interconnection topologies are arbitrarily switched with period 0.1 s among three graphs $\mathcal{G}_i$ $(i = 1, 2, 3)$, which are shown in Figure 1. For simplicity, all nonzero weighting factors of the graphs are taken as (1).

Each agent uses the reduced-order observer-based protocol (4). Take $F = -0.8$ and $G = [0.9\ 0.1]$. To solve the Sylvester equation (7), one can get $T = [9.1676\ -4.6282\ -1.9688]$, which satisfies that $\begin{bmatrix} C \\ T \end{bmatrix}$ is nonsingular. Then, we know that $Q_1 = \begin{bmatrix} 1.0000 & 0 \\ 0 & 1.0000 \\ 4.6564 & -2.3508 \end{bmatrix}$ and $Q_2 = \begin{bmatrix} 0 \\ 0 \\ -0.5079 \end{bmatrix}$. Taking a positive definite matrix $Q = 4I$, we have $K = [3.1532\ -3.2555\ -2.7856]$ by solving the Riccati equation (8). Take $\kappa = 1.0243$, which satisfies condition (31).

Let $x_{i(j)}(t)$ $(j = 1, 2, 3)$ denote the jth component of x_i. The trajectories of $x_{i(j)}(t)$ are depicted in Figure 2, which shows that the multiagent system can achieve consensus. The trajectories of $v_i(t)$ and $v_i(t) - T\varpi(t)$ are depicted in Figure 3, which is also shown that $v_i(t) \to T\varpi(t)$ as $t \to \infty$.

For simplicity, we consider the group to consist of four followers and one leader; that is, $N = 4$. Assume that the interconnection topologies are arbitrarily switched among three graphs $\widehat{\mathcal{G}}_\sigma$ $(i = 1, 2, 3)$ and the communication graph given by Figure 4. All nonzero weighting factors of the graphs are taken as (1).

Take $\kappa = 1.86$, which satisfies condition (61). All other parameters used in protocol (50) are chosen as aforementioned. The trajectories of $x_{i(j)} - x_{0(j)}$, $j = 1, 2, 3$, are depicted in Figure 5, which shows that the follower agents can track the leader agent.

6. Conclusion

In this paper, we investigate the consensus problem for a group of agents with high-dimensional linear coupling dynamics under undirected switching interaction topology. We propose a strict proof of main result in [35] based on the Jordan decomposition method and generalize the proposed protocol to solve the consensus problem under undirected switching interconnection topology. To solve the leader-following consensus problem, we propose a neighbor-based track law for each following agent with a little simple modification to the reduced-order observer-based consensus protocol. The control parameters used in protocol can be constructed by solving the Riccati equation and the Sylvester equation. The parameter-dependent common Lyapunov function method is involved to analyze the consensus problems under undirected switching topology. Since common Lyapunov function method is conservative, the less conservative method should be probed. Of course, more generalized and interesting cases, such as switching directed interaction topology, random interaction topology, jointly connected convergence condition, and the effect of time delays arising in the communication between agents, will be investigated in our future work.

Acknowledgments

This work was supported by the National Nature Science Function of China under Grant nos. 61074123 and 61174063 and the open project of State Key Laboratory of Industrial Control Technology in Zhejiang University, China, under Grant no. ICT1218.

References

[1] A. Jadbabaie, J. Lin, and A. S. Morse, "Coordination of groups of mobile autonomous agents using nearest neighbor rules," *IEEE Transactions on Automatic Control*, vol. 48, no. 6, pp. 988–1001, 2003.

[2] T. Vicsek, A. Czirk, E. Ben-Jacob, I. Cohen, and O. Shochet, "Novel type of phase transition in a system of self-driven particles," *Physical Review Letters*, vol. 75, no. 6, pp. 1226–1229, 1995.

[3] N. Corson, M. A. Aziz-Alaoui, R. Ghnemat, S. Balev, and C. Bertelle, "Modeling the dynamics of complex interaction systems: from morphogenesis to control," *International Journal of Bifurcation and Chaos*, vol. 22, no. 2, Article ID 1250025, 20 pages, 2012.

[4] W. Ren and R. W. Beard, *Distributed Consensus in Multivehicle Cooperative Control: Theory and Applications*, Springer, Berlin, Germany, 2008.

[5] W. Yu, G. Chen, and M. Cao, "Some necessary and sufficient conditions for second-order consensus in multi-agent dynamical systems," *Automatica*, vol. 46, no. 6, pp. 1089–1095, 2010.

[6] F. Xiao and L. Wang, "Consensus problems for high-dimensional multi-agent systems," *IET Control Theory and Applications*, vol. 1, no. 3, pp. 830–837, 2007.

[7] R. Olfati-Saber, A. A. Fax, and R. M. Murray, "Consensus and cooperation in networked multi-agent systems," *Proceedings of the IEEE*, vol. 95, no. 1, pp. 215–233, 2007.

[8] Y. Hong, J. Hu, and L. Gao, "Tracking control for multi-agent consensus with an active leader and variable topology," *Automatica*, vol. 42, no. 7, pp. 1177–1182, 2006.

[9] J. Hu and Y. Hong, "Leader-following coordination of multi-agent systems with coupling time delays," *Physica A*, vol. 374, no. 2, pp. 853–863, 2007.

[10] W. Ren, "On consensus algorithms for double-integrator dynamics," *IEEE Transactions on Automatic Control*, vol. 53, no. 6, pp. 1503–1509, 2008.

[11] P. Lin and Y. Jia, "Further results on decentralised coordination in networks of agents with second-order dynamics," *IET Control Theory & Applications*, vol. 3, no. 7, pp. 957–970, 2009.

[12] W. Ren, K. L. Moore, and Y. Chen, "High-order and model reference consensus algorithms in cooperative control of multivehicle systems," *ASME Journal of Dynamic Systems, Measurement, and Control,*, vol. 129, no. 5, pp. 678–688, 2007.

[13] F. Jiang and L. Wang, "Consensus seeking of high-order dynamic multi-agent systems with fixed and switching topologies," *International Journal of Control*, vol. 83, no. 2, pp. 404–420, 2010.

[14] W. Ren and R. W. Beard, "Consensus seeking in multiagent systems under dynamically changing interaction topologies," *IEEE Transactions on Automatic Control*, vol. 50, no. 5, pp. 655–661, 2005.

[15] Y. Hong and X. Wang, "Multi-agent tracking of a high-dimensional active leader with switching topology," *Journal of Systems Science & Complexity*, vol. 22, no. 4, pp. 722–731, 2009.

[16] L. Gao, Y. Tang, W. Chen, and H. Zhang, "Consensus seeking in multi-agent systems with an active leader and communication delays," *Kybernetika*, vol. 47, no. 5, pp. 773–789, 2011.

[17] W. Ni and D. Cheng, "Leader-following consensus of multi-agent systems under fixed and switching topologies," *Systems & Control Letters*, vol. 59, no. 3-4, pp. 209–217, 2010.

[18] L. Gao, J. Zhang, and W. Chen, "Second-order consensus for multiagent systems under directed and switching topologies," *Mathematical Problems in Engineering*, vol. 2012, Article ID 273140, 21 pages, 2012.

[19] R. Yamapi, H. G. Enjieu Kadji, and G. Filatrella, "Stability of the synchronization manifold in nearest neighbor nonidentical van der Pol-like oscillators," *Nonlinear Dynamics*, vol. 61, no. 1-2, pp. 275–294, 2010.

[20] Y. Chen, J. Lü, F. Han, and X. Yu, "On the cluster consensus of discrete-time multi-agent systems," *Systems & Control Letters*, vol. 60, no. 7, pp. 517–523, 2011.

[21] J. Zhao, M. A. Aziz-Alaoui, and C. Bertelle, "Cluster synchronization analysis of complex dynamical networks by input-to-state stability," *Nonlinear Dynamics*, vol. 70, no. 2, pp. 1107–1115, 2012.

[22] Y. Sun, "Mean square consensus for uncertain multiagent systems with noises and delays," *Abstract and Applied Analysis*, vol. 2012, Article ID 621060, 18 pages, 2012.

[23] H. Li, "Observer-type consensus protocol for a class of fractional-order uncertain multiagent systems," *Abstract and Applied Analysis*, vol. 2012, Article ID 672346, 18 pages, 2012.

[24] X.-R. Yang and G.-P. Liu, "Necessary and sufficient consensus conditions of descriptor multi-agent systems," *IEEE Transactions on Circuits and Systems I*, vol. 59, no. 11, pp. 2669–2677, 2012.

[25] F. Sun, Z.-H. Guan, X.-S. Zhan, and F.-S. Yuan, "Consensus of second-order and high-order discrete-time multi-agent systems with random networks," *Nonlinear Analysis: Real World Applications*, vol. 13, no. 5, pp. 1979–1990, 2012.

[26] U. Münz, A. Papachristodoulou, and F. Allgöwer, "Consensus in multi-agent systems with coupling delays and switching topology," *IEEE Transactions on Automatic Cotrol*, vol. 56, no. 12, pp. 2976–2982, 2011.

[27] X. Wang, Y. Hong, J. Huang, and Z.-P. Jiang, "A distributed control approach to a robust output regulation problem for multi-agent linear systems," *IEEE Transactions on Automatic Control*, vol. 55, no. 12, pp. 2891–2895, 2010.

[28] Y. Su and J. Huang, "Cooperative output regulation of linear multi-agent systems," *IEEE Transactions on Automatic Control*, vol. 57, no. 4, pp. 1062–1066, 2012.

[29] Y. Hong, G. Chen, and L. Bushnell, "Distributed observers design for leader-following control of multi-agent networks," *Automatica*, vol. 44, no. 3, pp. 846–850, 2008.

[30] L. Gao, X. Zhu, and W. Chen, "Leader-following consensus problem with an accelerated motion leadera," *International Journal of Control, Automation and Systems*, vol. 10, no. 5, pp. 931–939, 2012.

[31] S. Bowong and R. Yamapi, "Adaptive observer based synchronization of a class of uncertain chaotic systems," *International Journal of Bifurcation and Chaos in Applied Sciences and Engineering*, vol. 18, no. 8, pp. 2425–2435, 2008.

[32] Z. Li, Z. Duan, G. Chen, and L. Huang, "Consensus of multiagent systems and synchronization of complex networks: a unified viewpoint," *IEEE Transactions on Circuits and Systems I*, vol. 57, no. 1, pp. 213–224, 2010.

[33] H. Zhang, F. L. Lewis, and A. Das, "Optimal design for synchronization of cooperative systems: state feedback, observer and output feedback," *IEEE Transactions on Automatic Control*, vol. 56, no. 8, pp. 1948–1952, 2011.

[34] L. Gao, X. Zhu, W. Chen, and H. Zhang, "Leader-following consensus of linear multi-agent systems with state-observer under switching topologies," *Mathematical Problems in Engineering*, vol. 2013, Article ID 873140, 12 pages, 2013.

[35] Z. Li, X. Liu, P. Lin, and W. Ren, "Consensus of linear multi-agent systems with reduced-order observer-based protocols," *Systems & Control Letters*, vol. 60, no. 7, pp. 510–516, 2011.

[36] J. H. Seo, H. Shim, and J. Back, "Consensus of high-order linear systems using dynamic output feedback compensator: low gain approach," *Automatica*, vol. 45, no. 11, pp. 2659–2664, 2009.

[37] Z. Li, Z. Duan, and G. Chen, "Dynamic consensus of linear multi-agent systems," *IET Control Theory & Applications*, vol. 5, no. 1, pp. 19–28, 2011.

[38] W. Dong, "Distributed observer-based cooperative control of multiple nonholonomic mobile agents," *International Journal of Systems Science*, vol. 43, no. 5, pp. 797–808, 2012.

[39] R. A. Horn and C. R. Johnson, *Matrix Analysis*, Cambridge University Press, New York, NY, USA, 1985.

[40] C. Chen, *Linear System Theory and Design*, Oxford University Press, New York, NY, USA, 1999.

[41] W. M. Wonham, *Linear Multivariable Control*, Springer, New York, NY, USA, 1985.

Hindawi Publishing Corporation
Abstract and Applied Analysis
Volume 2013, Article ID 398293, 13 pages
http://dx.doi.org/10.1155/2013/398293

Research Article

Nonlinear Filtering Preserves Chaotic Synchronization via Master-Slave System

J. S. González-Salas,[1] E. Campos-Cantón,[2] F. C. Ordaz-Salazar,[1] and E. Jiménez-López[3]

[1] *Academia de Matemáticas, Universidad Politécnica de San Luis Potosí, Urbano Villalón 500, 78369 San Luis Potosí, SLP, Mexico*
[2] *División de Matemáticas Aplicadas, Instituto Potosino de Investigación Científica y Tecnológica, Camino a la Presa de San José 2055, 78216 San Luis Potosí, SLP, Mexico*
[3] *Departamento de Físico Matemáticas, Universidad Autónoma de San Luis Potosí, Alvaro Obregón 64, Col. Centro 78000 San Luis Potosí, SLP, Mexico*

Correspondence should be addressed to E. Campos-Cantón; eric.campos@ipicyt.edu.mx

Received 17 December 2012; Revised 26 February 2013; Accepted 6 March 2013

Academic Editor: H. G. Enjieu Kadji

We present a study on a class of interconnected nonlinear systems and give some criteria for them to behave like a filter. Some chaotic systems present this kind of interconnected nonlinear structure, which enables the synchronization of a master-slave system. Interconnected nonlinear filters have been defined in terms of interconnected nonlinear systems. Furthermore, their behaviors have been studied numerically and theoretically on different input signals.

1. Introduction

In the study of nonlinear dynamics, much research was devoted to synchronization of chaotic systems, which have been unidirectional coupling [1], and one of the main applications is in secure communications systems [2]. Under unidirectional coupling, there is a master system that forces a slave system. Let us begin by considering a master system whose temporal evolution is ruled by the following equation:

$$\dot{\mathbf{y}} = f(\mathbf{y}), \tag{1}$$

where $\mathbf{y} \in \mathbb{R}^n$ is the state vector, with f defining a vector field $f : \mathbb{R}^n \to \mathbb{R}^n$. The slave system is given by

$$\dot{\mathbf{x}} = g(\mathbf{x}, \mathbf{y}), \tag{2}$$

where $\mathbf{x} \in \mathbb{R}^m$ is the state vector, and the function $g : \mathbb{R}^m \times \mathbb{R}^n \to \mathbb{R}^m$ describes the dynamics of the slave system and coupling. The master system behaves as an autonomous system and the slave system is a forced system that under certain conditions could behave as a nonautonomous system, where its dynamic is completely determined by the master system; that is, it means that the slave system acts in function of the master system. Hence, the slave system can be seen as a driven system by an external force, and then it can be studied as a filter when the input signal comes from a master system or any external signal unidirectional coupled.

There are several asymptotical behaviors reported based on master-slave configuration. Some cases are summarized as follows: *Identical Synchronization* (IS) implies coincidence of the corresponding states of the interacting systems [1]. *Lag Synchronization* (LS) occurs when the trajectory of one oscillator is delayed by a specific time and is identical to the trajectory of the other oscillator [3]. *Phase Synchronization* (PS) means the lock of chaotic oscillator phases, regardless of their amplitudes [4]. *Frequency Entrainment Synchronization* (FES) occurs when two systems are oscillating with the same frequency [5]. *Generalized Synchronization* (GS) is defined as the presence of some functional relationship between the states of the slave and master systems [6]. *Multimodal Generalized Synchronization* (MGS) is presented when there are several basins of attraction for the slave system, and generalized synchronization is also presented [7, 8]. The aforementioned chaotic synchronization phenomena tell us that some types of synchronization are stronger than others. Another characteristic of these asymptotic behaviors is that

they always can be described in terms of a functional relationship. For example, let Φ be the GS function which relates the master system with the slave system; that is, $\mathbf{y} = \Phi(\mathbf{x})$. In general, the way how synchronization phenomena can be detected is by means of the auxiliary method [6]; thus the way one can know that unidirectional coupled systems present GS is when they present asymptotic behavior:

$$\lim_{t \to \infty} \left| \mathbf{x}^1(t) - \mathbf{x}^2(t) \right| = 0, \tag{3}$$

where $\mathbf{x}^1(t)$ and $\mathbf{x}^2(t)$ are solutions of the slave and auxiliary systems, respectively, initialized with different initial condition $\mathbf{x}^1(0) \neq \mathbf{x}^2(0)$. If this limit is satisfied, it indicates that the slave system has lost its sensitivity to initial conditions, thus losing their autonomy. Thence, the trajectory of the response system depends on the input signal from master system. If we consider the slave system as a forced system, then we will see that its behavior depends on an external forcing, like a filter does.

Forced Synchronization (FS) is defined as a phenomenon that occurs when oscillations of several chaotic systems $\mathbf{x}^{(1)}(t), \mathbf{x}^{(2)}(t), \ldots, \mathbf{x}^{(k)}(t)$ show correlated behavior because of an external signal applied to these oscillators [9]. Meanwhile, the conditions in order that a chaotic system behaves as a filter for an external signal under a specific coupling are given in [10] where this phenomenon was called *nonlinear filtering* (NF). So, these three phenomena (GS, FS, and NF) can be recognized when the limit (3) is satisfied and can be studied from the viewpoint of forced chaotic systems. GS contains NF and MGS because these two phenomena present asymptotic behavior. Nevertheless, there exists a difference between NF and MGS. For MGS, the initial conditions determine the basin of attraction where the trajectory of the slave system converges, the fact despite that there exists a functional relationship between the slave and the master systems, the slave system does not behave like a filter. For NF, the slave system must act in function of the external force and never in function of its initial conditions.

The dynamic of at least one state of several chaotic systems has similar structure to low pass filter, for example, the first equation of the Lorenz system $\dot{x} = -\sigma x + \sigma y$, where x and y can be seen as the output and input signals of a low pass linear filter, respectively. The second equation of the Lorenz system can be seen as a low pass nonlinear filter, $\dot{y} = -y + x(\rho - z)$, where y is the output and x and z are the input signals of a low pass nonlinear filter. Without loss of generality, from the viewpoint of continuous dynamical systems, a filter can be seen as a forced dynamical system in which its response depends on its structure, given by their equations, and can be linear or nonlinear. Then a natural question would be the following: what is the effect on the response of forced nonlinear system given an input signal? In order to answer this question, we make a study of a chaotic system forced with different kinds of signals.

We are interested in explaining synchronization phenomenon of chaotic systems based on nonlinear interconnected structures, as these structures behave as a nonlinear filter that allows synchronization of master and slave systems. Thereby, the target is not to put forward a new nonlinear filter that can replace those designed with the specific purpose of preventing noise in the signal. Thus, the objective of this research is to show how the synchronization phenomenon underlies nonlinear interconnected structure. This kind of structure which is immersed in some chaotic systems could have some useful applications in filtering waves such as those originated from earthquakes and tsunamis, because they can be tuned to produce resonance at certain frequencies. So, the target of this work is to give features of the nonlinear filter as those given by the second and third equations of the Lorenz system in function of the parameters of the input signal u, which gives us a complementary perspective with respect to the analysis made in [9], where it was only proved and showed that a forced-chaotic system filters constant, sinus, and random signals. To achieve this goal, we make a study on the effect of nonlinear filter based on interconnected nonlinear systems for different input signals u, like sinusoidal, chaotic, and random signals. Several chaotic systems that have a similar structure to interconnected systems can be analyzed like a nonlinear filtering phenomenon.

The paper is organized as follows: Section 2 contains basic definitions of nonlinear filters based on n-interconnected systems; Section 3 presents a way how tuning the parameters of an n-interconnected system in order to the system behaves as a nonlinear filter; in Section 4 is the study of the response to amplitude and frequency of a nonlinear filter; Section 5 shows the response of the filter when the input signal is noise; Section 6 presents a study case of correlation coefficient analysis; in Section 7, we present the relation between nonlinear filters and chaotic systems; finally, conclusions are given in Section 8.

2. Nonlinear Filter Structure

In the theory of linear systems, it is very well known that a first-order low pass linear filter is given as follows:

$$\dot{x}_1 = k_1 x_1 + k_2 u, \tag{4}$$

where $x_1 \in \mathbb{R}$ is the output of the filter, and $k_1, k_2 \in \mathbb{R}$ are parameters of the filter (4). These parameters control attenuation and amplitude of the input signal, respectively, and $u \in \mathbb{R}$ is the input signal to be filtered. Based on the configuration of low pass filter given by (4), a low pass nonlinear filter is defined as follows.

Definition 1. Let $x_1 \in \mathbb{R}$ be an output signal, $u \in \mathbb{R}$ an input signal, and k_1, k_2, and $k_3 \in \mathbb{R}$ parameters. Thus, a low pass nonlinear filter can be defined as follows:

$$\dot{x}_1 = k_1 x_1 + \left(k_2 + k_3 x_1\right) u. \tag{5}$$

The parameter k_3 in the above definition is used to control the nonlinear term $x_1 u$. Notice that when $k_3 = 0$, the nonlinear term disappears, $k_3 x_1 u$, and then the nonlinear filter (5) behaves as a linear filter. The structure of nonlinear filters (5) has been used to generate chaos, as it can be seen in the Lorenz system [11], but its states are interconnected. Therefore, a natural question emerges around nonlinear filtering: what are the characteristics of two nonlinear filters if

they are interconnected and forced by the same signal u? An interconnected system via nonlinear filters is given as follows:

Definition 2. Let $x_1, x_2 \in \mathbb{R}$ be output signals, $u \in \mathbb{R}$ an input signal, and k_1, k_2, k_3, k_4, k_5, and $k_6 \in \mathbb{R}$ parameters. So, let us define an interconnected system via low pass nonlinear filters as follows:

$$\begin{aligned} \dot{x}_1 &= k_1 x_1 + (k_2 + k_3 x_2)\, u, \\ \dot{x}_2 &= k_4 x_2 + (k_5 + k_6 x_1)\, u. \end{aligned} \tag{6}$$

Thus the system (6) is called two-interconnected systems.

Now, in Definition 2, the parameters k_3 and k_6 are coupling parameters for the outputs x_1 and x_2, respectively. In general, an n-interconnected system can be defined by coupled x_n to the output x_{n+1} with $n > 2$. This n-interconnected system has a core based on low pass linear filters $\dot{x} = K\mathbf{x} + Bu$, where $\mathbf{x} \in \mathbb{R}^n$ is a state vector, $K \in \mathbb{R}^{n\times n}$ is a matrix, and $B \in \mathbb{R}^{n\times 1}$ is a constant vector. Thus, we can define n-interconnected system with the following expression:

$$\dot{x} = K\mathbf{x} + Bu + f(\mathbf{x}, u), \tag{7}$$

where the nonlinear function $f(\mathbf{x}, u) \in \mathbb{R}^n$ is constituted by terms $k_i x_j u$, $i \in \{1, 2, \ldots, 3n\}$, $j \in \{1, 2, \ldots, n\}$. An n-interconnected system (7) is studied in [12] where the authors found that its model produces hyperbolic chaos when it is forced by a sinusoidal wave. On the other hand, system (7) is formed by a linear part $K\mathbf{x}$, an input signal Bu, and a nonlinear part $f(\mathbf{x}, u)$, which can induce sensitivity to initial conditions $(x_1(0), x_2(0), \ldots, x_n(0))$. But a filter must act in function of the input signal and not in function of the initial condition. Therefore, it is important to find conditions in order to guarantee that an interconnected system behaves as a filter. Roughly speaking, the response of a filter only depends on the kind of input signal and if the interconnected systems depend on initial condition, this is classified as generalized forced synchronization phenomenon by forced systems [9]. Therefore, according to context, a nonlinear filter is defined in the next way.

Definition 3. Let $\mathbf{x}^i(t) = (x_1^i(t), x_2^i(t), \ldots, x_n^i(t))^T$ be a vector of output signals given by n-interconnected system (7) with initial condition $\mathbf{x}^i(0) = (x_1^i(0), x_2^i(0), \ldots, x_n^i(0))^T$. System (7) is called an n-interconnected nonlinear filter if it always presents asymptotic behavior:

$$\lim_{t\to\infty} \left|\mathbf{x}^{(1)}(t) - \mathbf{x}^{(2)}(t)\right| = 0. \tag{8}$$

In Definition 3, if $t \to \infty$ and the output of the n-interconnected system is independent of the initial conditions, then system (7) is considered an n-interconnected nonlinear filter.

3. Tuning of the Parameters

We select the entries of the matrices K and B in order for condition (8) to be satisfied. Let us start by considering $\boldsymbol{\delta}(t) = \mathbf{x}^{(1)}(t) - \mathbf{x}^{(2)}(t)$, and then $\dot{\delta}(t) = \dot{\mathbf{x}}^{(1)}(t) - \dot{\mathbf{x}}^{(2)}(t)$. Now, by using (7) we deduce that $\dot{\boldsymbol{\delta}} = K\boldsymbol{\delta}(t) + f(\mathbf{x}^{(1)}, u) - f(\mathbf{x}^{(2)}, u)$ which can be rewritten as follows:

$$\begin{aligned} \boldsymbol{\delta}(t) = \boldsymbol{\delta}(0)\, e^{Kt} + e^{Kt} \int_0^t e^{Ks} \Big(& f\left(\mathbf{x}^{(2)}, u\right) \\ & - f\left(\mathbf{x}^{(1)}, u\right)\Big)\, ds. \end{aligned} \tag{9}$$

In order to describe the asymptotic behavior of (9), we state the following theorem.

Theorem 4. *If system* (7)*, forced by signal u, satisfyies the following conditions:*

(1) *there exists a positive constant k such that* $\mathrm{Re}\{\lambda\} \le -k$*, for every eigenvalue* λ *of the linear part of system* (7)*;*

(2) $f(\mathbf{x}, u)$ *is a continuous Lipschitz; that is, there exists a positive function* $C[u] < \infty$ *such that* $|f(\mathbf{x}^{(2)}, u) - f(\mathbf{x}^{(1)}, u)| \le C[u]|\mathbf{x}^{(2)} - \mathbf{x}^{(1)}|$,

then, system (7) *is a filter for u, provided that* $k > \overline{C[u]}$*, where*

$$\overline{C[u]} := \lim_{t\to\infty} \frac{1}{t} \int_0^t C\left[u(s)\right] ds. \tag{10}$$

Proof. Let $\mathbf{x}^{(1)}(t), \mathbf{x}^{(2)}(t)$, and $\boldsymbol{\delta}(t)$ defined be before. We want to prove that $k > \overline{C[u]}$ implies $\lim_{t\to\infty}|\boldsymbol{\delta}(t)| = 0$. From (9) we have the following estimate:

$$\begin{aligned} |\boldsymbol{\delta}(t)| &\le \left\|e^{Kt}\right\| |\boldsymbol{\delta}(0)| + \left\|e^{Kt}\right\| \\ &\quad \times \int_0^t \left\|e^{K(-s)}\right\| \left|f\left(\mathbf{x}^{(2)}, u\right) - f\left(\mathbf{x}^{(1)}, u\right)\right| ds \\ &\le e^{\|K\||t|} |\boldsymbol{\delta}(0)| + e^{\|K\||t|} \\ &\quad \times \int_0^t e^{\|K\|-s|} \left|f\left(\mathbf{x}^{(2)}, u\right) - f\left(\mathbf{x}^{(1)}, u\right)\right| ds. \end{aligned} \tag{11}$$

Using hypothesis (1), we obtain from the previous inequality the following estimate:

$$\begin{aligned} |\boldsymbol{\delta}(t)| &\le e^{-kt} |\boldsymbol{\delta}(0)| \\ &\quad + e^{-kt} \int_0^t e^{ks} \left|f\left(\mathbf{x}^{(2)}, u\right) - f\left(\mathbf{x}^{(1)}, u\right)\right| ds. \end{aligned} \tag{12}$$

If we multiply by e^{kt}, the last expression results in

$$e^{kt} |\boldsymbol{\delta}(t)| \le |\boldsymbol{\delta}(0)| + \int_0^t e^{ks} \left|f\left(\mathbf{x}^{(2)}, u\right) - f\left(\mathbf{x}^{(1)}, u\right)\right| ds. \tag{13}$$

Using the hypothesis (2), it follows that

$$e^{kt} |\boldsymbol{\delta}(t)| \le |\boldsymbol{\delta}(0)| + \int_0^t e^{ks} C[u]\, |\boldsymbol{\delta}(s)|\, ds. \tag{14}$$

Application of Gronwall's inequality yields

$$|\boldsymbol{\delta}(t)| \le |\boldsymbol{\delta}(0)|\, e^{-t(k-(1/t)\int_0^t C[u(s)]ds)}, \tag{15}$$

which proves the theorem. □

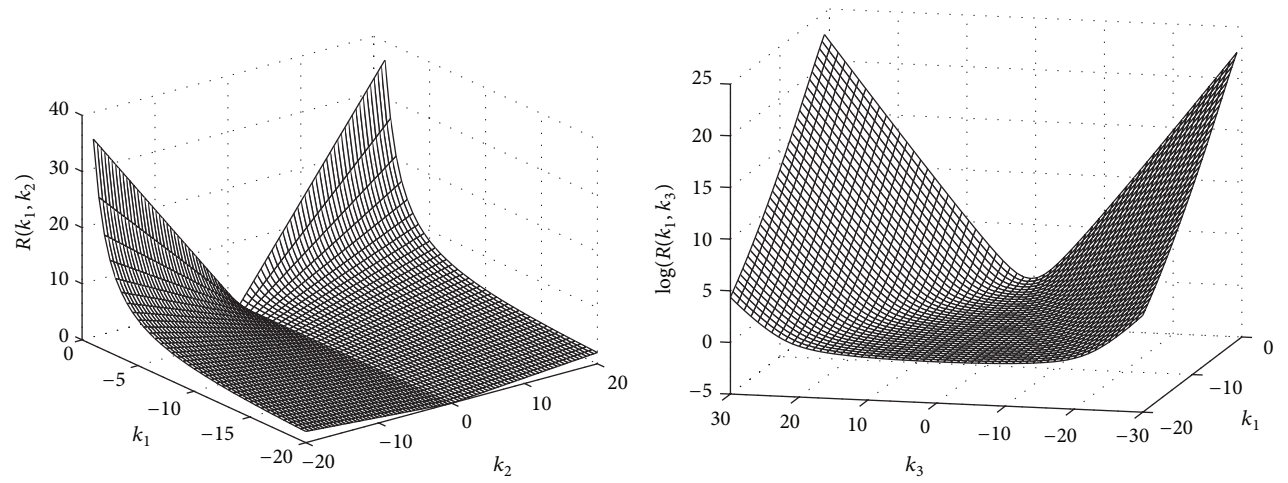

Figure 1: The maximal range of values of the filter (5) in function of its parameters when it is forced by $u = \sin t$: (a) $R(k_1, k_2)$ and (b) $R(k_1, k_3)$.

We can infer from the above theorem that all elements of the matrix K must be negative; that is, $k_i < 0$ for $i = 1, \ldots, n$. On the other hand, due to the fact that (9) does not depend on matrix B, then its terms are not conditioned and they can take any real value. These will be carried out in the remainder of this paper.

3.1. A Low Pass Nonlinear Filter. The analyzed case is the one-interconnected system given by (7); this case is confined to the particular case of the filter given by (5); where its elements are $x = x_1 \in \mathbb{R}$, $A_{1\times1} = k_1$, $B_{1\times1} = k_2$, and $f(x_1, u) = uk_3$. According to the first condition of the above theorem, we have $k_1 < 0$, and now considering the nonlinear part of the filter, if the Lipschitz condition is satisfied when $|f(x_1)^{(1)} - f(x_1)^{(2)}| \leq |k_3||u||\delta(t)|$, giving as a result $c[u] = |k_3||u|$, therefore the parameter k_3 can be any real value. Now, the interest is that the one-interconnected system behaves as a nonlinear filter; then Theorem 4 needs to be satisfied by $k_1 < -|k_3|\overline{|u|}$. If the input signal is a constant, $u = \mu$ ($\mu \in Z$) and $\mu \leq -k_1/|k_3|$, then the response of the filter converges to zero; otherwise it diverges. Another case is when the input signal is $u = \mu \sin(\omega t)$, we have the following:

$$\begin{aligned} |\delta(t)| &\leq |\delta(0)|\, e^{k_1 t + |k_3| \int_0^t |\mu \sin(\omega s)| ds} \\ &\leq |\delta(0)|\, e^{k_1 t + |k_3||\mu| \int_0^t ds}, \end{aligned} \tag{16}$$

which converges $\mu \leq -k_1/|k_3|$. Generally, condition (8) is always satisfied for oscillating functions u with $|u(t)| \leq M$. However, for the case that u is a polynomial of grade greater than 1, that is, $u = a_n t^n + a_{n-1} t^{n-1} + \cdots + a_0$ for $n > 1$, condition (8) is not satisfied.

Due to the fact that our interest is to tune the value of the parameters k_1, k_2, and k_3, we make a numerical study on the effect of these parameters on the response of x_1 when the one-interconnected system (7) is being forced by the sinusoidal input signal $u = \sin(t)$. After a transient time, we calculate the maximal range of values of the one-interconnected system (7) by obtaining $R(k_i, k_j) = \mathrm{MAX}\{x_1(t)\} - \mathrm{MIN}\{x_1(t)\}$ ($i \neq j$), where $\mathrm{MAX}\{x_1(t)\}$ and $\mathrm{MIN}\{x_1(t)\}$ are the maximum and minimum values, respectively, of the response time series $x_1(t)$ in function of the parameters k_i, k_j. For example, if we want to calculate $R(k_1, k_2)$, then we fix the value of k_3 and simulate different time series of the one-interconnected system (7) for different values of k_1, k_2. In general, the value of $R(k_i, k_j)$ is calculated in function of the parameters which are varied and in each case condition (8) is verified if it is satisfied. Figures 1(a) and 1(b) show the graphs of $R(k_1, k_2)$ for $k_3 = -1$ and $R(k_1, k_3)$ for $k_2 = 1$, respectively. These graphs show that the one-interconnected system (7) increments exponentially the amplitude of its response when the parameter k_3 increases its magnitude; meanwhile, the amplitude of x_1 is mildly incremented in a linear rate in function of the magnitude of the parameter k_2.

3.2. Interconnected Nonlinear Filters. Now, the first case is a two-interconnected system (6); the matrices $K_{2\times2}$, $B_{2\times1}$, and the nonlinear function $f(\mathbf{x}, u) : \mathbb{R}^2 \times \mathbb{R} \to \mathbb{R}^2$ are assumed as follows:

$$\begin{aligned} K &= \begin{pmatrix} k_1 & 0 \\ 0 & k_4 \end{pmatrix}, \qquad B = \begin{pmatrix} k_2 \\ k_5 \end{pmatrix}, \\ f(\mathbf{x}, u) &= \begin{pmatrix} k_3 u x_2 \\ k_6 u x_1 \end{pmatrix}. \end{aligned} \tag{17}$$

System (6) is asked to behave as a nonlinear filter, so the conditions of Theorem 4 are used to select the value of the parameters $\{k_i\}$. From the first condition of the theorem, we realize that $k_1, k_4 < 0$, $\{k_2, k_5\} \in \mathbb{R}$, and if $A > B \int_0^t |u| ds$, where $A = \max\{k_1, k_4\}$ and $B = \max\{k_3, k_6\}$, then system (6) is a filter for the signal u. In order to know more about the characteristics of the values of the parameters, we calculate

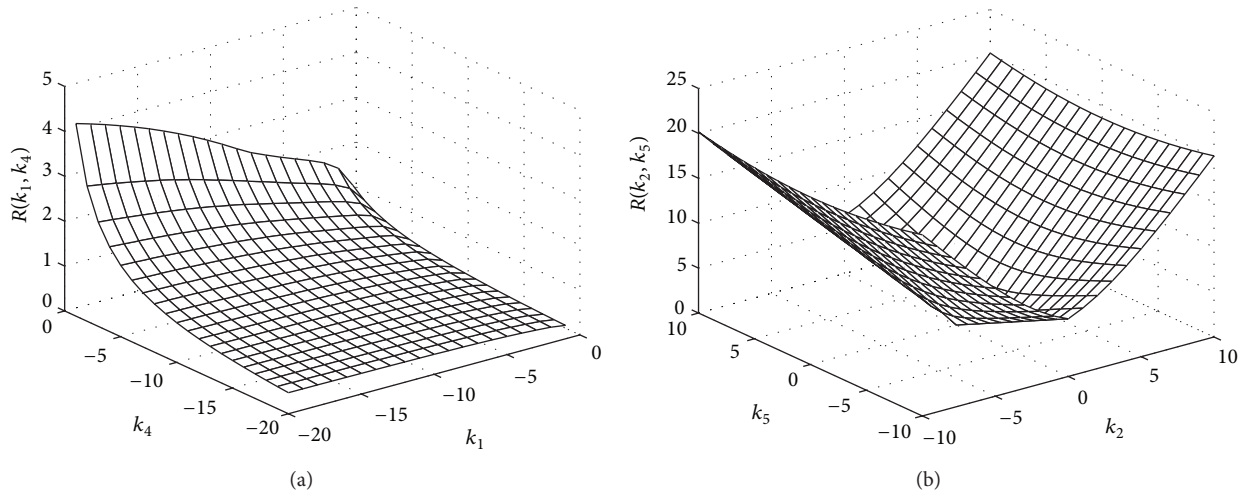

FIGURE 2: The maximal range of values of the filter (17) in function of its parameters when the filter is forced by $u = \sin t$. (a) $R(k_1, k_4)$ and (b) $R(k_2, k_5)$.

the eigenvalues of the Jacobian of system (6), which results in the following:

$$\lambda_{1,2} = \frac{1}{2}\left(k_1 + k_4 \pm \sqrt{\left(k_1 + k_4\right)^2 - 4\left(k_1 k_4 - k_3 k_6 u^2\right)}\right). \tag{18}$$

Our purpose is that system (6) converges; then $\mathrm{Re}\{\lambda_i\}$ must be negative. Therefore, we need to guarantee that $k_1 k_4 \geq k_3 k_6 u^2$ is true. Due to $u^2 \geq 0$, then the parameters k_3 and k_6 need to be opposite sign, that is, either $k_3 < 0$, $k_5 > 0$ or $k_3 > 0, k_6 < 0$. We choose arbitrarily the first relation of signs.

The effect of the parameters $\{k_i\}$ on the response x of the interconnected nonlinear filters is computed by $R(k_i, k_j)$ when system (6) is forced by $u = \sin(t)$. Several calculations were made and for each of them we verify that the nonlinear filtering condition (8) was satisfied. Figure 2(a) shows $R(k_1, k_4)$ when the parameters of the filter (6) are fixed to $k_2 = k_5 = k_6 = 1$, $k_3 = -1$. Figure 2(b) shows $R(k_2, k_5)$ for $k_1 = k_4 = k_3 = -1$ and $k_6 = 1$.

In the remainder of this paper, we studied the effect of the parameters input signal u on the response of the coupled filter (6); that is, we tune the parameters of the filter, vary the parameter's values of the input signal, and observe the effect of the response. Therefore, we need to fix k_i $(i = 1, \ldots, 6)$. Our interest is focus on the study of the response to the input u when the linear filters x_1, x_2 are coupled in a nonlinear way. Without loss of generality and seeking clarity in our study, we consider $k_5 = 0$. The rest of the parameter values could vary in the intervals $k_1 < 0$, $k_4 < 0$, $k_3 k_6 < 0$, $\{k_2, k_5\} \in \mathbb{R}$, which is a rich variety of values where the filter works. We can select any value in these intervals and produce similar responses; nevertheless, we fix the values to $k_1 = -1$, $k_2 = 28$, $k_3 = -1$, $k_4 = -2.66$, $k_5 = 1$, which will be used in the rest of the paper.

4. Response to the Amplitude and Frequency

In this section, we present a study on the effect of the filter's response (6) as function of parameter's values of the sinusoidal input signal $u(t) = \mu \sin(\omega t)$. Figure 3(a) shows the output signals of the n-interconnected nonlinear filter for the cases $\mu = 1$, $\omega = 3$ and $\mu = 1$, $\omega = 5$. One can see that the orbits have a form of a Lissajous curve and the amplitude of the output signal as the frequency of the input signal is increased. In general, to see the effect of amplitude μ on the filter's response, we calculate the length of the Lissajous L in this way

$$L = \int_0^T \sqrt{\left(\dot{x}_1\right)^2 + \left(\dot{x}_2\right)^2} dt, \tag{19}$$

where T is the period of the orbit $(x_1(t), x_2(t))$. The effect of the input signal's frequency ω on the length L of the orbit of the filter's response is shown in Figure 3(b). Thus, L falls exponentially according to the increment of the frequency ω. System (6) presents a rejection to high frequencies because it is a low pass filter.

Now, fixing the frequency to $\omega = 1.0$ and varying the amplitude μ, we observe that new frequency components appear in the Fourier Transform (FT) of the output signal x_1. When the amplitude increases, then more peaks of frequency appear as multiples of the input signal's frequency. As is shown in Figures 4(a) and 4(b), $\mu = 1$ and 5, respectively. This is a characteristic of a nonlinear filter that linear filters do not present.

The nonlinear filters display assorted behaviors, that is, contrary to the example shown in Figure 4, where the amplitude is fixed to $\mu = 10$ and frequency ω is varied. Figures 5(a) and 5(b) show the FT of the response of the filter (6) for $\omega = 1$ and $\omega = 2$, respectively. Comparing both plots of Figure 5, we see that frequency peaks appear at multiples of input signal's frequency ω.

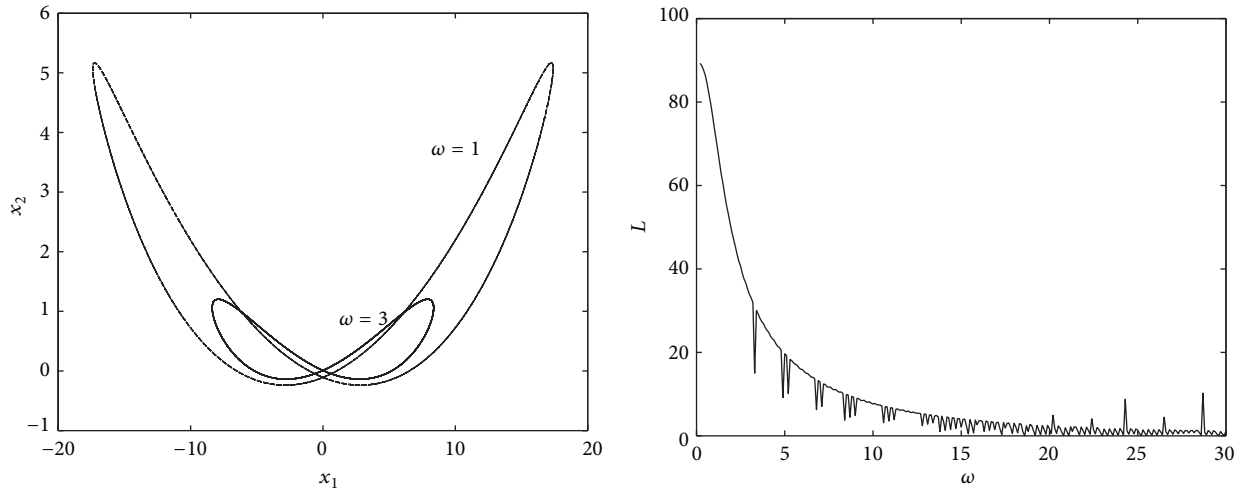

Figure 3: (a) The orbits of two Lissajous curves calculated by forcing system (6) with $\mu = 1$ and $\omega = 1, 3$. (b) We can see how the size of the Lissajous curve L falls exponentially, as ω increments its value.

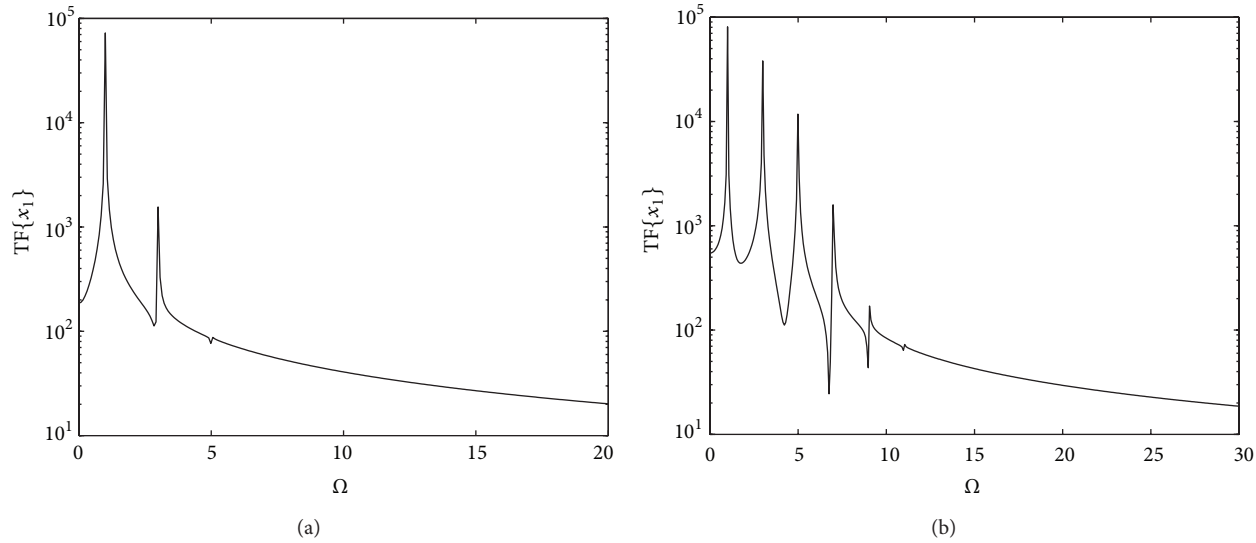

Figure 4: Both plots are the FT for the state x_1 of the filter (6) when it is filtering the input signal $u = \mu \sin(t)$ for the cases (a) $\mu = 1.0$ and (b) $\mu = 5$. These graphs show that when μ is incremented, new component frequency peaks appear in the power spectrum of the filter's response.

4.1. A Theoretical Justification. For the purpose of giving a theoretical justification of the behavior of the filter (6) when it is forced by the sinusoidal signals, we can see in the interconnected nonlinear filter (6) that $\dot{x}_1$ and $\dot{x}_2$ are linear first-order differential equations which can be rewritten in the next form:

$$x_1(t) = \mu e^{k_1 t}\left(k_2 \int e^{-k_1 t} \sin(\omega t)\, dt + k_4 \int e^{-k_1 t} \sin(\omega t)\, x_2(t)\, dt\right), \tag{20}$$

$$x_2(t) = k_6 \mu e^{k_5 t} \int e^{-k_5 t} \sin(\omega t)\, x_1(t)\, dt. \tag{21}$$

Without loss of generality and for seeking clarity, we consider the parameter $k_5 = 0$. Applying integration by parts to (20) and considering that the states $x_1(t)$ and $x_2(t)$ are functions that depend on time and frequency and that μ is a constant, we have the following:

$$\begin{aligned} x_1(t) = \frac{-\mu}{\omega^2 + k_1^2}\Big(&k_2\left(k_1 \sin(\omega t) + \omega \cos(\omega t)\right) \\ &+ k_3\left(k_1 \sin(\omega t) + \omega \cos(\omega t)\, x_2(t)\right) \\ &- k_4 e^{k_1 t} \int e^{-k_1 t}\left(k_1 \sin(\omega t) + \omega \cos(\omega t)\right) \dot{x}_2 dt\Big). \end{aligned} \tag{22}$$

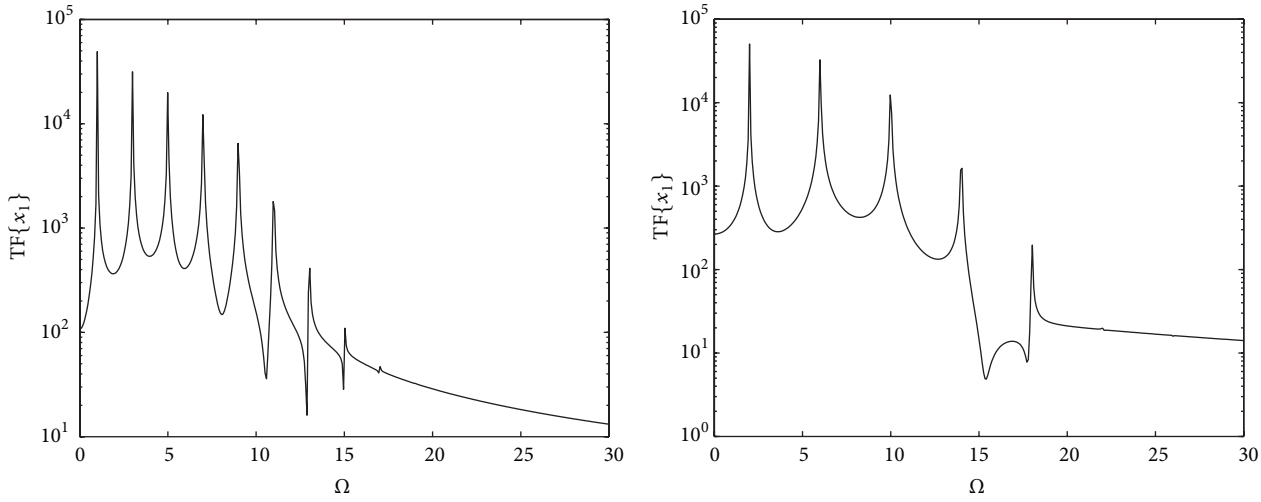

Figure 5: Both plots are the FT of the state x_1 of the filter (6) when it is filtering the input signal $u = 10\sin(\omega t)$ for the cases (a) $\omega = 1$ and (b) $\omega = 2$.

And for (21) we have

$$x_2(t) = \frac{-\mu k_6}{\omega^2 + k_5^2}\left(\left(k_5\sin(\omega t) + \omega\cos(\omega t)\right)x_1(t) - e^{k_5 t}\int e^{-k_5 t}\left(k_5\sin(\omega t) + \omega\cos(\omega t)\right)\dot{x}_1 dt\right). \tag{23}$$

Note that in (22) and (23), the magnitude values of $x_1(t)$ and $x_2(t)$ decrease when the frequency ω increases. Furthermore, since the terms

$$e^{k_1 t}\int e^{-k_1 t}\left(k_1\sin(\omega t) + \omega\cos(\omega t)\right)\dot{x}_2 dt, \quad e^{k_5 t}\int e^{-k_5 t}\left(k_5\sin(\omega t) + \omega\cos(\omega t)\right)\dot{x}_1 dt \tag{24}$$

have factors $(\omega^2 + k_5^2)^n$, $(\omega^2 + k_1^2)^n$ for $n \leq -2$, then we approximate (22) and (23) to

$$x_1(t) \approx -\frac{\mu}{\omega^2 + k_1^2}\left(k_2 G_1(t) + k_3 G_1(t)\, x_2(t)\right), \tag{25}$$

$$x_2(t) \approx -\frac{\mu k_6}{\omega^2 + k_5^2} G_2(t)\, x_1(t), \tag{26}$$

where $G_1(t) = k_1\sin(\omega t) + \omega\cos(\omega t)$, $G_2(t) = k_5\sin(\omega t) + \omega\cos(\omega t)$ are periodic functions with period given by the input signal. Substituting (25) in (26), we have

$$x_1(t) \approx -\frac{\mu k_2 G_1(t)}{\omega^2 + k_1^2} + \frac{\mu^2 k_4 k_8 G_1(t) G_2(t)}{\left(\omega^2 + k_1^2\right)\left(\omega^2 + k_5^2\right)} x_1(t). \tag{27}$$

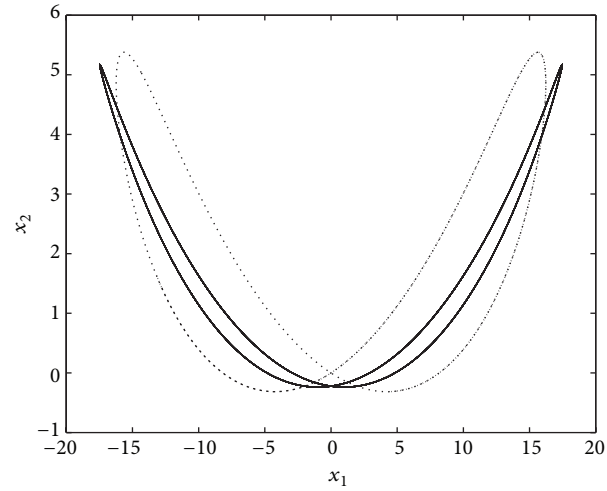

Figure 6: Comparison of Lissajouses. Lissajous with solid line corresponds to the solution of system (6) and Lissajous with dashed line corresponds to its approximated solution plotted with the parametric equations (28) and (29).

Now, solving for $x_1(t)$ from (27), it results that

$$x_1(t) \approx \frac{-\mu k_2\left(\omega^2 + k_5^2\right) G_1(t)}{\omega^4 + \left(k_1^2 + k_5^2\right)\omega^2 + k_1^2 k_5^2 - \mu^2 k_3 k_6 G_1(t) G_2(t)}. \tag{28}$$

And for $x_2(t)$ it results that

$$x_2(t) \approx \frac{\mu^2 k_2 k_6 G_1(t) G_2(t)}{\omega^4 + \left(k_5^2 + 1\right)\omega^2 + k_5^2 - \mu^2 k_3 k_6 G_1(t) G_2(t)}. \tag{29}$$

Figure 6 shows the orbit of the solution of (28) and (29) and the orbit of the numerical solution of the filter (6) when

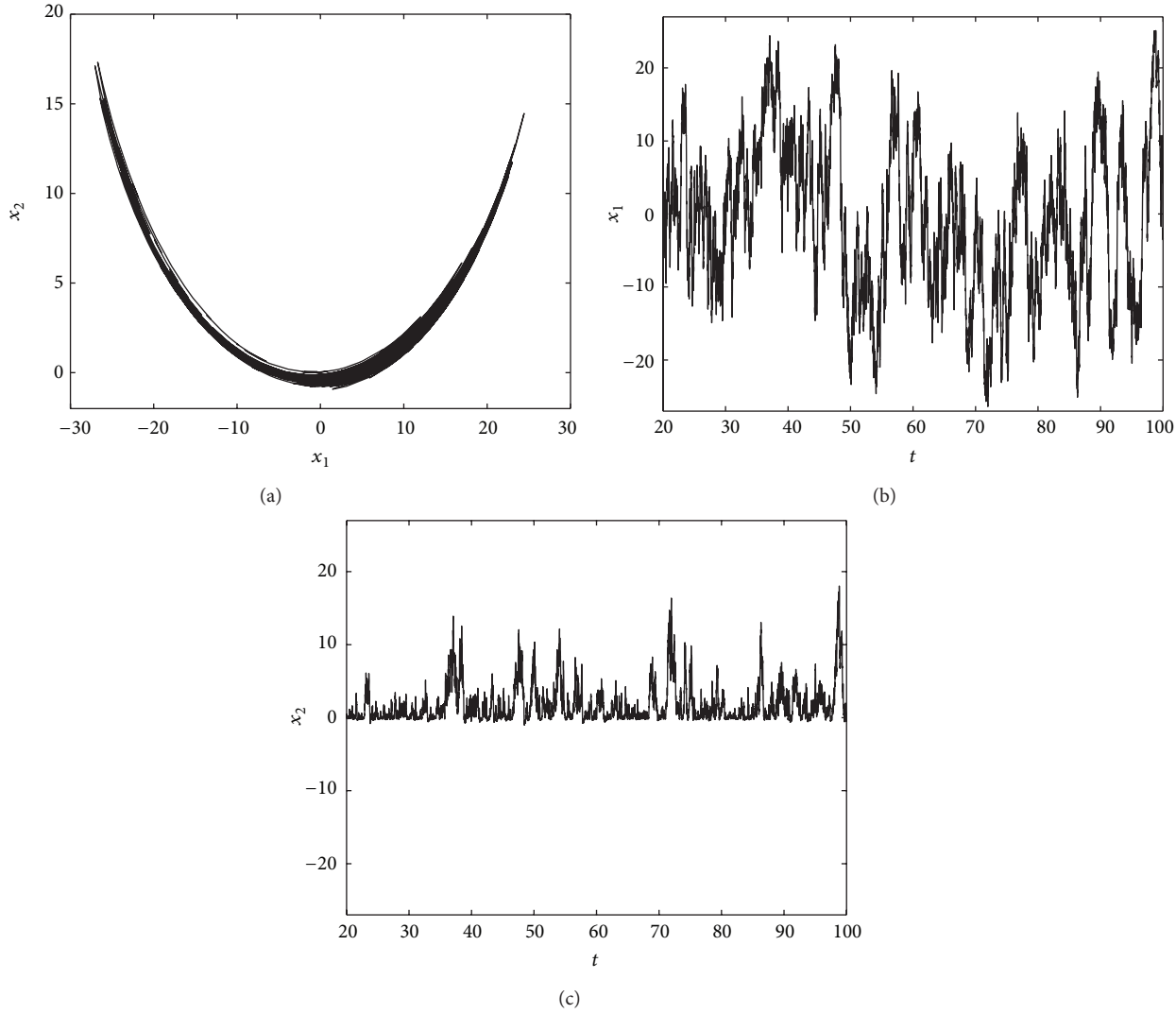

FIGURE 7: Plots of the filter's response (6) when a random input signal $u = 10\eta(t)$ is filtered. (a) The phase space (x_1, x_2). The time series (b) $x_1(t)$ and (c) $x_2(t)$.

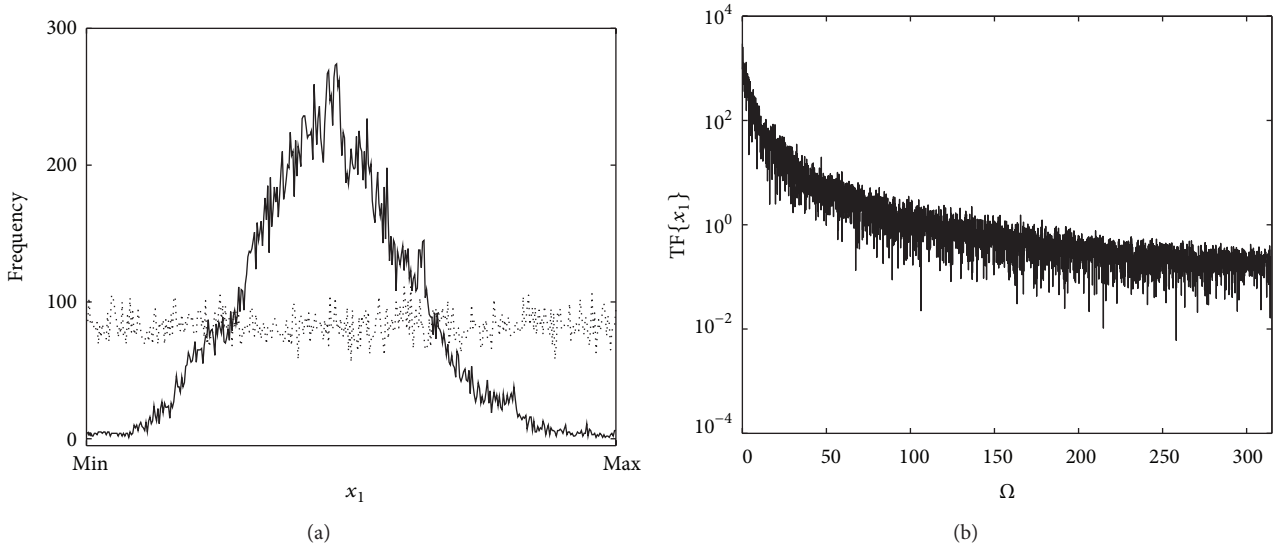

FIGURE 8: Response of the filter (6) when it is forced by the random signal $u = \eta(t)$. (a) Graphs of the histograms of the state x_1 (continuous line) and histogram of the external input signal u (dotted line). (b) TF of the component x_1.

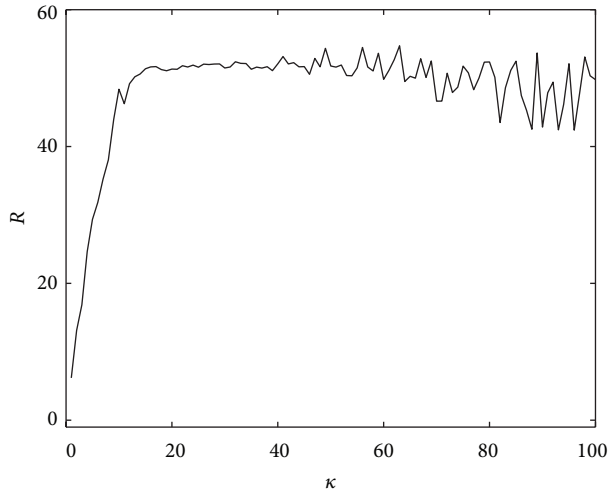

Figure 9: Range of values of the state x_1 in function of the κ when system (6) filters random signal.

$\mu = 1.0$ and $\omega = 1.0$. The thin Lissajous curve is calculated with (6) and another with (28) and (29). We can see that both orbits oscillate in a Lissajous curve of one knot and the same symmetric form with respect to the y-axis, but slightly different amplitude.

Now, we analyze the FT of the equations of system (6) which are given as follows:

$$j\Omega X_1(\Omega) = k_1 X_1(\Omega) + k_2 \mathrm{FT}\{u\} + k_3 \mathrm{FT}\{u x_2\}, \quad (30)$$

$$j\Omega X_2(\Omega) = k_5 X_2 + k_6 \mathrm{FT}\{u x_1\}(\Omega), \quad (31)$$

where $\mathrm{FT}\{x_i\} = X_i(\Omega)$ is the FT of the signal x_i. For the case when $u = \mu \sin(\omega t)$, we have

$$\begin{aligned}\Omega X_1(\Omega) = {} & -jk_1 X_1(\Omega) + \frac{k_3\mu}{2}\left(X_2(\Omega+\omega) - X_2(\Omega-\omega)\right) \\ & + k_2\mu\pi\left(\delta(\Omega+\omega) - \delta(\Omega-\omega)\right), \\ \Omega X_2(\Omega) = {} & -jk_5 X_2(\Omega) + \frac{k_6\mu}{2}\left(X_1(\Omega+\omega) - X_1(\Omega-\omega)\right).\end{aligned} \quad (32)$$

Now, solving for $X_1(\Omega)$ and $X_2(\Omega)$, we have

$$\begin{aligned}X_1(\Omega) = {} & \frac{\mu}{\Omega + jk_1}\left[k_2\pi\left(\delta(\Omega+\omega) - \delta(\Omega-\omega)\right)\right. \\ & \left. + \frac{k_3}{2}\left(X_2(\Omega+\omega) - X_2(\Omega-\omega)\right)\right],\end{aligned} \quad (33)$$

$$X_2(\Omega) = \frac{\mu k_6}{2(\Omega + jk_5)}\left[X_1(\Omega+\omega) - X_1(\Omega-\omega)\right]. \quad (34)$$

Equations (33) and (34) show that variables x_1, x_2 have the form of low pass filters (as we commented previously). Thus, the terms $X_2(\Omega-\omega)$ and $X_2(\Omega+\omega)$ in (33) are as follows:

$$\begin{aligned}X_2(\Omega-\omega) &= \frac{k_6\mu}{2(\Omega - \omega + jk_5)}\left[X_1(\Omega) - X_1(\Omega-2\omega)\right], \\ X_2(\Omega+\omega) &= \frac{k_6\mu}{2(\Omega + \omega + jk_5)}\left[\left(X_1(\Omega+2\omega) - X_1(\Omega)\right)\right],\end{aligned} \quad (35)$$

and using (33) and (35), we obtain

$$\begin{aligned}X_1(\Omega) = {} & \frac{\mu D}{\Omega + jk_1}\left[k_2\pi\left(\delta(\Omega+\omega) - \delta(\Omega-\omega)\right) + \frac{\mu k_3 k_6}{2}\right. \\ & \left.\times\left(\frac{X_1(\Omega+2\omega)}{2(\Omega+\omega+jk_5)} + \frac{X_1(\Omega-2\omega)}{2(\Omega-\omega+jk_5)}\right)\right],\end{aligned} \quad (36)$$

where

$$D = \frac{2\left((\Omega + jk_5)^2 - \omega^2\right)(\Omega + jk_1)}{2\left(\left((\Omega + jk_5)^2 - \omega^2\right)(\Omega + jk_1) + \mu^2 k_3 k_6 (\Omega + jk_5)\right)}. \quad (37)$$

Equation (36) has the terms $X_1(\Omega - 2\omega)$ and $X_1(\Omega + 2\omega)$, which are calculated by developing recursively (33), giving as a result

$$\begin{aligned}X_1(\Omega-2\omega) = {} & \frac{\mu}{\Omega - 2\omega + jk_1}\left[k_2\pi\left(\delta(\Omega-\omega) - \delta(\Omega-3\omega)\right)\right. \\ & \left. + \frac{k_3}{2}\left(X_2(\Omega-\omega) - X_2(\Omega-3\omega)\right)\right], \\ X_1(\Omega+2\omega) = {} & \frac{\mu}{\Omega + 2\omega + jk_1}\left[k_2\pi\left(\delta(\Omega+3\omega) - \delta(\Omega+\omega)\right)\right. \\ & \left. + \frac{k_3}{2}\left(X_2(\Omega+3\omega) - X_2(\Omega+\omega)\right)\right].\end{aligned} \quad (38)$$

Equations (33) and (38) show that $X_1(\Omega)$ have terms which contain factors $\delta(\Omega - 3\omega)$, $\delta(\Omega - \omega)$, $\delta(\Omega + \omega)$, and $\delta(\Omega + 3\omega)$ and if we develop recursively n times (33), then new terms of the form $\mu^{|k|}\delta(\Omega - (2k+1)\omega)D_k$ for $-n \le k \le n$ appear in the solution of $X_1(\Omega)$, where D_k is a so complex factor which depends on every parameter and variable of (32) and for $\mu < 1.0$ the quotient $|\mu^k|/|D_k| \approx 0$. Therefore, when the amplitude μ is incremented, then the amplitude of the peaks $\delta(\Omega - (2k+1)\omega)$ does too. For this reason, the numerical evidence shows that if the parameter input signal μ is incremented, then apparently new components of frequency appear in the spectrum $X_1(\Omega)$. These frequencies always form part of $X_1(\Omega)$ but with a very small amplitude. They are so small that they look like noise.

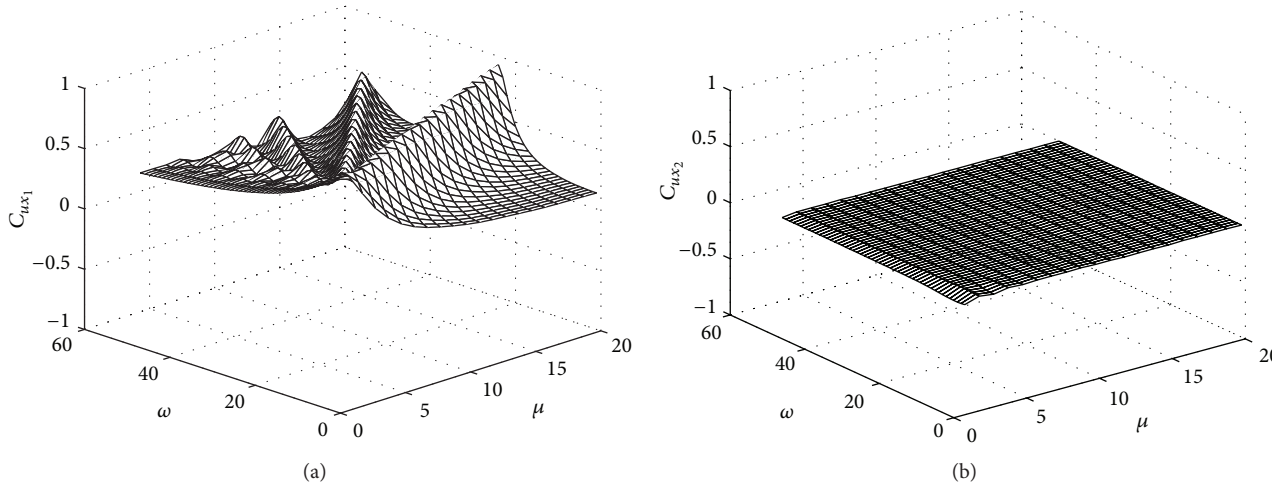

FIGURE 10: Correlation between the response of the filter (6) and the input signal $u = \mu \in (\omega t)$: (a) C_{ux_1} and (b) C_{ux_2}.

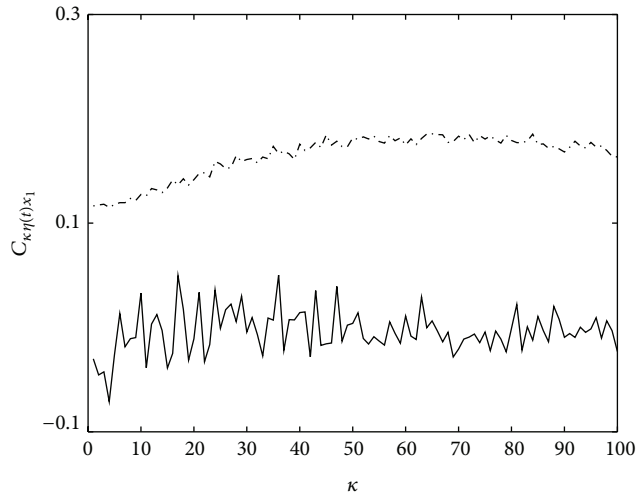

FIGURE 11: Correlation in function of the parameter of the random input signal κ. Dashed line and continuous line correspond to C_{ux_1} and C_{ux_2}, respectively.

5. Response to Random Signals

Now, let $u = \kappa\eta(t)$, where $\eta(t)$ is a random signal equidistributed on the interval $[-1, 1]$ and κ is its amplitude. When $u = 10\eta(t)$ is the input signal of the filter (6), the phase space of the response is a limit cycle that has the form of a quarter moon which is shown in Figure 7(a). As a first glimpse the filter's response seems to be a periodic orbit like in the case of the sinusoidal input signal, but the time series $x_1(t)$ and $x_2(t)$, which are respectively shown in Figures 7(b) and 7(c), are aperiodic signals.

The following remarks are pertinent.

(i) The output signal of the filter has a normal (or Gaussian) distribution when the input signal is random with uniform distribution. For the case $u = \eta(t)$, Figures 8(a) and 8(b) show the histogram and the FT of the x_1 signal, respectively, where one can see that the FT of the response has an exponential decay.

(ii) The filter presents saturation after a threshold value of the amplitude of input signal $u = \kappa\eta(t)$. Figure 9 shows the range of values $R(\kappa) = \text{MAX}\{x_1\} - \text{MIN}\{x_1\}$ of the response x_1 versus the amplitude of the parameter κ.

To justify the exponential decay of the filter's response when it is forced with random signal, we consider $\text{FT}\{u\} = K_1$, where K_1 is a constant which depends on κ, the amplitude of the random signal, and $x_3 \ll \text{FT}\{u\}$. Thus the following terms of (30) are $k_2\text{FT}\{u\} = k_2K_1$ and $\text{FT}\{ux_2\} \approx K_2$, where K_2 depends on κ too. So, the FT results are

$$j\Omega X_1(\Omega) \approx -X_1(\Omega) - K_2 + rK_1, \tag{39}$$

and for the magnitude of $X_1(\Omega)$ we have

$$\left|X_1(\Omega)\right| \approx \left|\frac{rK_1 + K_2}{1 + \Omega^2}\right|. \tag{40}$$

Figure 8(b) shows the form of the curve $|X_1(\Omega)|$ which corresponds to (40).

6. Correlation Coefficient

Because a filter acts in function of the input signal, another way to characterize the effect of the input signal on the filter's response is to compute the correlation between the input and output signals. If we have time series of N data, the correlation coefficient C_{xy} of series $x(i)$ and $y(i)$ is defined as

$$C_{xy} = \frac{\sum_{i=1}^{N}(x(i) - \overline{x})(y(i) - \overline{y})}{(N-1)S_xS_y}, \tag{41}$$

where $\overline{x}$, $\overline{y}$ are the means and s_x, s_y are the standard deviations of the series $x(i)$ and $y(i)$, respectively. We calculate correlation coefficients for different input signals and the

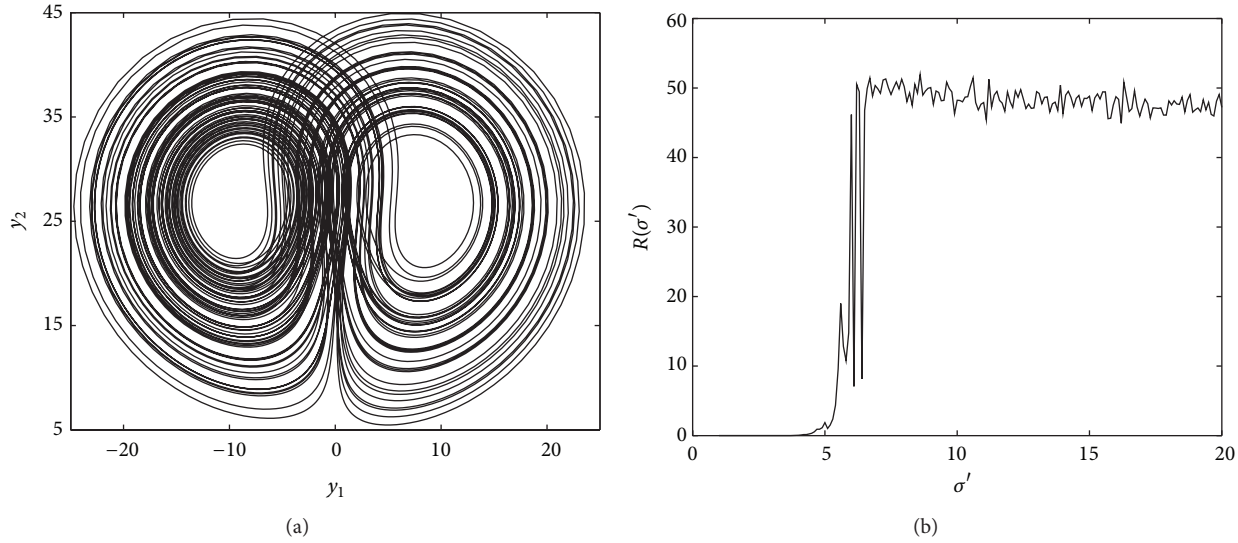

Figure 12: (a) Orbit of the filter (43) when the external input is $u = y_1$ of system (42). (b) The maximal range of response of system (43).

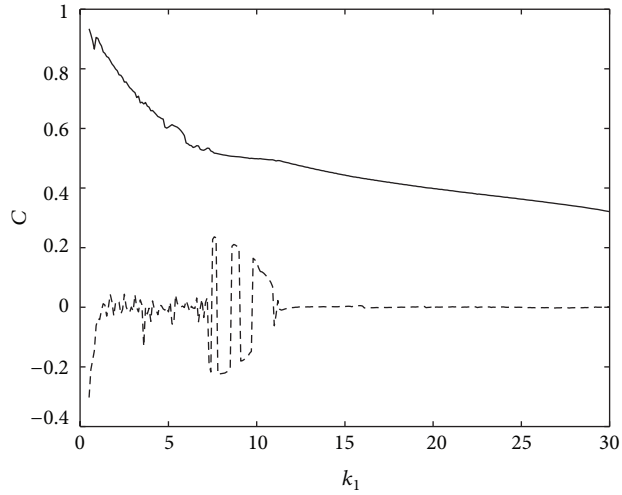

Figure 13: Correlation between state variables against the parameter κ_1. The continuous line and the dashed line correspond to $C_{y_1y_2}$, $C_{y_1y_3}$, respectively.

Table 1: Coefficient correlations between different input signals and the responses x_1, x_2 of the filter (6).

External force u	C_{x_1u}	C_{x_2u}
$\sin(t)$	0.7455	−0.0021
The state variable x_1 of the Rössler system	0.7453	0.0574
$\eta(t)$	0.1160	0.0630

output signals x_1 and x_2 which are given in Table 1. The first two cases in Table 1 correspond to a periodic and chaotic signals, $C_{ux_1} \approx 0.745$ and $C_{ux_2} \approx 0.0$, and the last case considers a random signal as an input signal.

We make a further numerical study of the coefficient correlation in function of the parameters of the sinusoidal input signal. In Figure 10(a), we can see that the correlation between sinusoidal external signals is not constant and that it depends on both parameters μ and ω. On the contrary, Figure 10(b) shows that the absence of correlation between the response x_2 and their respective forces is independent of almost the whole range of values of the input signal parameters.

On the other hand, the last row in Table 1 shows that $C_{ux_1} \approx 0.1160$ and $R_{ux_2} \approx 0.0630$. This means that the filter's response (6) does not have correlation when the input is a random signal. Despite the fact that the amplitude of the parameter κ is increased, the output signal of the filter does not have correlation with input signal (random), as shown in Figure 11. Therefore, the correlation between the input random signal and its filter's response cannot be induced by incrementing the value of its amplitude. A similar result occurs for the sinusoidal signal and its response x_2.

7. Low Pass Filters in Chaotic Systems

The Lorenz system is a very well-known third-order chaotic system [11] which is defined as

$$\begin{aligned} \dot{y}_1 &= -\sigma y_1 + \sigma y_2, \\ \dot{y}_2 &= r y_1 - y_2 - y_1 y_3 \\ &= -y_2 + (r - y_3)\, y_1, \\ \dot{y}_3 &= y_1 y_2 - b y_3 = -b y_3 + y_2 y_1, \end{aligned} \tag{42}$$

where $\mathbf{y} = (y_1, y_2, y_3)^T$ is the state vector and σ, r, and b are parameters. Each component of system (42) is defined based on low pass filters. For example, the first equation is a linear low pass filter, where the state variables y_1 and y_2 are the input and output signals, respectively. The second and third equations comprise a *two*-interconnected nonlinear filter whose outputs are y_2 and y_3, and the input signal is

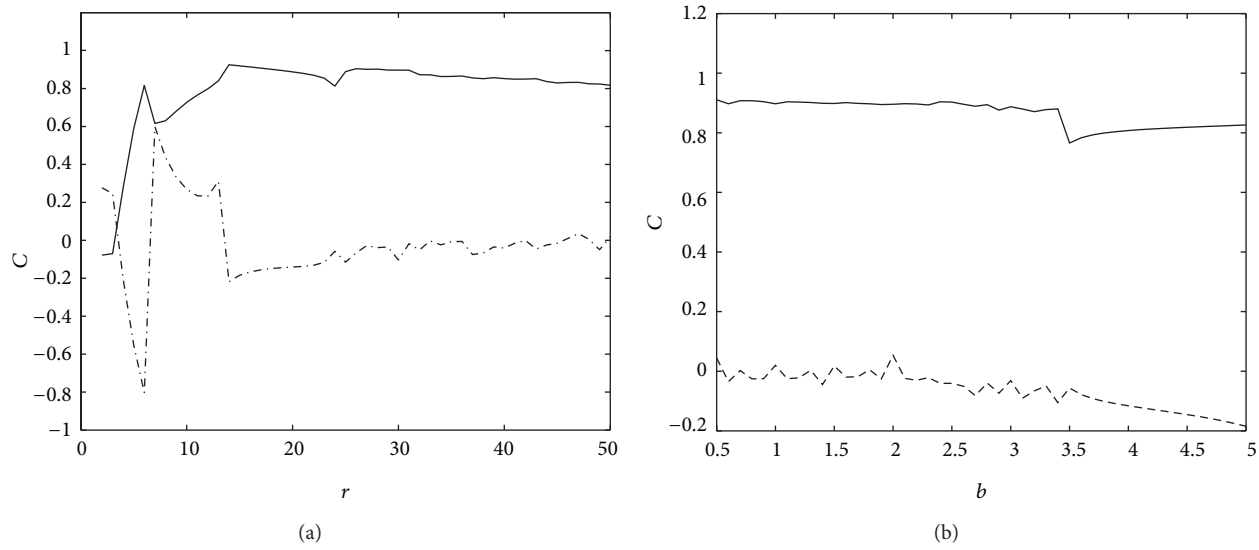

Figure 14: Correlations between the state variables of the Lorenz system (42) against the parameters (a) r and (b) b. Each continuous line and dashed line correspond to $C_{y_1y_2}, C_{y_1y_3}$, respectively.

$u = y_1$. The *two*-interconnected nonlinear filter of the Lorenz system (42) can be rewritten in terms of (7) as follows:

$$K = \begin{pmatrix} -1 & 0 \\ 0 & -b \end{pmatrix}, \qquad B = \begin{pmatrix} r \\ 0 \end{pmatrix}, \qquad f(x,u) = \begin{pmatrix} uy_3 \\ uy_2 \end{pmatrix}, \tag{43}$$

where $x_1 = y_2$, $x_2 = y_3$, and $u = y_1$. The projection of the Lorenz attractor onto the plane (y_1, y_2) is shown in Figure 12(a) for the following parameter's values: $\sigma = 10$, and $b = 2.66$, and $r = 28.0$. In order to study the response of the interconnected system (43) when the input signal is the state variable y_1, we have calculated $R(\sigma)$ which is the maximal range of values of the time series y_2. In Figure 12(b), we can see that $R \approx 0$ for $0 \leq \sigma \leq 5$; this means that the solution converges to a fixed point. For $\sigma \in [5, 7]$, there is a transition period in the behavior of the filter, and for $\sigma \geq 7$ the range of values of the filter's response is approximately constant.

When calculating the correlation coefficient between the components of the *two*-interconnected system (43), it results that $C_{y_1y_2} = 0.9022$, $C_{y_1y_3} = -0.0384$, and $C_{y_2y_3} = -0.0424$. The high correlation between the state variables y_1 and y_2 occurs because of y_1 is a simple low pass lineal filter for the signal y_2 without any nonlinear term included in its equation (see $\dot{y}_1$ in (42)). On the other hand, the time series y_1 has no correlation with y_3 which could be induced by the nonlinear term settles in the equation $\dot{y}_3$ of system (42). Now, we put a parameter to control the amplitude of the input signal such that $u = \kappa_1 y_1$ and calculate $C_{y_1y_2}$ and $C_{y_2y_3}$ as a function of the parameter k_1. In Figure 13, it is shown that only $C_{y_1y_2}$ is affected when the value of κ_1 is incremented, while the absence of correlation between states y_2 and y_3 remains for all values of κ_1. For $\kappa_1 > 32$, the trajectories of system (43) diverge.

We have shown by means of numerical experiments in previous sections that the absence of correlation between the external force u and the state variable x_2 of the filter response generally does not depend on the parameters of the input signal. Similar result occurs when the Lorenz autonomous system is considered like a *two*-interconnected system which is forced by the signal $u = y_1$. As shown in Figure 13, there exists a high correlation between the state variables y_1 and y_2, and an absence of correlation between state variables y_2 and y_3. But can the correlation between the state variables y_1 and y_2 be incremented by changing the value of the parameters of the Lorenz system? With the purpose of answering this question, we have calculated $C_{y_1y_2}, C_{y_1y_3}$ as a function of the autonomous Lorenz system parameter r keeping the value of the parameter b constant and vice versa. Figure 14(a) shows that for $r < 15$ approximately, correlations $C_{y_1y_2}, C_{y_1y_3}$ have a transition period, and for $r \geq 15$, the correlations return to their previously showed behavior: $C_{y_1y_2} \approx 1.0$ and $C_{y_1y_3} \approx 0$. Figure 14(b) shows that the parameter b does not affect the correlation between y_1 and the responses y_2, y_3.

If Lorenz system parameters are tuned so that the Lorenz system behaves as a filter and can be used as a slave system, then generalized synchronization of master and slave systems always appears.

8. Conclusions

An n-interconnected nonlinear system given by (6) always behaves as a filter if the condition given by Theorem 4 is satisfied. Despite of the nonlinearities in the structure of n-interconnected nonlinear system, its dynamical behavior does not depend on the initial conditions but it does as a function of the input signal. The nonlinear filter's response to sinusoidal input signal presents several interesting phenomena such as (i) frequency components at multiples of the input signal's frequency (ii) when the amplitude of the input

signal increases, the number of peaks of the filter's response increases (iii) the amplitude of the filter's response falls exponentially as a function of the input signal's frequency.

The Lorenz system is described in terms of low pass filters which consists of a linear low pass filter and a *two*-interconnected nonlinear low pass filter. This gives us the possibility to describe all the systems that conform the Lorenz family and others with similar structure in terms of low pass filters.

In several studies of chaos synchronization, specifically in forced systems $\dot{\mathbf{x}} = f(\mathbf{x}, u)$, $\mathbf{x} \in \mathbb{R}^n$, it has been found that generalized synchronization of response systems occurs for specific external signals u, but all these cases satisfy condition (8). Then, the general synchronization phenomenon and the phenomenon of nonlinear filter are seen to be the same. Nevertheless, condition (8), in generalized synchronization phenomenon, could not be satisfied, because of the trajectories generated with different initial conditions asymptotically could go to a different basin of attractions. This characteristic is different to the phenomenon of nonlinear filter which by definition condition (8) needs to be always satisfied if a system behaves like a nonlinear filter. Several chaotic systems have a similar structure to n-interconnected system, so that we conjecture that this study can help to distinguish between generalized synchronization behavior and nonlinear filtering behavior of an n-interconnected system.

Acknowledgments

The authors would like to thank Emanuel Rodríguez-Orozco for reading the paper and giving constructive comments. E. Jiménez-López is a doctoral fellow of CONACYT in the Graduate Program on Applied Science at UASLP, and IPICYT for the hospitality during his sojourn in DMAp-IPICYT. E. Campos-Cantón acknowledges CONACYT for the financial support through Project no. 181002.

References

[1] L. M. Pecora and T. L. Carroll, "Synchronization in chaotic systems," *Physical Review Letters*, vol. 64, no. 8, pp. 821–824, 1990.

[2] I. Campos-Cantón, E. Campos-Cantón, J. S. Murgúa-Ibarra, and M. E. Chavira-Rodríguez, "Secure communication system using chaotic signals," *Ingeniería, Investigación y Tecnología*, vol. 10, no. 1, 2009.

[3] M. G. Rosenblum, A. S. Pikovsky, and J. Kurths, "From phase to lag synchronization in coupled chaotic oscillators," *Physical Review Letters*, vol. 78, no. 22, pp. 4193–4196, 221997.

[4] M. G. Rosenblum, A. S. Pikovsky, and J. Kurths, "Phase synchronization of chaotic oscillators," *Physical Review Letters*, vol. 76, no. 11, pp. 1804–1807, 1996.

[5] V. S. Anishchenko, T. E. Vadivasova, D. È. Postnov, and M. A. Safonova, "Synchronization of chaos," *International Journal of Bifurcation and Chaos in Applied Sciences and Engineering*, vol. 2, no. 3, pp. 633–644, 1992.

[6] H. D. I. Abarbanel, N. F. Rulkov, and M. M. Sushchik, "Generalized synchronization of chaos: the auxiliary system approach," *Physical Review E*, vol. 53, no. 5, pp. 4528–4535, 1996.

[7] E. Campos, J. Urías, and N. F. Rulkov, "Multimodal synchronization of chaos," *Chaos*, vol. 14, no. 1, pp. 48–54, 2004.

[8] L. Ontañón-García, E. Campos-Cantón, R. Femat, I. Campos-Cantón, and M. Bonilla-Marín, "Multivalued synchronization by poincar coupling," *Communications in Nonlinear Science and Numerical Simulation*.

[9] J. S. González Salas, E. Campos Cantón, F. C. Ordaz Salazar, and I. Campos Cantón, "Forced synchronization of a self-sustained chaotic oscillator," *Chaos*, vol. 18, no. 2, Article ID 023136, p. 9, 2008.

[10] E. C. Cantón, J. S. C. Salas, and J. Urías, "Filtering by nonlinear systems," *Chaos*, vol. 18, no. 4, Article ID 043118, p. 4, 2008.

[11] E. N. Lorenz, "Deterministic nonperiodic flow," *Journal of the Atmospheric Sciences*, vol. 20, pp. 130–141, 1963.

[12] L. V. Turukina and A. Pikovsky, "Hyperbolic chaos in a system of resonantly coupled weakly nonlinear oscillators," *Physics Letters A*, vol. 375, no. 11, pp. 1407–1411, 2011.

Hindawi Publishing Corporation
Abstract and Applied Analysis
Volume 2013, Article ID 483269, 7 pages
http://dx.doi.org/10.1155/2013/483269

Research Article

Effective Synchronization of a Class of Chua's Chaotic Systems Using an Exponential Feedback Coupling

Patrick Louodop,[1] Hilaire Fotsin,[1] Elie B. Megam Ngouonkadi,[1] Samuel Bowong,[2] and Hilda A. Cerdeira[3]

[1] *Laboratory of Electronics, Department of Physics, Faculty of Science, University of Dschang, P.O. Box 67, Dschang, Cameroon*
[2] *Laboratory of Applied Mathematics, Department of Mathematics and Computer Science, Faculty of Science, University of Douala, P.O. Box 24157, Douala, Cameroon*
[3] *Instituto de Física Teórica-UNESP, Universidade Estadual Paulista, Rua Dr. Bento Teobaldo Ferraz 271, Bloco II, Barra Funda, 01140-070 São Paulo, SP, Brazil*

Correspondence should be addressed to Hilda A. Cerdeira; cerdeira@ift.unesp.br

Received 17 February 2013; Accepted 4 March 2013

Academic Editor: René Yamapi

A robust exponential function based controller is designed to synchronize effectively a given class of Chua's chaotic systems. The stability of the drive-response systems framework is proved through the Lyapunov stability theory. Computer simulations are given to illustrate and verify the method.

1. Introduction

Shortly after Pecora and Carroll showed the possibility of synchronizing chaotic elements [1], applications stretched out in many fields [2–4] giving rise to interdisciplinary research, since this phenomenon appears in many systems in a variety of ways [5–12]. Much research was done developing different strategies in the quest of effective synchronization such as adaptive synchronization [13–15], inverse synchronization [16], and antisynchronization [17–24]. The robustness of many of these methods, as surprising as it may appear, has already been demonstrated in many cases in the presence of noise, perturbations, or parameter mismatches [25–27].

For applications such as telecommunications, where the transmission of messages is not possible unless transmitter and receiver are synchronized [10–12], the investigation of new chaotic systems as well as the most effective means of synchronization is always of great importance. Thus, mathematical models [28, 29], mechanical systems [30], and electronic circuits [10, 13] are continually built. One of the best known electronic circuits is the Chua's oscillator [31, 32]. Although Chua's circuit is one of the simplest circuits in the literature, it has various complex chaotic dynamics properties which has made it a topic of extensive study [31–34]. A modified version of the circuit has also been topic of attention [33–35]. Its theoretical analysis and numerical simulations agree very well with experimental results.

Recently, some authors proposed a nonlinear controller in order to force synchronization with the purpose of saving energy [22, 23]. The nonlinear controllers used are based on bounded nonlinear functions [22, 23]. In this work we apply the exponential function based nonlinear controller to achieve synchronization between the drive-response systems when disturbances are present. Our controller has certain properties which makes it more advantageous to use it, such as the following properties: (1) it is easy to implement in practice; (2) it needs no adaptation algorithm; hence its electrical circuit remains simple; (3) it is faster than the synchronization based on fixed feedback gain which is usually used.

This work is organized as follows. In Section 2, the problem is formulated and the assumptions are given. Section 3 presents the main results. We use Lyapunov stability theory to study the robustness of our proposed controller. We show

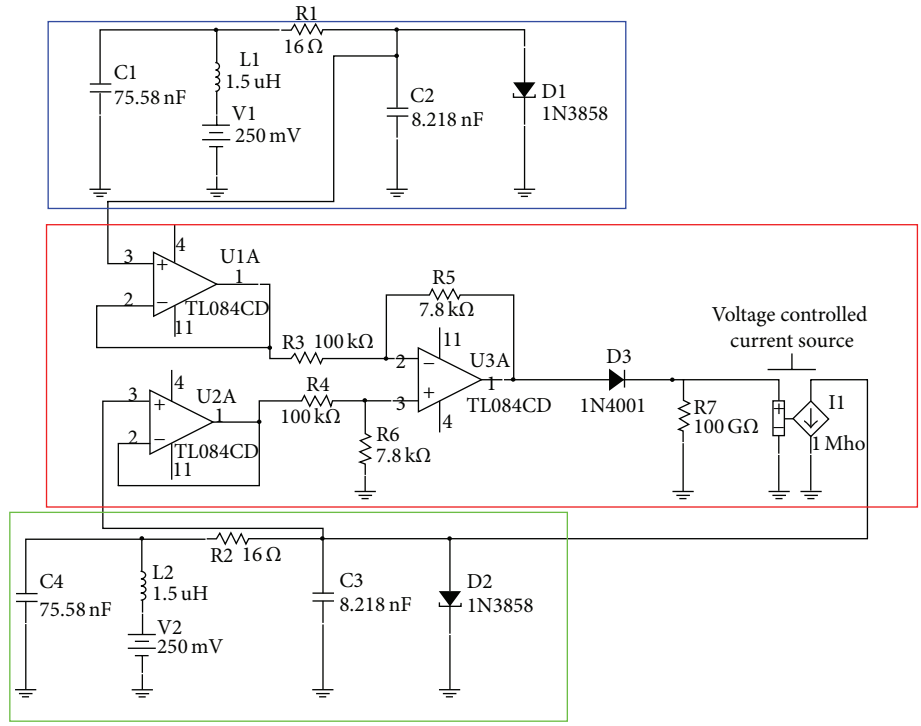

Figure 1: Scheme of the circuit for the whole system: transmitter (blue box), controller (red box), and receiver (green box).

that with this controller the drive and response systems are practically synchronized—the errors between the master system and the slave system do not tend to zero but to a limit value. In this case, it is shown that the derivative of Lyapunov function is contained in a closed domain to which the error between master and slave system converges. Since the error is sufficiently small, using the principle of the "ultimate boundedness property," we arrive to the conclusion that the system is globally stable because the derivative of the Lyapunov function is negatively definite. Ultimate boundedness is in particular compatible with local instability about zero and implies global stability. This was demonstrated by Ding and Cheng in [36]. They proposed a new criterion of globally uniformly ultimate boundedness for discrete-time nonlinear systems which helps to relax the condition of stability based on Lyapunov function. The same ideas were successfully applied by de la Sen and Alonso [37], while in [38], Bitsoris et al. work on the robust positive invariance and ultimate boundedness of nonlinear systems with unknown parameters and disturbances, where only their bounds of variance are known. In Section 4, numerical results are presented and we compare the given scheme with that using the simple fixed gain based controller. The conclusions are given in Section 5.

2. Formulation of the Problem

In this paper, we study the master-slave synchronization of a class of Chua's chaotic systems, represented in Figure 1 and described by the equations that follow.

The master system is given by:

$$\begin{aligned} \dot{x}_1(\tau) &= \alpha\left[x_2(\tau) - x_1(\tau) - Rf\left(x_1(\tau)\right)\right] + d(\tau), \\ \dot{x}_2(\tau) &= \beta\left[x_1(\tau) - x_2(\tau) + Rx_3(\tau)\right], \\ \dot{x}_3(\tau) &= \gamma\left[v(\tau) - x_2(\tau)\right], \end{aligned} \tag{1}$$

where τ is a dimensionless time, $x_i(t)$, $i = 1, 2, 3$, are the state variables, $v(\tau)$ is an external force, and α, β, γ, and R are positive constant parameters of the system. The function $f(x_1(\tau))$ represents the nonlinearity of the system and $d(\tau)$ the disturbances. The function $f(x_1(\tau))$ defines Chua's circuit, which is given by $f(x_1) = a_2x(\tau) + 0.5(a_1 - a_2)(|x_1(\tau) + 1| - |x_1(\tau) - 1|)$ [31, 33, 34], while the modified Chua's system is obtained using $f(x_1(\tau)) = ax_1^3$ [12] or $f(x_1(\tau)) = a_1(x_1 - b)^3 - a_2(x_1 - b) + a_3$ [32]. The latter represents the behavior of a tunnel diode [32]. For an autonomous system $v(\tau)$ is constant and $d(\tau) = 0$.

The slave system is given by

$$\begin{aligned} \dot{y}_1(\tau) &= \alpha\left[y_2(\tau) - y_1(\tau) - Rf\left(y_1(\tau)\right)\right] + U(\tau), \\ \dot{y}_2(\tau) &= \beta\left[y_1(\tau) - y_2(\tau) + Ry_3(\tau)\right], \\ \dot{y}_3(\tau) &= \gamma\left[v(\tau) - y_2(\tau)\right], \end{aligned} \tag{2}$$

where $y_i(\tau), i = 1, 2, 3$, is the slave state variables and $U(\tau)$ the feedback coupling.

Here we present a scheme to solve the synchronization problem for system (1). That is to say, if the uncertain system (1) is regarded as the drive system, a suitable response system

should be constructed to synchronize it with the help of the driving signal x. In order to do so, we assume the following:

(i) There is a bounded region $\mathcal{U} \subset R^3$ containing the whole basin of the drive system (1) such that no orbit of system (1) ever leaves it.

(ii) The disturbance $d(\tau)$ is bounded by an unknown positive constant D, namely,

$$\|d(\tau)\| \leq D, \tag{3}$$

where $\|\cdot\|$ denotes the euclidian norm of a vector.

(iii) All chaotic systems are supposed to be confined to a limited domain; hence there exists a positive constant L such that

$$\left\|f\left(y_1(\tau)\right) - f\left(x_1(\tau)\right)\right\| \leq L\left\|y_1(\tau) - x_1(\tau)\right\|. \tag{4}$$

We will now try to synchronize the systems described in (1) and (2) designing an appropriate control $U(\tau)$ in system (2) such that

$$\left\|y_i(\tau) - x_i(\tau)\right\| \leq r, \quad \text{for } \tau \longrightarrow \infty, \tag{5}$$

where r is a sufficiently small positive constant.

Let us define the state errors between the transmitter and the receiver systems as

$$e_i(\tau) = y_i(\tau) - x_i(\tau), \quad \text{with } i = 1, 2, 3, \tag{6}$$

and the feedback coupling as

$$U(\tau) = -\varphi\left(\exp\left(ke_1(\tau)\right) - 1\right), \tag{7}$$

where φ and k are positive fixed constants.

Introducing the definition of the systems (1), (2), and (7) into (2), the dynamics of the error states (6) becomes

$$\begin{aligned} \dot{e}_1(\tau) &= \alpha\left[e_2(\tau) - e_1(\tau) - R\left(f\left(y_1\right) - f\left(x_1\right)\right)\right] \\ &\quad - d(\tau) - \varphi\left(\exp\left(ke_1\right) - 1\right), \\ \dot{e}_2(\tau) &= \beta\left[e_1(\tau) - e_2(\tau) + Re_3(\tau)\right], \\ \dot{e}_3(\tau) &= -\gamma e_2(\tau). \end{aligned} \tag{8}$$

The problem is now reduced to demonstrating that with the chosen control law $U(\tau)$, the error states e_i, $i = 1, 2, 3$, in (8) are at most a sufficiently small positive constant r, which will prove the proposition.

3. Main Results

If we consider the master-slave chaotic systems (1) and (2) with all the aforementioned assumptions (3) and with the exponential function based feedback coupling given by the relation (7), we will show that the overall system will be practically synchronized, that is, $\|y_i(\tau) - x_i(\tau)\| \leq r$, where r is a sufficiently small positive constant for large enough τ.

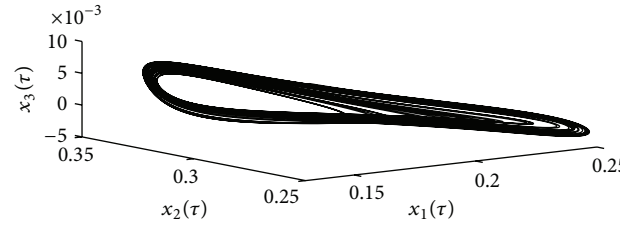

Figure 2: 3D chaotic attractor of the tunnel diode based modified Chua's system.

In order to do so, let us consider the following Lyapunov function:

$$V = \frac{1}{2}\left[\frac{e_1^2}{\alpha} + \frac{e_2^2}{\beta} + \frac{Re_3^2}{\gamma}\right]. \tag{9}$$

Differentiating the function V with respect to time yields

$$\begin{aligned} \dot{V} &= 2e_1e_2 - e_1^2 - e_2^2 - R\left(f\left(y_1\right) - f\left(x_1\right)\right)e_1 \\ &\quad - \frac{d(\tau)}{\alpha}e_1 - \frac{\varphi}{\alpha}\left[\exp\left(ke_1\right) - 1\right]e_1 \\ &= -\left(e_1 - e_2\right)^2 - R\left(f\left(y_1\right) - f\left(x_1\right)\right)e_1 \\ &\quad - \frac{d(\tau)}{\alpha}e_1 - \frac{\varphi}{\alpha}\left[\exp\left(ke_1\right) - 1\right]e_1. \end{aligned} \tag{10}$$

Expanding the exponential function as follows:

$$\begin{aligned} \exp\left(ke_1\right) - 1 \simeq ke_1 + \sum_{i=1}^{n}\frac{\left(ke_1\right)^{2i}}{2i!} + \sum_{i=1}^{n}\frac{\left(ke_1\right)^{2i+1}}{(2i+1)!} \\ + \theta\left(e_1\right) + \zeta\left(e_1\right), \end{aligned} \tag{11}$$

where $\theta(e_1)$ and $\zeta(e_1)$ constitute the rest of the expansion in order greater than n for odd part and for even part of the development, respectively, and substituting by the maximum value of the disturbance, D, it follows that

$$\begin{aligned} \dot{V} &\leq RLe_1^2 + \frac{D}{\alpha}\left|e_1\right| \\ &\quad - \frac{\varphi}{\alpha}\left(ke_1 + \sum_{i=1}^{n}\frac{\left(ke_1\right)^{2i}}{2i!} + \theta\left(e_1\right)\right)e_1. \end{aligned} \tag{12}$$

Hence, we have

$$\begin{aligned} \dot{V} &\leq \left(RL - \frac{\varphi}{\alpha}k\right)e_1^2 \\ &\quad + \frac{1}{\alpha}\left(D + \varphi\sum_{i=1}^{n}\frac{\left(k\left|e_1\right|\right)^{2i}}{2i!} + \left|\theta\left(e_1\right)\right|\right)\left|e_1\right|, \end{aligned} \tag{13}$$

$$\begin{aligned} \dot{V} &\leq \left(RL - \frac{\varphi}{\alpha}k\right)e_1^2 \\ &\quad + \frac{1}{\alpha}\left(D + \varphi\sum_{i=1}^{n}\frac{(kr)^{2i}}{(2i)!} + \Theta(r)\right)r, \end{aligned} \tag{14}$$

where $\Theta(r) \geq \max(\theta(e_1))$.

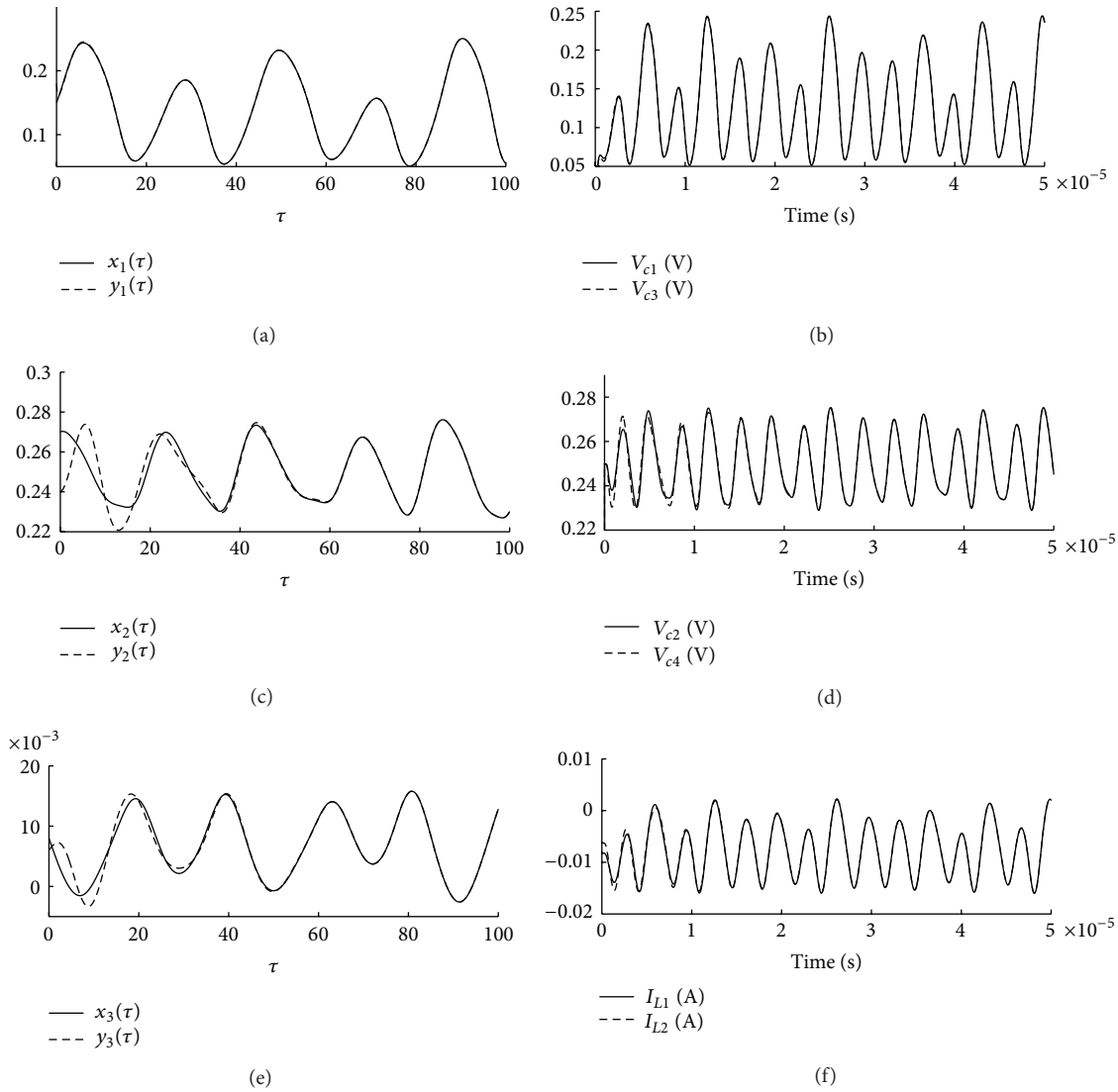

FIGURE 3: Time evolution of the master system (solid lines) and slave system (dashed lines) from Matlab simulations (left) and Pspice simulations (right).

Here we use r as an upper bound for the error in each axis. Then we see that the derivative of the Lyapunov function (12) is lower than that in (13), which in turn is smaller than the one given by (14). Thus expression (14) is maximized and the radius of the close domain to which the error is attracted is determined. Defining

$$\varphi \geq \frac{\alpha RL}{k}, \qquad \phi = \left(\frac{D + \Theta(r)}{\alpha} + \frac{RL}{k} \sum_{i=1}^{n} \frac{(kr)^{2i}}{(2i)!} \right) r, \quad (15)$$

one obtains

$$\dot{V} \leq -\psi e_1^2 + \phi, \quad \text{where } \psi = \left| RL - \frac{\varphi}{\alpha} k \right|. \quad (16)$$

Equation (16) is in principle a form of the ultimate boundedness property in the sense that if the error is sufficiently small, then the system is globally stable because the upper-bound is negative [36]. From (16), it follows that if

$$\|e_1\| > \sqrt{\frac{\phi}{\psi}} \quad (17)$$

therefore, $\dot{V}(\tau) < 0$; hence $V(\tau)$ decreases, which implies that $\|e_1\|$ decreases. It then follows from standard invariance arguments as in [23] that asymptotically for increasing time the error satisfies the following bound

$$\|e_1\| < C, \quad (18)$$

for any $C > \sqrt{\phi/\psi}$.

So if ϕ is sufficiently small, the bound for the synchronization error will also be sufficiently small. Therefore, the synchronization state error would be contained within a neighborhood of the origin, as we wanted to prove. In

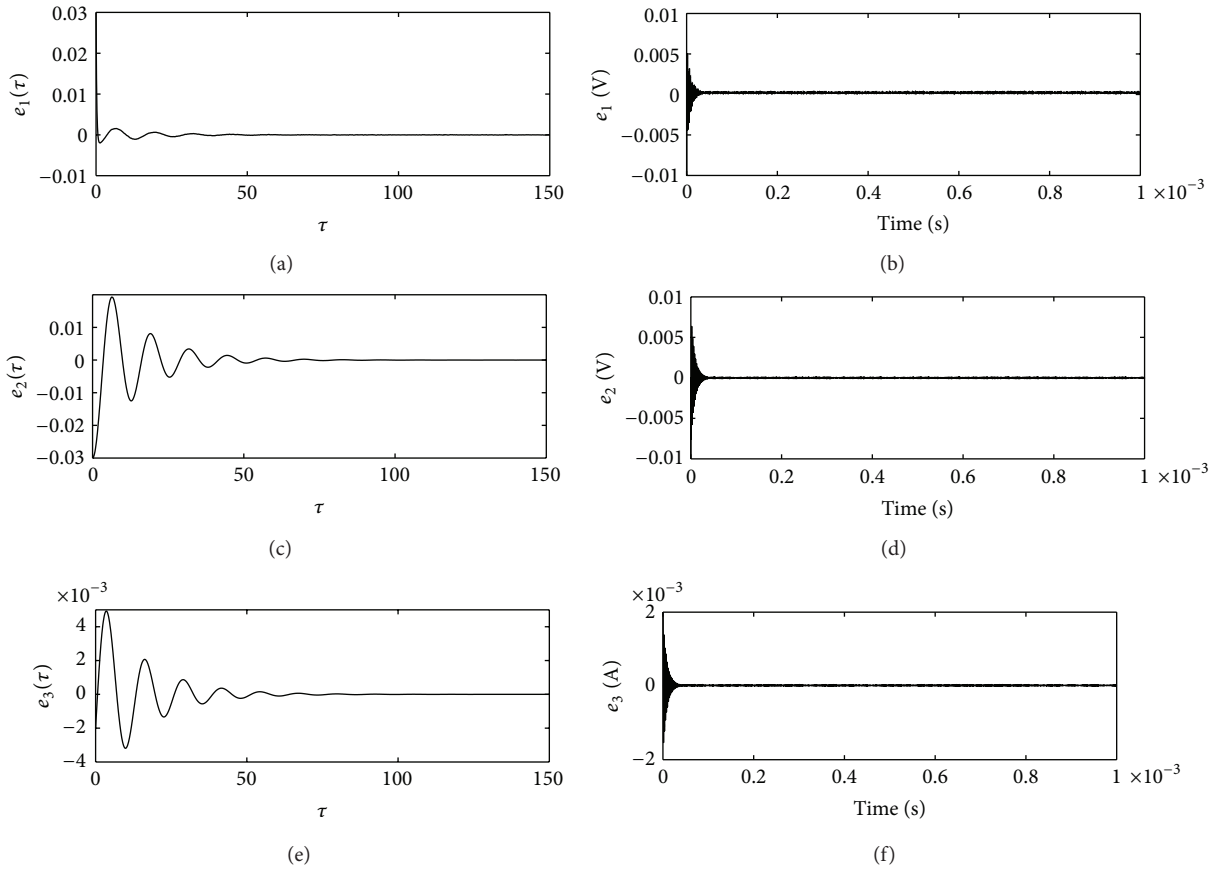

Figure 4: Time evolution of the synchronization errors from Matlab simulations (left) and Pspice simulations (right).

addition as $V(\tau)$ decreases, then there exists a continuous and strictly increasing function ϱ and a finite integer η, such that

$$V\left(e\left(\tau+\eta\right),\tau+\eta\right)-V\left(e\left(\tau\right),\tau\right)\leq-\varrho\left(\left\|e\left(\tau\right)\right\|\right), \tag{19}$$

where $e(\tau)=(e_1(\tau),e_2(\tau),e_3(\tau))$.

Thus, the Lyapunov function respects [36, Theorem 3.1] and then (8) is globally uniformly ultimate bounded near the origin.

4. Numerical Simulations

4.1. Chaotic Systems. In this section, we present some numerical results for the circuit shown in Figure 1, to illustrate the effectiveness of the proposed scheme, where the three-dimensional tunnel diode based modified Chua's system [35] is used as transmitter (blue box) and receiver (green box), the controller appears inside the red box. With the initial conditions selected as $(x_1(0),x_2(0),x_3(0))=(0.15,0.27,0.008)$ and $(y_1(0),y_2(0),y_3(0))=(0.18,0.24,0.006)$ and with the given system's parameters: $\alpha=2.507463$, $\beta=0.2985075$, $\gamma=0.20875$, $R=16$, $e=0.250$, $a_1=1.3242872$, $a_2=0.06922314$, $a_3=0.00539$, and $b=0.167$, the systems behave chaotically as shown in Figure 2. The disturbances $d(\tau)$ are given by the relation $d(\tau)=0.001\,\mathrm{wgn}(1,1,1)(x_1(\tau)+x_2(\tau))$, where wgn(1, 1, 1) is Matlab white gaussian noise generator.

4.2. Simulation Results and Discussion. The controller's parameters are $\varphi=10$ and $k=3$. The controller circuit was realized through the following relations: $k=R_5/V_TR_3=R_6/V_TR_4$ and $\varphi=R_7I_s$ where $V_T\simeq0.026$ Volt and $I_s\simeq10^{-12}$ are diode characteristics. The Voltage controlled current source (VCCS) is used to minimize as much as possible the mutual influence of between the slave system (Green box) and the controller (Red box) and to only generate the current which obliges the response system to follow the drive system. The graphs of Figures 3 and 4 show that the synchronization is reached around the dimensionless time $\tau=60$.

Remark 1. In Pspice simulations, the synchronization is reached for high values of R_7 particularly if $R_7>100\,\mathrm{k}\Omega$. R_7 role is to increase the value of the VCCS output current by increasing the value of the voltage at its landmarks.

Considering the case without disturbances, if we compare the proposed scheme with the one for which the controller is given by the following relation:

$$U\left(t\right)=-\zeta e_1\left(\tau\right), \tag{20}$$

where ζ is a positive constant chosen equal to φ, it appears that, as one can visually appreciate on the graphs of Figures 5 and 6, the exponential function based nonlinear controller is faster than the linear controller with fixed gain.

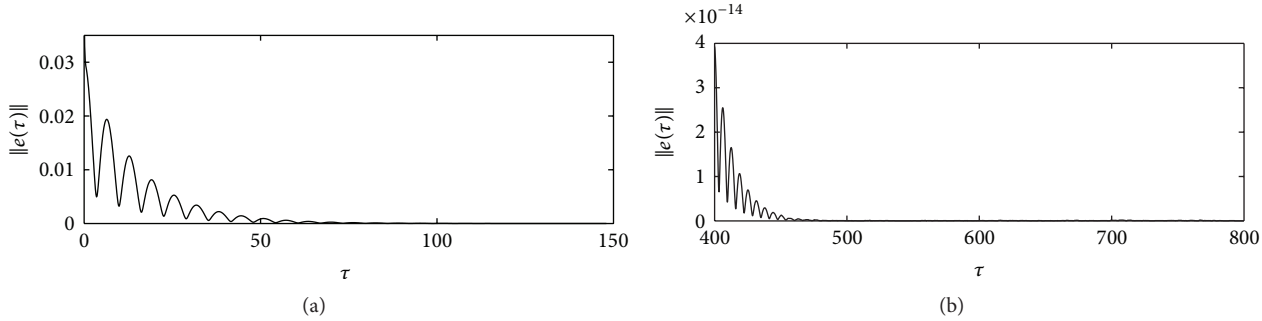

Figure 5: Time evolution of the synchronization errors norm with the propose scheme (7).

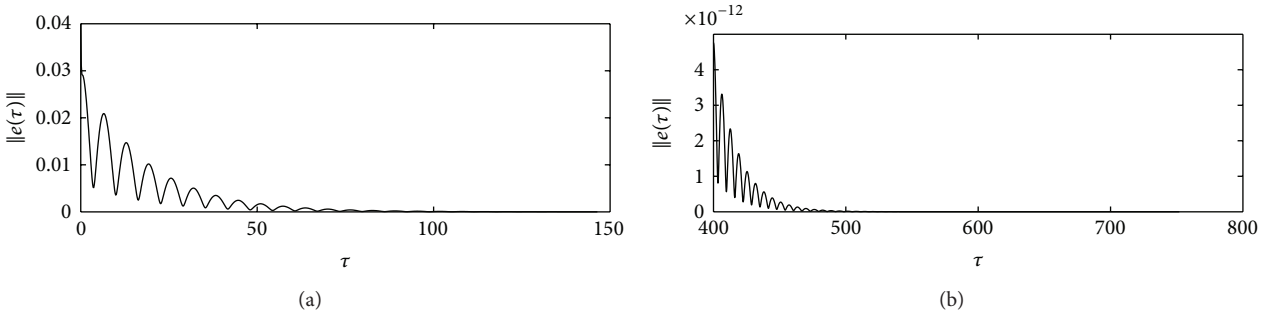

Figure 6: Time evolution of the synchronization errors norm with linear controller (20).

5. Conclusion

In this paper the synchronization between two different delayed chaotic systems is studied via a simple—exponential function based—nonlinear controller. Although different initial conditions and disturbances make synchronization more difficult, a simple exponential function based nonlinear controller is designed which facilitates the task. This is proven through the Lyapunov stability theory; it is shown that both master-slave systems should be practically synchronized. It is important to note that the proposed scheme improves the linear controller with fixed gain usually used. To show the effectiveness of the proposed strategy, some numerical simulations are given; they show the efficiency of the proposed strategy in front of the linear fixed gain based controller. The electronic circuit of the used controller is also given followed by some simulations.

Acknowledgments

The authors thank the hospitality of the University of Yaounde I and the Abdus Salam International Centre for Theoretical Physics. H. A. Cerdeira acknowledges support by the CNPq-ProAfrica, project no. 490265/2010-3 (Brazil). P. Louodop acknowledges M. André Romet for support throughout this work.

References

[1] L. M. Pecora and T. L. Carroll, "Synchronization in chaotic systems," *Physical Review Letters*, vol. 64, no. 8, pp. 821–824, 1990.

[2] X. Li, X. Guan, and D. Ru, "The damping time of EEG with information retrieve and autoregressive models," in *Proceedings of the 5th IFAC Symposium on Modelling and Control in Biomedical Systems*, Melbourne, Australia, August 2003.

[3] S. K. Han, C. Kurrer, and Y. Kuramoto, "Dephasing and bursting in coupled neural oscillators," *Physical Review Letters*, vol. 75, no. 17, pp. 3190–3193, 1995.

[4] J. S. Lin, C. F. Huang, T. L. Liao, and J. J. Yan, "Design and implementation of digital secure communication based on synchronized chaotic systems," *Digital Signal Processing*, vol. 20, no. 1, pp. 229–237, 2010.

[5] N. Islam, B. Islam, and H. P. Mazumdar, "Generalized chaos synchronization of unidirectionally coupled Shimizu-Morioka dynamical systems," *Differential Geometry*, vol. 13, pp. 101–106, 2011.

[6] B. Blasius, A. Huppert, and L. Stone, "Complex dynamics and phase synchronization in spatially extended ecological systems," *Nature*, vol. 399, no. 6734, pp. 354–359, 1999.

[7] S. Sivaprakasam, I. Pierce, P. Rees, P. S. Spencer, K. A. Shore, and A. Valle, "Inverse synchronization in semiconductor laser diodes," *Physical Review A*, vol. 64, no. 1, pp. 138051–138058, 2001.

[8] I. Wedekind and U. Parlitz, "Synchronization and antisynchronization of chaotic power drop-outs and jump-ups of coupled semiconductor lasers," *Physical Review E*, vol. 66, no. 2, Article ID 026218, pp. 1–4, 2002.

[9] A. Fradkov, H. Nijmeijer, and A. Markov, "Adaptive observer-based synchronization for communication," *International Journal of Bifurcation and Chaos in Applied Sciences and Engineering*, vol. 10, no. 12, pp. 2807–2813, 2000.

[10] K. M. Cuomo and A. V. Oppenheim, "Circuit implementation of synchronized chaos with applications to communications," *Physical Review Letters*, vol. 71, no. 1, pp. 65–68, 1993.

[11] S. Bowong, "Stability analysis for the synchronization of chaotic systems with different order: application to secure communications," *Physics Letters A*, vol. 326, no. 1-2, pp. 102–113, 2004.

[12] S. Bowong and J. J. Tewa, "Unknown inputs' adaptive observer for a class of chaotic systems with uncertainties," *Mathematical and Computer Modelling*, vol. 48, no. 11-12, pp. 1826–1839, 2008.

[13] H. Fotsin and S. Bowong, "Adaptive control and synchronization of chaotic systems consisting of Van der Pol oscillators coupled to linear oscillators," *Chaos, Solitons and Fractals*, vol. 27, no. 3, pp. 822–835, 2006.

[14] A. Astolfi, D. Karagiannis, and R. Ortega, *Nonlinear and Adaptive Control with Applications*, Springer, London, UK, 2008.

[15] G. Feng and R. Lozano, *Adaptive Control Systems*, Reed Elsevier, 1999.

[16] E. M. Shahverdiev, R. A. Nuriev, L. H. Hashimova, E. M. Huseynova, R. H. Hashimov, and K. A. Shore, "Complete inverse chaos synchronization, parameter mismatches and generalized synchronization in the multi-feedback Ikeda model," *Chaos, Solitons and Fractals*, vol. 36, no. 2, pp. 211–216, 2008.

[17] V. Sundarapandian, "Global chaos anti-synchronization of Liu and Chen systems by nonlinear control," *International Journal of Mathematical Sciences & Applications*, vol. 1, no. 2, pp. 691–702, 2011.

[18] X. Zhang and H. Zhu, "Anti-synchronization of two different hyperchaotic systems via active and adaptive control," *International Journal of Nonlinear Science*, vol. 6, no. 3, pp. 216–223, 2008.

[19] H. Zhu, "Anti-synchronization of two different chaotic systems via optimal control with fully unknown parameters," *Information and Computing Science*, vol. 5, pp. 11–18, 2010.

[20] X. Gao, S. Zhong, and F. Gao, "Exponential synchronization of neural networks with time-varying delays," *Nonlinear Analysis. Theory, Methods & Applications A*, vol. 71, no. 5-6, pp. 2003–2011, 2009.

[21] S. Zheng, Q. Bi, and G. Cai, "Adaptive projective synchronization in complex networks with time-varying coupling delay," *Physics Letters A*, vol. 373, no. 17, pp. 1553–1559, 2009.

[22] J. Cai, M. Lin, and Z. Yuan, "Secure communication using practical synchronization between two different chaotic systems with uncertainties," *Mathematical & Computational Applications*, vol. 15, no. 2, pp. 166–175, 2010.

[23] P. Louodop, H. Fotsin, and S. Bowong, "A strategy for adaptive synchronization of an electrical chaotic circuit based on nonlinear control," *Physica Scripta*, vol. 85, no. 2, Article ID 025002, 2012.

[24] M. Roopaei and A. Argha, "Novel adaptive sliding mode synchronization in a class of chaotic systems," *World Applied Sciences Journal*, vol. 12, pp. 2210–2217, 2011.

[25] Z. Sun and X. Yang, "Parameters identification and synchronization of chaotic delayed systems containing uncertainties and time-varying delay," *Mathematical Problems in Engineering*, vol. 2010, Article ID 105309, 15 pages, 2010.

[26] S. T. Kammogne and H. B. Fotsin, "Synchronization of modified Colpitts oscillators with structural perturbations," *Physica Scripta*, vol. 83, no. 6, Article ID 065011, 2011.

[27] C. K. Ahn, "Robust chaos synchronization using input-to-state stable control," *Pramana*, vol. 74, no. 5, pp. 705–718, 2010.

[28] D. J. D. Earn, P. Rohani, and B. T. Grenfell, "Persistence, chaos and synchrony in ecology and epidemiology," *Proceedings of the Royal Society B*, vol. 265, no. 1390, pp. 7–10, 1998.

[29] S. Bowong, "Optimal control of the transmission dynamics of tuberculosis," *Nonlinear Dynamics*, vol. 61, no. 4, pp. 729–748, 2010.

[30] Z. Yang, G. K. M. Pedersen, and J. H. Pedersen, "Model-based control of a nonlinear one dimensional magnetic levitation with a permanent-magnet object," in *Automation and Robotics*, chapter 21, pp. 359–374.

[31] L. O. Chua, "The genesis of Chua's circuit," *AEU. Archiv fur Elektronik und Ubertragungstechnik*, vol. 46, no. 4, pp. 250–257, 1992.

[32] L. O. Chua, T. Yang, G. Q. Zhong, and C. W. Wu, "Synchronization of Chua's circuits with tune-varying channels and parameters," *IEEE Transactions on Circuits and Systems I*, vol. 43, no. 10, pp. 862–868, 1996.

[33] Y. Z. Yin, "Experimental demonstration of chaotic synchronization in the modified Chua's oscillators," *International Journal of Bifurcation and Chaos in Applied Sciences and Engineering*, vol. 7, no. 6, pp. 1401–1410, 1997.

[34] X. X. Liao, H. G. Luo, G. Zhang, J. G. Jian, X. J. Zong, and B. J. Xu, "New results on global synchronization of Chua's circuit," *Acta Automatica Sinica*, vol. 31, no. 2, pp. 320–326, 2005.

[35] A. Y. Markov, A. L. Fradkov, and G. S. Simin, "Adaptive synchronization of chaotic generators based on tunnel diodes," in *Proceedings of the 35th IEEE Conference on Decision and Control*, pp. 2177–2182, December 1996.

[36] Z. Ding and G. Cheng, "A new uniformly ultimate boundedness criterion for discrete-time nonlinear systems," *Applied Mathematics*, vol. 2, pp. 1323–1326, 2011.

[37] M. de la Sen and S. Alonso, "Adaptive control of time-invariant systems with discrete delays subject to multiestimation," *Discrete Dynamics in Nature and Society*, vol. 2006, Article ID 41973, 27 pages, 2006.

[38] G. Bitsoris, M. Vassilaki, and N. Athanasopoulos, "Robust positive invariance and ultimate bounded- ness of nonlinear systems," in *Proceedings of the 20th Mediterranean Conference on Control and Automation (MED)*, pp. 598–603, Barcelona, Spain, July 2012.